Doctoral Thesis

Asphaltene based Oxidized Carbons: New Catalysts for Synthetic Transformations

Hyosic Jung

Department of Chemistry

Ulsan National Institute of Science and Technology

2021

Asphaltene based Oxidized Carbons: New Catalysts for Synthetic Transformations

Hyosic Jung

Department of Chemistry

Ulsan National Institute of Science and Technology

Asphaltene based Oxidized Carbons: New Catalysts for Synthetic Transformations

A thesis/dissertation submitted to
Ulsan National Institute of Science and Technology
in partial fulfillment of the
requirements for the degree of
Doctor of Philosophy

Hyosic Jung

09/29/2020

Approved by

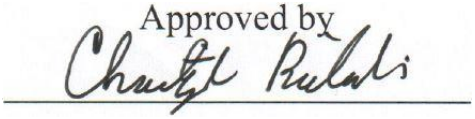

Advisor
Christopher W. Bielawski

Asphaltene based Oxidized Carbons: New Catalysts for Synthetic Transformations

Hyosic Jung

This certifies that the thesis/dissertation of Hyosic Jung is approved.

09/29/2020

Signature

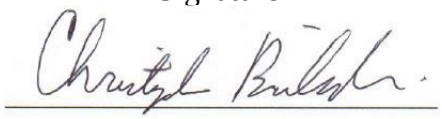

Advisor: Christopher W. Bielawski

Signature

Jong-Beom Baek: Thesis Committee Member #1

Signature

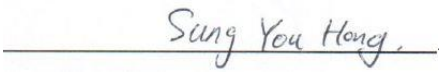

Sung You Hong: Thesis Committee Member #2

Signature

Young S. Park: Thesis Committee Member #3

Signature

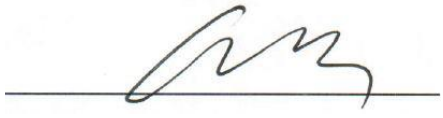

Hyeon Suk Shin: Thesis Committee Member #4

Some portions of this thesis were submitted to the journal entitled "*Communications Chemistry*". The article was accepted for publication and finally published. It is my understanding that the article may be re-used as part of this thesis without permission from the publisher (Nature Publications); see https://www.nature.com/nature-research/reprints-and-permissions/permissions-requests. Likewise, other portions of this dissertation were submitted to the journal entitled "*RSC Advances*". It is my understanding that the article may be re-used as part of this thesis without permission from the publisher (RSC Publications); see https://www.rsc.org/journals-books-databases/journal-authors-reviewers/licences-copyright-permissions/

Abstract

Since the terminology of catalysis was introduced in the 1800s, catalysts have been considered the essential materials to facilitate chemical reactions. Predominantly, metal-based catalysis has driven various synthetic reactions until now. Although metal-based catalysts are commonplace and have been well-studied in the context of a wide variety of transformations, increasing costs, high toxicity, and limited resources have warranted the development of alternatives. Among potential candidates, carbocatalysts, materials mostly comprising carbon elements, have attracted attention to promoting a broad range of transformations. For example, graphene oxide (GO) has been broadly utilized as a catalyst for various organic transformations. However, the high oxygen content and large particle size prevented further utilization under harsh synthetic conditions (e.g., microwave irradiation or light) where unexpected side reactions occurred.

In this dissertation, we introduced asphaltene oxide (AO) as a new class of carbocatalyst for various types of organic synthesis and overcame the limitations mentioned above. Asphaltene, as a precursor material, often thrown away from petroleum refining processes, was composed of polycyclic aromatic hydrocarbons (PAHs). Initially, we hypothesized that AO's finite surface area compared to GO might be used in applications inaccessible to other carbocatalyst, such as microwave-assisted reactions. Initially, AO was synthesized using a modified Hummers' method, a standard protocol for preparing GO from graphite. In the following research, it was found that AO successfully promoted various synthetic applications, including etherifications, condensations, C-C cross-couplings, and Fischer indole syntheses from the utilization of microwave reactors.

In an effort to expand usage in organic synthesis, we focused on contemporary drawbacks that carbocatalysts encountered. Carbocatalysts are commonly known as heterogeneous catalysts. Even if carbocatalyst has been well-studied and substituted metal-based catalysts in various organic synthesis, these heterogeneous features have inherent limitations such as catalysis deactivation. For this reason, we hypothesized that increasing the oxygen content of AO would enhance its solubility in a manner that improves catalytic activity when compared to heterogeneous counterparts. Indeed, refluxing asphaltene in 60% nitric acid afforded a derivative that exhibited good solubility in both organic solvents and aqueous media; as such, hereafter, the material was termed 'soluble AO' (sAO). These solubility features made sAO accessible to a relatively in-depth analysis of the structure and molecular weight compared to other carbocatalysts. Furthermore, sAO effectively functioned as a catalyst for esterifications, Fischer indole condensations, multicomponent reactions, and cationic polymerizations with remarkable

catalytic. Furthermore, it was possible to be utilized in both microwave reactions and aqueous media synthesis.

Table of Contents

List of Figures

List of Tables

Chapter 1: Introduction

1.1 The past and present catalysis

"There is probably no chemical reaction which cannot be influenced catalytically."

-Wilhelm Ostwald awarded the 1909 Nobel Prize in Chemistry-

Catalysts, an essential tool for conducting reactions, have been used to produce alcohol from sugar by fermentation much earlier[1]. In 1540, Valerius Cordus used sulfuric acid to promote alcohol conversion to ethers, which was first known to use inorganic catalysts[2]. As such, catalysis has been around in human history for a long time while nobody understood the catalysis phenomenon. In 1835, the terminology of catalysis was eventually coined by Jöns Jacob Berzelius[3]. In the 1880s, Wilhelm Ostwald[4] performed reactions that were catalyzed by acids/bases and established that the reaction rate is related to the catalyst's strength. Besides, he afresh defined that "Catalysts are substances which change the velocity of a reaction without modification of the energy factors of the reaction"[5]. In the present day, catalysis is defined as "a substance that increases the rate of a reaction without modifying the overall standard Gibbs energy change in the reaction" by IUPAC (see Figure 1.1)[6].

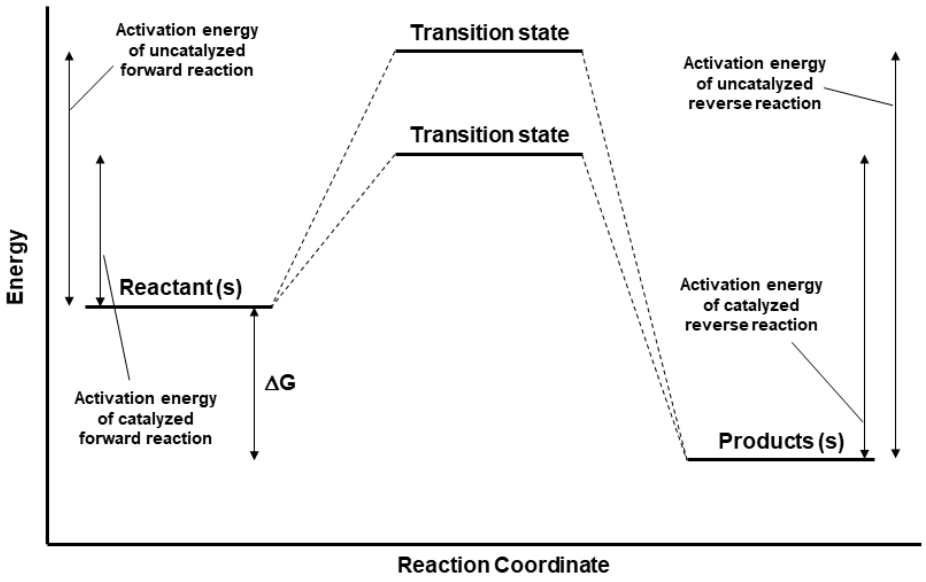

Figure 1.1 Energy diagram for catalyzed and uncatalyzed reactions.

Catalysts could be generally divided into the two classes, homogeneous or heterogeneous, depending on the mixture phase with the reactant. As such, the difference of catalyst solubility in the reactant caused the pros and cons of heterogeneous and homogeneous systems, respectively. In detail, heterogeneous catalysts are solid compounds and occupy a different phase with the reactants. Since a heterogeneous catalyst is not miscible with reactants, it is readily separated from a reaction mixture straightforwardly using filtration and facilitates recycling in other reaction batches. These advantages have fulfilled financial requirements in the industrial manufacturing process. However, the most critical limitation for the heterogeneous catalyst is the catalytic activities come from the surface of the material[7]. Once the reactant molecules completely occupied the catalysts' surface, the further reaction did not make progress until the product was detached from the surface. In this process, the catalyst underwent deactivation, which is the loss over catalytic activity and selectivity. Furthermore, the heterogeneous catalyst mechanism was often an unknown process due to the involuntary side reactions on the surface and the limitation of characterization methods.

However, a homogeneous catalyst was mixed with the reactant in the same phase into the reaction. In other words, each of the catalyst molecules is participated in chemical reactions and accomplished a high degree of interaction with reactant molecules. As such, homogeneous catalysts mostly show higher catalytic activities than heterogeneous catalysts. Moreover, these catalysts' active sites and reaction mechanisms were usually well-defined because of more direct analysis techniques such as liquid-state nuclear magnetic resonance (NMR), gas chromatography-mass spectrometry (GC-MS), and single-crystal X-ray diffraction. The homogeneous catalyst was also prone to modification using different ligands and additives to improve the catalytic activity[8]. Despite these advantages, the separation of the catalyst from the reaction mixture is a generally complicated and expensive process. By extension, the homogeneous catalysts are often irrecoverable and hard to recycle after the reaction[9].

According to the Nobel foundation’s statistics, the chemical and enzymatic catalysis fields achieved about 14% of the Nobel Prizes in chemistry between 1901 and 2012. Most of all, transition metal-based catalysts[10-14] drove the development and advancement of catalysis chemistry. To introduce some cases in the Nobel award related to catalysis, Paul Sabatier excogitated the reduction of carbon dioxide using hydrogen in the presence of Nickel as the catalyst at high temperature and pressure. He had been recognized and won the Nobel Prize in chemistry in 1912[15, 16]. After half a century, Karl Ziegler discovered the titanium-based catalyst, a combination of $TiCl_4$ and $Al(C_2H_5)_2Cl$, and Giulio Natta successfully prepared the stereoregular poly(propylene) using the modified titanium catalyst[17]. The Ziegler-Natta catalysts have been used to polymerize terminal alkenes (e.g., polyethylene, polypropylene, and polybutadiene) and vigorously utilized in commercial plastics and rubber

manufacturing[18]. Both Karl Ziegler and Giulio Natta were recognized and awarded the Nobel Prize in Chemistry in 1963. The 2005 Nobel Prize was awarded to Yves Chauvin[19], Robert H. Grubbs[20-22], and Richard R. Schrock[23-25] for discovering useful molecular rearrangement known as metathesis. In this metathesis, transition metal catalysts (Grubbs catalysts and Schrock catalysts are based on ruthenium and molybdenum, respectively; see Figure 1.2) promote breaking double bonds and re-make between carbon atoms in ways that cause atom groups to change places. Similarly, various transition metal-catalyzed carbon-carbon bond formations were investigated to synthesize the complex organic molecules[12, 26]. Typically, Richard F. Heck[27, 28], Ei-ichi Negishi[29], and Akira Suzuki[30] discovered the palladium-catalyzed cross couplings in organic synthesis and awarded the Nobel Prize in 2010. Transition metal-based catalysts have been regarded as the most dependable and essential materials in the whole catalysis history.

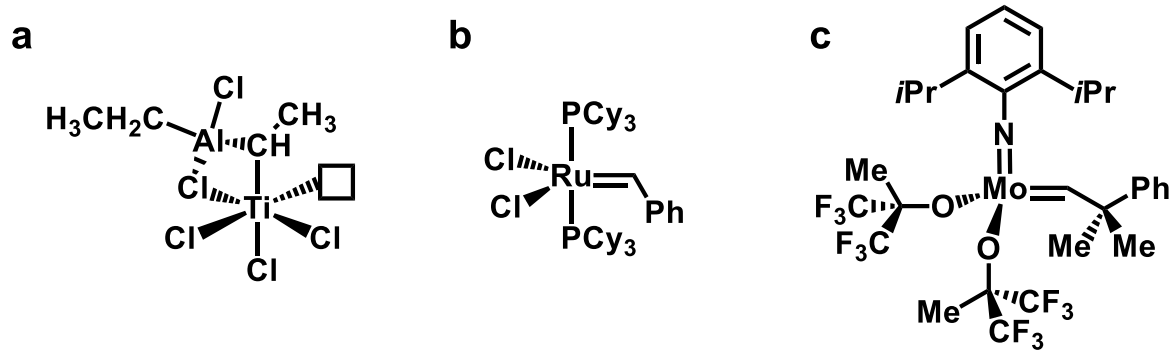

Figure 1.2 Representative transition metal catalysts awarded in Nobel Prize. (a) Ziegler-Natta catalyst. (b) 1st generation Grubbs catalyst. (c) Schrock catalyst.

Even though transition metal-based catalysts had made remarkable progress in organic, inorganic, and biomolecular synthesis, inherent limitations of metal and ligand resources have still been considered in catalyst fields. Firstly, various transition metals and ligands are commonly expensive due to the scarcity of resources. Therefore, the utilization of transition metal-based catalysts is not economically suited for large-scale reactions in the industrial process. Secondly, transition metals are generally toxic, and as a result, serious problems in the field of electronic devices and pharmaceuticals have been caused by the residue of metals from products[31, 32]. Finally, transition metals are often sensitive under moisture and oxygen atmosphere. Due to the undesirable sensitivity, transition metal-catalyzed synthesis has been required for unique environments, complex instruments, and techniques. Based upon these intrinsic drawbacks, alternative materials such as organocatalysts and carbocatalysts have been attractive and interesting in catalyst fields for metal-free synthetic transformations[33].

1.2 Carbocatalysts

Carbocatalysts are defined as the primary carbon-composed materials used for the various organic or inorganic synthetic transformation as a catalyst. Due to its benefits, such as abundant resources in nature, economical and environment-friendly, carbocatalysts have been considered alternative candidates instead of transition metal-based catalysts. Historically, charcoal has been utilized in the oxidation process as carbocatalyst. In the 1920s, Rideal and Wright demonstrated that oxalic acid was oxidized to afford carbon dioxide and water under oxygen absorbed charcoal[34]. The oxidation was conducted in the absence of charcoal to demonstrate the catalytic ability, but the reactions did not facilitate. Also, oxygen absorbed charcoal promoted the oxidative dehydrogenation that converted ethylbenzene to styrene. In another example of carbocatalyst, Ritter and coworkers investigated that 4-chlorophenol was oxidatively decomposed in the presence of graphite and hydrogen peroxide to yield hydrochloric acid, water, and carbon dioxide[35]. While graphite showed the lower catalytic activity than iron powder/ions, the process may be described that the graphite acted similar to the iron ion in the Fenton reaction[36]. Furthermore, other carbon isotope structures such as carbon nanotubes (CNTs) and fullerene (C_{60}) participated as carbocatalyst for synthetic transformations. Surface functionalized CNTs was effectively catalyzed the oxidative dehydrogenation of *n*-butanes to butenes[37]. C_{60} has demonstrated the ability of activation of hydrogen and successfully catalyzed the hydrogenation of nitrobenzene to aniline[38].

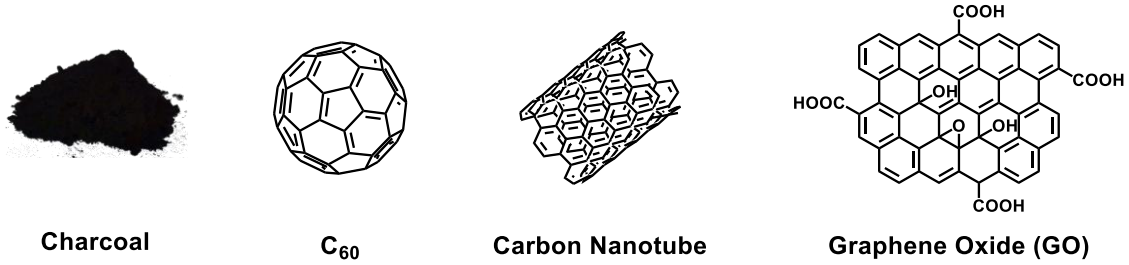

Figure 1.3 Representative pictures or structures of typical carbocatalysts, including charcoal, buckminsterfullerene (C_{60}), carbon nanotubes (CNTs), and graphene oxide (GO).

Even though the aforementioned carbon-based materials have successfully performed varied synthetic reactions, most of them showed unsatisfied catalytic activity than transition metal catalysts. In 2010, Bielawski and coworker reported that graphene oxide (GO) effectively facilitated selective oxidations, a broad range of alcohols to their aldehyde and ketone, and hydration alkynes to their

corresponding methyl ketones[39]. Since GO was discovered as carbocatalyst, chemists have focused on seeking the utilization of GO in place of transition metal-based catalysts. As a result, GO has been afforded to promote various organic transformations such as oxidation[40-42], reduction reactions[43], C-C cross couplings[44-46], polymerizations[47], and many others[48, 49]. For example, nitroarene derivatives underwent a reduction pathway and converted to the corresponding aminoarene products in the presence of GO[50]. Furthermore, GO was enabled to selectively hydrogenate nitro substrates, which possessed the reducible functional groups such as alkenes or alkynes. Besides, GO was found to facilitate polymerizations with different monomers (e.g., benzyl alcohol and vinyl) through dehydration or cationic pathway affording to GO mediated polymers, enhanced mechanical or electrical properties[51, 52]. As such, GO has been tremendously and extensively developed in the carbocatalyst field and the material field.

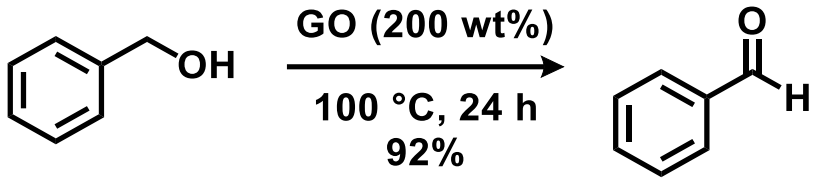

Figure 1.4 Graphene oxide (GO) catalyzed selective oxidation of benzyl alcohol to benzaldehyde.

1.3 What is asphaltene?

Asphaltene is classified as insoluble, the heaviest aromatic hydrocarbons, and polar components in crude oil[53]. Also, asphaltene has a complex colloidal structure and is easily agglomerated in solution. The terminology of "Asphaltene" was coined by French chemist Boussingault in 1837[54, 55]. Even though the definition of asphaltene has been tried to unify for a long time, it has not been precisely defined by physical and chemical ways due to the complicated molecule mixture, uncertain molecular weight, and structure. Therefore, asphaltene is operationally defined by its solubility features, soluble in toluene and insoluble in *n*-hexane and *n*-heptane[56].

The aggregated asphaltene caused troubles in the oil refining process and transportation for a long time. In detail, asphaltene provoked that (i) excessive coke was produced in the process of pyrolysis, catalytic and hydrogenation classification (ii) catalyst efficiency was reduced due to low reactivity of asphaltene (iii) catalysts was rapidly deactivated by the accumulation of coke (iv) fouling was formed on the wall of the pipeline during the transport of crude oil. Subsequently, asphaltene is

directly related to critical points of economic issues in the oil refining industry due to the reasons mentioned earlier. That is why asphaltene has been focused on studying the ways of purification from crude oils and also the more in-depth analysis to investigate the molecular weight and structure.

As mentioned above, since π-π interactions between aromatic benzene rings of asphaltene were dominated, resulting in the formation of the agglomerated macromolecules, the molecular structure of asphaltene is challenging to define. In 1967, Yen and coworkers first suggested a model explain the structure of asphaltenes, known as Yen model[57]. The model was proposed that asphaltene was composed of different chemical moieties, such as polycyclic aromatic hydrocarbons (PAHs), connected to a different length of alkyl chains. Furthermore, the Yen model was recently developed to the Yen-Mullins model (see Figure 1.5), specified the structure of asphaltenes from the molecular level to aggregated cluster level[58]. In 2015, individual molecular architectures of asphaltene were finally clarified by Gross groups using atomic-resolution low-temperature atomic force microscopy (AFM) and scanning tunneling microscopy (STM)[59]. This microscopy study directly demonstrated the previously proposed model structure of asphaltenes composed to the diverse size of PAHs mixture with heteroatoms (e.g., nitrogen and sulfur) and diverse length of alkyl chains. Even though mass spectrum (MS) applied of asphaltene had limitations such as fragmentation, gas-phase aggregation, and the inability to volatilize the heaviest asphaltene fraction, molecular weight analysis of asphaltene was previously carried out and resulted in obtaining range from 400 Da to 10000 Da[60, 61]. Since then, by applying the time-resolved fluorescence depolarization (TRFD) method, the molecular weight of asphaltene was calculated by correlation times and obtained an average 750 Da (range of 500-1000 Da)[62-66].

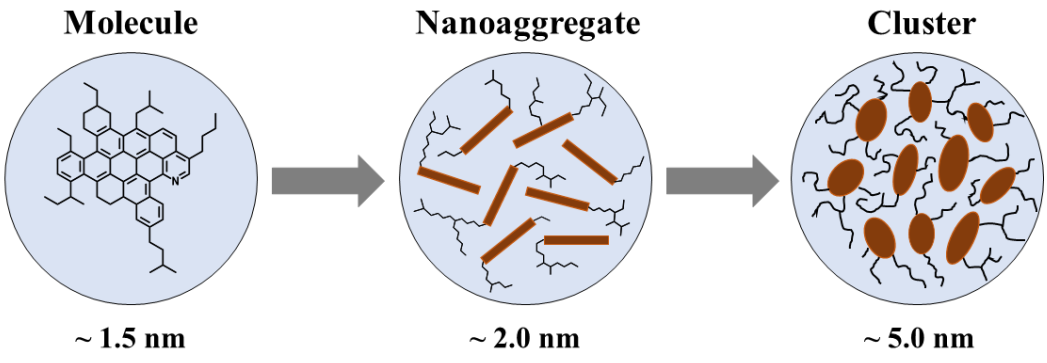

Figure 1.5 Yen-Mullins model. The representative single molecular architecture of asphaltenes was shown polycyclic aromatic hydrocarbons (PAHs) with alkyl chains (left image). PAHs molecules formed nanoaggregates with about 2 nm (center image). Nanoaggregates formed clusters with about 5 nm (right image).

According to previous reports, oxidation for asphaltene has traditionally been precipitation/separation methods from crude oil. In 1971, asphaltene was directly heated to reflux in nitric acid to obtain water-soluble asphaltene[67]. Furthermore, partially oxidized asphaltene treated by $KMnO_4$ has been shown to facilitate its precipitate from crude oil[68]. Ozonized asphaltene, which enhanced hydrophilic properties, facilitated the more robust interaction with other asphaltene[69]. As a result, asphaltene has induced the aggregation of each other and reduced viscosity in bitumen. As such, oxidized asphaltene with different methods has been studied to resolve the economic issues in the oil refinery industry.

1.4 Contents of the Dissertation

In chapter 2 of this dissertation, synthesizing a novel class of carbocatalyst using asphaltene and giving scope to catalysis ability for diverse synthetic transformation will be described. Asphaltene was oxidized using a modified Hummers' method, a general preparation method for GO. The structure of asphaltene oxide (AO) was analyzed by Fourier-transform infrared spectroscopy (FT-IR), x-ray photoelectron spectroscopy (XPS), and elemental analysis. Further analysis for a deeper understanding of the functional groups on AO was performed using different chemical tests, targeting either the inhabited epoxide, carboxylic acid, and hydroxy groups. To unveil the application of AO for synthetic reaction, we adopted the oxidation of alcohol, the benchmark transformation for carbocatalyst. However, AO facilitated not an oxidation pathway but a condensation route on account of the acidic properties of AO. Furthermore, Claisen-Schmidt-type condensation and C-C cross-coupling reactions were also accomplished with the aid of AO. Based on these experiment results, we analyzed the origins of AO's catalyst activity compared to the results obtained from analogous experiments using GO. Finally, AO was successfully utilized in a microwave-assisted synthesis that has hitherto impossible with other reported oxidized carbons because of its comparatively small particle size and unique composition.

In chapter 3 of this dissertation, further studies on AO by enhancing the degree of oxidation will be introduced. A homogeneous catalyst system is commonly more activated than a heterogeneous catalyst. A new oxidation method to prepare soluble asphaltene oxide (sAO) was successfully achieved using more strong acid reagent. Compared to AO, the most significant difference feature of sAO is soluble in organic solvents (e.g., methanol, ethanol, THF, DMSO, DMF, and acetone) and even water. Furthermore, due to the solubility of sAO, the material afforded to conduct in-depth characterization using matrix-assisted laser desorption/ionization-time of flight (MALDI-TOF), NMR, AFM, and mass spectrum. By taking these advantages of sAO, various synthetic transformations such as esterifications, the Fischer indole condensations, multicomponent reactions, and cationic polymerizations were

successfully performed with high reactivity. Further application of sAO offered microwave-assisted reaction as well as aqueous media eco-friendly synthesis. This approach expands the realization of metal-free catalysts and helps promote synthetic reactions under homogeneous conditions.

Chapter 2: Using Asphaltene Oxide as Carbocatalyst for Various Synthetic Transformations

2.1 Introduction

The rapidly developing field of carbocatalysis[70], which is defined as chemical reactions conducted by carbon-based materials, provides interesting peculiarities. For instance, compared to a metal-based catalyst, carbocatalysts are generally economical, environmentally friendly, demand a relatively comfortable workup process because of their heterogeneous system, and display less toxicity without reactivity loss. Historically, various carbon isotopes such as charcoal[71], carbon nanotubes (CNTs)[37], and buckminsterfullerene (C_{60})[38] had been selected and utilized in broad transformations. Furthermore, the field of carbocatalysis burgeoned after it was revealed that the high chemical potential of the graphene oxide (GO) could be used to promote synthetic transformation. Indeed, GO has been afforded to facilitate oxidations[39], C-C cross-couplings[72-74], condensations[75], reduction[43], and many types of organic synthesis[76, 77]. The broad reactivity of GO is caused by the multitude of different oxygen-containing functional groups and relatively high acidity (pH measured to be a 3.0 at 1.0 mg/mL in water)[78].

Despite these advantages, GO and other carbocatalysts have trouble with fundamental and practical shortcomings. The catalytic activities are mysterious in origin(s) because GO is a berthollide and characteristics such as unknown basal structure and edge part, numerous oxygen functional groups, and an uncertain size of surface areas that depend on the degree of oxidation and exfoliation. Besides, GO has been discovered not to tolerate the high temperature, light, or microwaves and was rapidly decomposed because of its comparatively high oxygen content (the C/O ratio of GO is typically ~2)[79].

We hypothesized that discovering novel carbocatalyst precursors originated from asphaltene might be a solution for the drawbacks described above. Asphaltenes are residual molecules found from crude oil along with the heavier, aromatic, and saturated hydrocarbon[62]. Because of enhanced fuel quality, transportation costs, and increased production efficiency, the study of asphaltene directly focused on extraction and removal methods during oil refining processes[63]. Since asphaltene is composed of a mixture of various sizes of polycyclic aromatic hydrocarbons (PAHs), it is generally defined in terms of not its chemical form but its solubility (soluble in toluene and insoluble in hexane)[68].

However, the mixture structures of asphaltene were first-ever unveiled by Gross team using atomic force microscopy (AFM), and asphaltene was demonstrated to be mixtures of PAHs[59]. Since the aromatic based structures that were verified are comparable to two-dimensional carbons, asphaltene was labeled 'nanographene' and thus enabled to be used as a substitute for a small molecular model of graphite or graphene.

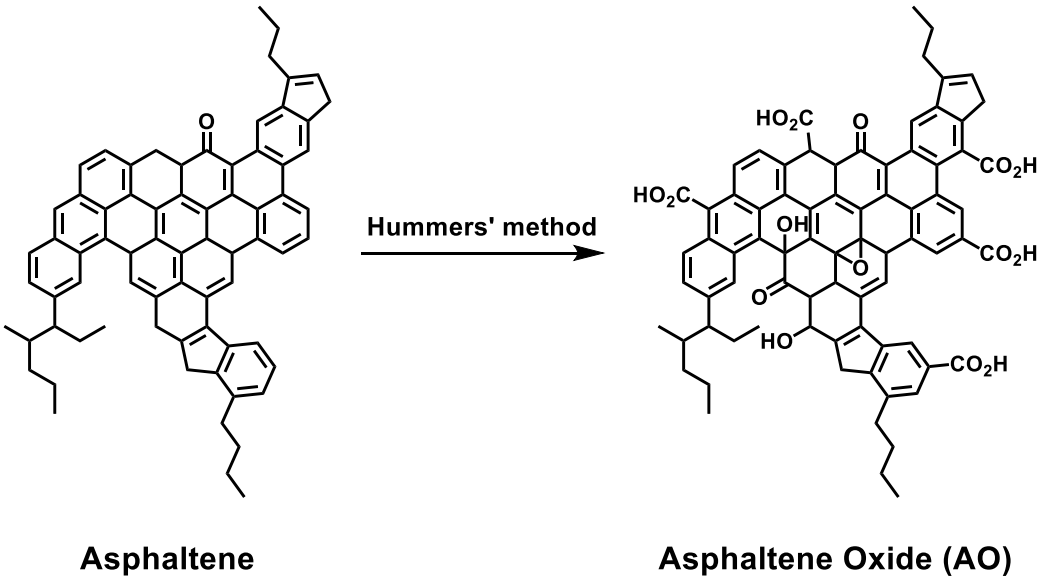

Figure 2.1 Oxidation of asphaltene using Hummers' method affords asphaltene oxide (AO).

Oxidizing asphaltene reported formerly was found to facilitate separation from crude oil[68] or reduce the viscosity of bitumen[69]. In detail, oxidizing asphaltene treated by potassium permanganate[68] or ozone[69] brought out enhanced hydrophilicity and enabled to precipitate from crude oil. We assumed that such asphaltene oxide (AO) might operate as a suitable catalyst owing to the inexpensive cost of the precursor while providing performance in the catalysis chemistry exhibited by GO and other carbocatalysts[80]. Furthermore, AO may investigate the logical mechanism and catalytically-active sites on other oxidized carbons and advance the development of the carbocatalysis field. Herein we provide the synthesis procedure for AO and explain the application of this material in diverse transformations. Moreover, we describe the novel perspective to the origins of the catalytic activities displayed by GO and demonstrate how AO can be applied to a new synthetic process that is unreachable to other carbocatalysts.

2.2 Result and Discussion

Initially, asphaltene was washed with *n*-heptane to eliminate the residual oil impurities and then directly synthesize AO using modified Hummers' method[81]. Briefly, asphaltene was oxidized by potassium permanganate in sulfuric acid at 35 ℃ for 3h, and the resulting particles were washed with an aqueous solution of HCl (1.0 M) to eliminate heavy metal impurities like vanadium and nickel and so on[82]. The FT-IR spectrum recorded for the product to prove oxidation of asphaltene revealed strong IR absorption bands that were assigned to hydroxyl (ν_{O-H} = 3400 cm^{-1}), carbonyl ($\nu_{C=O}$ = 1700 cm^{-1}), and epoxide (ν_{C-O} = 1220 and 1160 cm^{-1}) stretching frequencies (see Figure 2.2.a). Furthermore, AO featured a relatively high oxygen content (13.1 wt%; c.f., a ~1.4 wt% oxygen content was determined for the starting material), based on elemental analysis results (see Table C.2.1). Also, X-ray photoelectron spectroscopy (XPS) survey spectra supported that not only the oxygen content of AO was significantly higher than that of the starting material, but the aforementioned structural assignments were observed (see Figure 2.2.b-c).

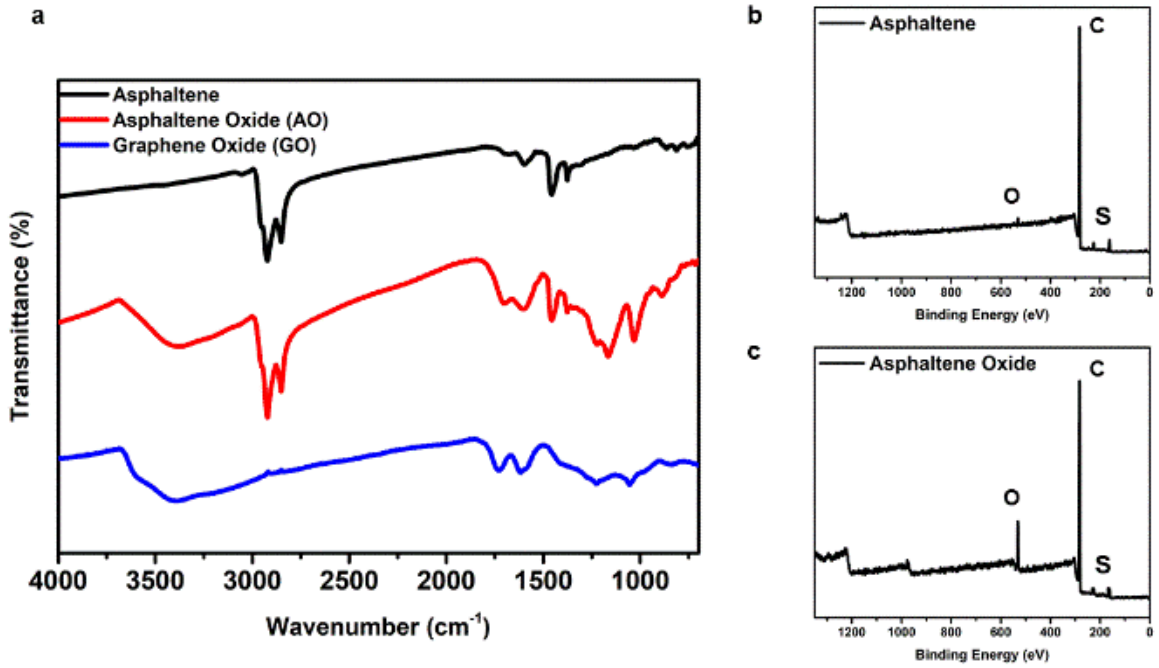

Figure 2.2 Summary of characterization data. (a) FT-IR spectra were recorded for asphaltene (black line), AO (red line), and GO (blue line). (b) XPS survey spectra recorded for asphaltene (c) XPS survey spectra recorded for AO (indicated).

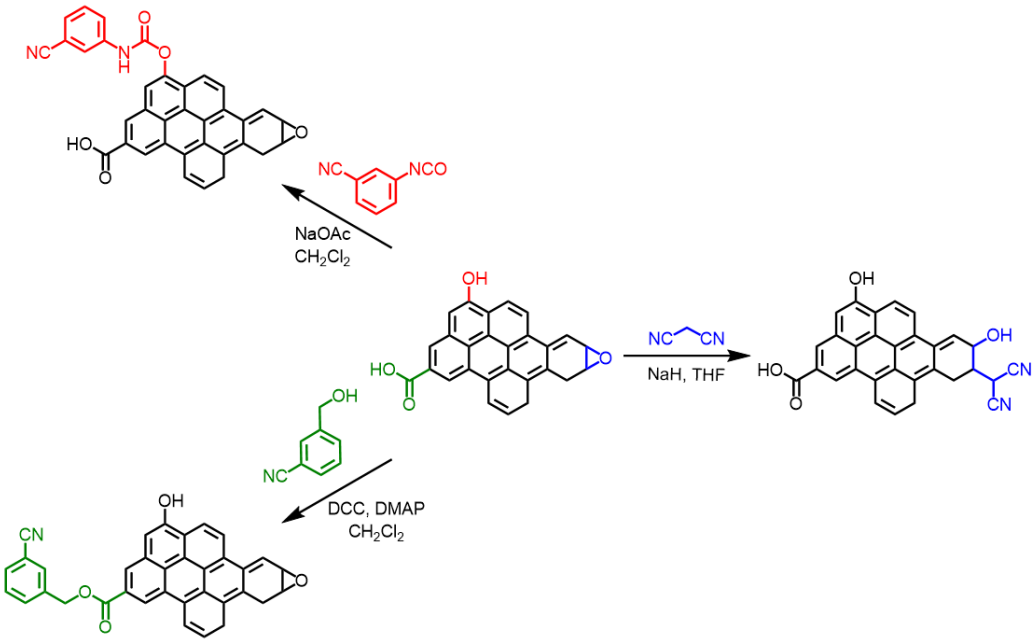

Figure 2.3 Chemical tests used to quantify the functional groups displayed on GO and AO. The starting material shown in the center represents a truncated form of GO or AO and features pendant carboxylic acid, hydroxy, and epoxide groups. By using the reagents shown, the carboxylic acid groups were converted to esters, the hydroxyl groups were converted to carbamates, and epoxide groups were ring-opened. In all cases, the corresponding products feature nitrile groups (CN) that could be quantified using IR spectroscopy and elemental analyses.

As shown in Figure 2.3, a series of chemical tests were devised to quantify the oxygen-based functional groups present on AO and reveal the structure of the material. The reagents, contained nitrile group, were utilized to preferentially react with either the existent carboxylic acid, hydroxy, or epoxide groups, and nitrile feature conducted to facilitate characterization using FT-IR spectroscopy and elemental analysis. First, AO was reacted with 3-cyanobenzyl alcohol under Steglich esterification condition and afforded the corresponding ester derivative[83]. FT-IR spectroscopy recorded for the ester derivative appeared a new signal assigned to a nitrile group ($\nu_{C\equiv N}$ = 2225 cm^{-1}) and showed a bathochromic shift of the carbonyl stretching frequency ($\nu_{C=O}$, from 1700 cm^{-1} to 1650 cm^{-1}). Next, introducing AO to 3-cyanophenyl isocyanate resulted in an attenuated hydroxyl stretching frequency (ν_{O-H} = 3400 cm^{-1}) and the appearance of strong signals that were assigned to nitrile ($\nu_{C\equiv N}$ = 2225 cm^{-1}), amido (ν_{N-H} = 3070 cm^{-1}), and carbamyl ($\nu_{C=O}$ = 1550 cm^{-1}) groups. Finally, using f previously reported by Swager to form C-C bonds via the ring-opening of the epoxide groups on GO[84], AO was treated with malononitrile under basic conditions. The intensity of the epoxide groups (ν_{C-O} = 1220 cm^{-1}) measured in the AO starting material decreased, and the formation of a new nitrile frequency ($\nu_{C\equiv N}$ =

2180 cm^{-1}) was observed. Elemental analysis data recorded for not only modified AOs of the reactions as mentioned above but also modified GOs enabled quantification of the resident functional groups using the respective nitrogen contents. The corresponding functional groups resulted in carboxylic acid (2.3×10^{-3} mol/g; c.f. 3.6×10^{-4} mol/g for GO), hydroxy (1.4×10^{-3} mol/g; c.f. 1.1×10^{-4} mol/g for GO) and epoxide (5.4×10^{-4} mol/g; c.f. 1.2×10^{-3} mol/g for GO). The differences in constituent functional groups measured for AO and GO were attributed to the former's relatively small size and effectively explained why differential reactivities were observed (vide infra). Furthermore, the pH of a suspension of AO in water ($[AO]_0$ = 1.0 mg/mL) was measured to be 3.5; for comparison, a GO suspension was 3.0 under identical conditions, and these data supported the hypothesis as mentioned above[85].

Table 2.1 Summary of functional group quantification data obtained for AO and GO[a]

Functional Group	AO (mol/g)	GO (mol/g)
carboxylic acid	$> 2.3 \times 10^{-3}$	$> 3.6 \times 10^{-4}$
hydroxy	$> 1.4 \times 10^{-3}$	$> 1.1 \times 10^{-4}$
epoxide	$> 5.4 \times 10^{-4}$	$> 1.2 \times 10^{-3}$

[a] The calculations were based on the elemental analysis data (see Table C.2.2 and Table C.2.3)

Since the of aldehydes/carboxyl (oxidation) or ether (condensation) with their corresponding alcohols is regarded as benchmark transformation for carbocatalysts[39], our initial efforts were directed toward exploring the chemistry of alcohol with AO. As summarized in Table 2.2, reactions with benzyl alcohol were optimized with various AO loading (5-20 wt%) and predetermined temperature (100-150 ℃) under neat conditions. To our surprise, AO was found to be a preferential catalyst for condensations instead of oxidations. The corresponding ether product was successfully obtained in yields of up to 82% from benzyl alcohol using 10 wt% loading of AO at 150 ℃ for 3h. Furthermore, AO facilitated to convert a series of alcohols, featured different functional groups, to the expected ethers (see Table A.2.2). Electron-rich functionalized alcohols generally afforded the product with higher conversions than electron-poor substrates. To sum up, based on a consistent experiment result with an acid-catalyzed process, the etherification synthesis was prominently affected by AO's unique structure and composition. In accordance with results reported for GO[51], benzyl alcohol or methoxy group functionalized derivatives was polymerized with the aid of AO at 200 ℃ and afforded the corresponding

poly(phenylene methylene)s in good yields (see Table A.2.4) and showed the potential of the carbon-based material as a useful polymerization catalyst.

As part of an effort to identify the AO's catalytically active sites, a series of control experiments were performed. Based on the results mentioned above, the hypothesis is an acidic feature of the catalyst promoted that condensation chemistry. Condensation was conducted with AO in the presence of an excess base (i.e., pyridine) to confirm the hypothesis[77, 86]. As a result, the ether product was not observed under these conditions. Presumably, pyridine made neutralization of the acidic parts in AO and suppressed the reaction. This result has supported the hypothesis that the catalytically active sites came from acidic. Since sulfur elemental on AO was detected by elemental analysis, sulfonic acid groups might be existing on the surface and serve the catalytic ability. To identify this assumption, benzenesulfonic acid (pH is 2.3 at 1.0 mg/mL in water), a truncated model for sulfonic acid groups on AO, was introduced to benzyl alcohol under optimized etherification conditions. As a result, the product was formed, not the benzyl ether, but a polymeric material, and it revealed that sulfonic acids did not affect the catalytic activity. Another control experiment performed with mellitic acid, called 'graphitic acid' (pH 2.4 at 1.0 mg mL^{-1} in water) due to a relatively large C/O ratio (1:1), also did not afford benzyl ether as a product. In accord with atomic absorption spectrometry (AAS) and inductively coupled plasma optical emission spectrometry (ICP-OES) data, AO contained vanadium (ca. 50 ppm) and nickel (ca. 30-200 ppm). However, it was verified that the residue metals impurities on AO did not influence the catalytic activity by performing the etherification with asphaltene, which also contained vanadium and nickel in similar concentrations as AO.

Table 2.2 Condensation of benzyl alcohol under various conditions[a]

Catalyst	Catalyst Loading (wt%)	Temperature (℃)	Benzyl Ether[b] (%)	Benzaldehyde[b] (%)
AO	5	100	10	0
AO	5	120	41	0
AO	5	150	61	6
AO	10	100	17	0
AO	10	120	60	0
AO	10	150	82	9
AO	20	100	24	0
AO	20	120	68	0
AO	20	150	73	7
--	--	150	0	<10
Asphaltene	20	150	0	0
Mellitic acid	20	150	0	0
AO + Pyridine[c]	10	150	0	0
$PhSO_3H$	10	150	0	0

[a] Unless otherwise noted, all reactions were performed with benzyl alcohol using the indicated catalyst loading and temperature for 3 h (see Table A.2.1 for reaction time optimization). [b] Conversion of benzyl alcohol to benzyl ether or benzaldehyde was calculated by ^{1}H NMR spectroscopy against an external standard (18-crown-6). [c] 10 wt% AO and 0.1 mL of pyridine.

Table 2.3 A summary of various AO-catalyzed condensations used to prepare chalcones

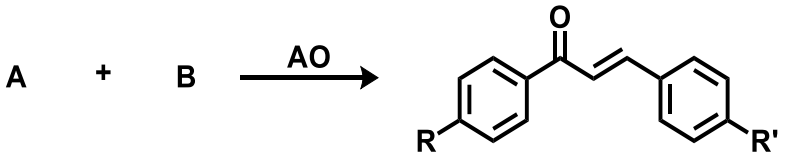

Entry	A	B	Yield[c] (%)
1[a]	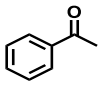	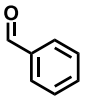	72
2[a]	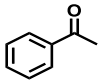	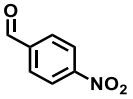	78
3[a]	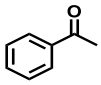	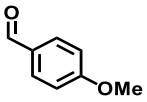	70
4[a]	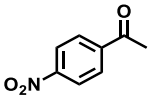		63
5[a]	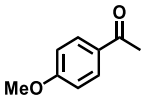	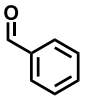	44
6[b]	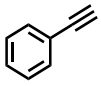		43
7[b]	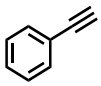	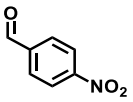	40
8[b]	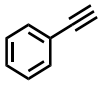	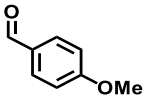	48

[a] Aldol condensations were performed neat condition in 1:1 stoichiometry (0.5 mmol each) of ketone : aldehyde using 50.0 mg of AO at 80 ℃ for 16 h. [b] Hydration-aldol condensations were performed neat condition in 1:1 stoichiometry (0.5 mmol each) of alkyne : aldehyde using 50.0 mg of AO at 100 ℃ for 16 h. [c] All products were purified using column chromatography.

When the etherification reaction with benzyl alcohol was finished, the catalyst was collected by filtration and then re-used to assess AO's recyclability after the synthetic transformation. AO was quickly recovered in up to 95% yields because of its insolubility in organic solvents. Even though the

C/O ratio of the recovered AO lower than that, the measured for the original material (14:1 vs. 7:1, respectively; see Table C.2.4), FT-IR signals corresponding to hydroxyl and carbonyl stretching frequencies were maintained (see Figure B.2.3). The recovered catalyst was successfully utilized over multiple cycles for etherification with minimal loss in catalytic activity. (see Table A.2.3). In detail, benzyl alcohol was converted to benzyl ether in a yield of 80% after the first cycle and subjecting the catalyst to five (5) successive reactions was afforded the ether product with a 70% yield (conditions per cycle: 10 wt% catalyst loading, 150 ℃, and 3h).

Next, efforts were directed toward another type of acid-catalyzed condensation[75] using AO. Claisen-Schmidt type reactions are typical acid-catalyzed condensation and produce chalcones, which are invaluable material based on many pharmaceutical agents[87]. As summarized in Table 2.3, The expected chalcone derivatives were obtained by various benzaldehydes and acetophenones, containing electron-donating or -withdrawing functional groups in good yields (up to 78%; see Table 2.3, entries 1-5). Considering that the Claisen-Schmidt-type reaction mechanism involves dehydration, multiple transformations in tandem are possible with the catalytic ability of AO. To test this hypothesis, phenylacetylene was introduced in 200 wt% loading of AO at 100 ℃ for 24 h and successfully converted to acetophenone in a yield of 86% (see Table A.2.5). Based on these results, we hypothesized that terminal alkynes enable to couple with aldehydes. We also reasoned that the water formed upon condensation promoted the hydration of the terminal alkynes in situ, and the resulting ketones may be subjected to further condensation reactions. To check our hypothesis, phenylacetylene and various benzaldehydes derivatives with electron-donating or withdrawing groups were reacted in the presence of AO. As a result, the expected chalcone products were obtained from the substrates above through tandem-hydration-aldol condensation in isolated yields over the two steps (up to 48%; see Table 2.3, entries 6-8).

C-C bond formations chemistry has been interesting topics in the synthesis of a pharmaceutical agent, medicinal and fine chemicals, and historically evolved with the support of transition metal catalysts, such as those based on nickel, palladium, and copper[88]. However, acidic carbocatalyst, including GO, have also been considered for C-C cross-coupling reactions[72-74] with specific substrates because metal-based catalysts have several drawbacks. For instance, xanthene is inclined to oxidation in the ambient atmosphere, and the oxidized substrates are possible to transform a xanthenyl cation via GO-catalyzed dehydration. Consequently, xanthenyl cation is prone to nucleophilic attack[89]. Considering that the C-C cross-coupling reaction mechanism, AO was also proved a significant catalyst for coupling xanthene to veratrole. As summarized in Table 2.4, xanthene and veratrole, introducing AO and co-catalyst (tosylic acid monohydrate; $TsOH \cdot H_2O$) were performed C-C cross-coupling

reaction, and the resulting product (9-(3,4-dimethoxyphenyl)-9H-xanthene) was obtained to competitive yield with these reported for GO under same conditions. Furthermore, a tolerable yield of the coupled products was also acquired without added co-catalysts.

Table 2.4 Summary of C–C cross-coupling reactions[a]

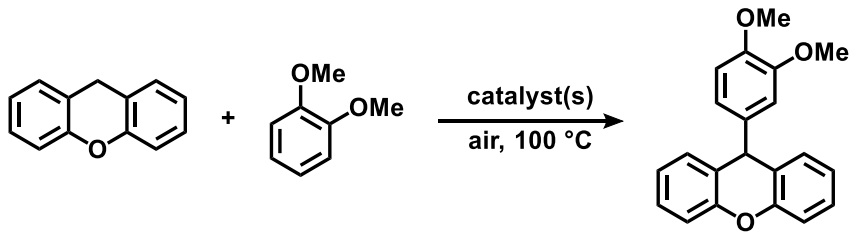

Entry	$TsOH \cdot H_2O$ ($\times 10^{-2}$ mmol)	Catalyst	Reaction Time (h)	Yield[b] (%)
1	1.0	AO	24	63
2	1.0	GO	24	66
3	1.0	AO	30	76
4[c]	-	AO	24	40
5[c]	-	GO	24	45
6[c]	-	Asphaltene	24	0

[a] Unless otherwise noted, all reactions were performed with xanthene (0.5 mmol), veratrole (1.0 mmol), 20.0 mg of catalyst, and $TsOH \cdot H_2O$ (1.0×10^{-2} mmol) as a co-catalyst at 100 ℃ for 24 h. [b] Isolated yields after purification using column chromatography. [c] Reaction was performed without a co-catalyst.

To discover the origins of catalytic activity for AO[90], we considered the effects of catalyst loading, particle size, and elemental composition compared to the results obtained from analogous experiments using GO[81]. The cross-coupling chemistry describes above is appropriate as the basis for the analysis because AO and GO functioned similarly. As we mentioned above in table 2.4 (entries 1-2 and 4-5), catalyst loading was not a key determinant of reaction performance. Next, the particle sizes

of AO and GO were measured to be 40 nm and 1400 nm, respectively, using dynamic light scattering (DLS). Even though the particle size of AO was 35 times smaller than GO, similar yields of the same cross-coupled products were obtained using identical quantities of AO or GO (63% vs. 66%, respectively)[72]. Based on these results, we determined that the particle size did not also affect the catalytic activity. However, the elemental composition was shown an optimistic correlation with the catalytic activity. Even though the C/O ratios of AO and GO were measured to be 6.7 and 1.5 using elemental analysis, respectively, the former observed a higher yield of product (63% vs. 27%) when the catalysts, normalized to their respective oxygen contents, were performed the cross-coupling reactions (see Table A.2.6). A similar tendency was shown when the reactions were performed in the absence of a co-catalyst (16% vs. 40%). To sum up these experiments, we concluded that the performances shown by these catalysts were not defined only by their absolute oxygen content but also contributed to the relatively high C/O ratio of the improved activity shown by AO.

Although GO has been a direct and effective strategy, the substitution for metal-based catalyst, its utility still has limitations under harsh reaction conditions. For instance, it is generally known that GO goes through a rapid reduction process when elevated temperatures and microwave irradiation[91, 92] exposed to the material, and it has been reported GO is possible to explode under a closed reaction system[93]. This phenomenon is why gaseous byproducts, including CO_2, CO, and H_2O, were provoked an explosion during reduction. Indeed, notwithstanding the commercialization of microwave-assisted chemistry[94], the development of carbocatalysts utilization has been prevented by safety issues. Since AO is a truncated GO model with lower oxygen contents and a smaller particle size[62], we supposed that AO might be more suitable and safer for a microwave reactor. To clarify the supposition, GO and AO was subjected to microwave at 150 ℃ for 15 min. As a result, GO exploded in the microwave vessel, but AO did not affect under irradiation (see Figure 2.4).

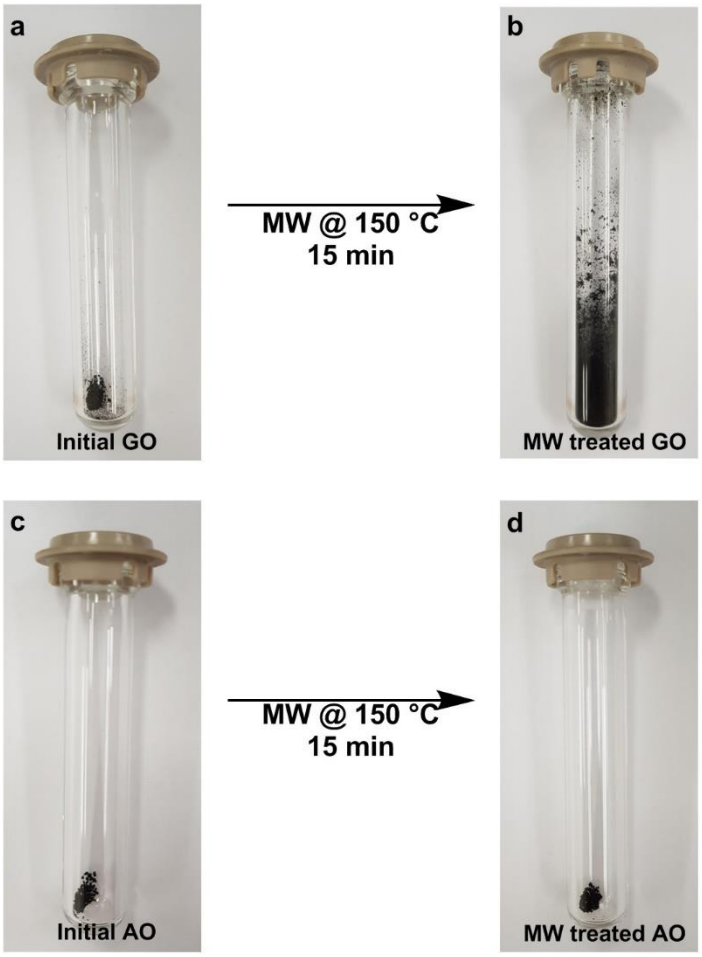

Figure 2.4 Photographs of GO taken (a) before and (b) after being subjected to microwaves at 150 ℃ for 15 min. Photographs of AO taken (c) before and (d) after being subjected to microwaves at 150 ℃ for 15 min.

When benzyl alcohol was radiated under AO as a catalyst in a microwave, the conversion of benzyl alcohol to benzyl ether increases and reaction time was reduced compared to an analogous thermal reaction. In detail, benzyl alcohol was converted to benzyl ether in yields of up to 90% within 15 min in a microwave (see Table A.2.7); for comparison, 3 hours reaction time was required under thermal conditions. Furthermore, microwave irradiation is also possible to expansion of the scope of etherifications such as electron-deficient substrates. For instance, 4- methoxy benzyl alcohol, which was not converted to the expected ether under an analogous thermal reaction, successfully afforded the products in high yields (80%) under microwave conditions (see Table A.2.8). However, the oxygen weight percentage of AO also decreased after used in a microwave reaction (c.f., 13.1% in the starting material to 9.3% in the recovered catalyst), and it means that the catalyst also undergoes reduction upon

microwave irradiation[95]. Regardless, the recovered AO was successfully and repeatedly promoted microwave-assisted etherification over multiple cycles (see Table A.2.9) to retain catalyst activity. For comparison, benzyl alcohol introduced GO under similar conditions was converted to benzyl ether and benzaldehyde in 53% and 6%. Also, GO went through extensive reduction on the surface (oxygen contents decrease from 42.5 to 9.3 wt%), and the explosion of the mixture was observed.

To additional examine the potential of carbocatalysis in a microwave, the Fischer indole synthesis, the condensation of a substituted phenylhydrazine and a carbonyl compound under acidic conditions, was selected[96]. The expected products, called for indole, have been employed in biologically-active heterocycles. As shown in Figure 2.5, AO successfully facilitated phenylhydrazine and cyclohexanone condensation to afford the corresponding annulated indole in a 44% isolated yield after 1 h at 100 ℃ under microwave conditions. For comparison, it takes 18 hours of reaction time to achieve the same product yield in a general thermal reactor at the same temperature. The reaction temperature was elevated up to 150 ℃ to improve performance, and a 62% yield was achieved in consequence.

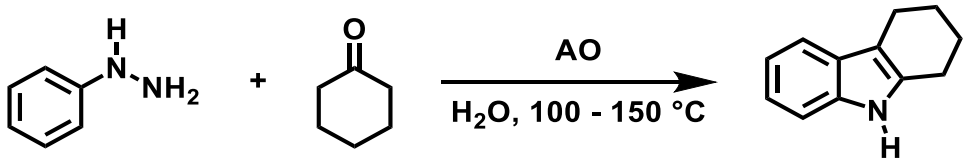

Figure 2.5 A Fischer indole synthesis using AO. Relatively high yields were obtained when the reaction was performed in a microwave reactor.

2.3 Conclusions

In summary, the oxidized form of asphaltene, which is an inexpensive petroleum byproduct, was defined and successfully utilized in various synthesis chemistry. Indeed, AO functions preferentially as an acid catalyst. As such, AO was demonstrated an effective carbocatalyst for condensations, cross-couplings, polymerizations, and other useful synthetic transformations. For comparison, other carbocatalysts, including GO, often facilitates an unsuspected reaction pathway and thus affords a mixture of products through competing mechanisms (i.e., oxidation vs. dehydration). Moreover, AO was successfully used for microwave-assisted reaction, the first example of its kind for a carbocatalyst, and AO significantly promoted numerous reactions under such conditions. The results described herein (i) substantiate asphaltene oxide and potentially other truncated forms of oxidized

carbons as effective catalysts for promoting synthetic transformations and (ii) demonstrate that the unique structure and composition of AO overcome of limitations that other oxidized carbons have.

2.4 Experimental Section

Chemicals and Materials

All reagents were purchased from Sigma Aldrich Inc., Alfa-Aesar, Tokyo Chemical Inc., or Acros Organics and used as received. Asphaltene (blown asphalt 5-10) was kindly supplied by Korea Petroleum. All solvents were supplied by Daejung Chemical unless otherwise noted.

Unless otherwise noted, all experiments were performed under ambient conditions. All microwave reactions were conducted using an Anton Paar GmbH-Monowave 300 microwave reactor.

Separation of asphaltene

Asphaltene (10.0 g) was dissolved with *n*-heptane (2.0 L) and then sonicated to help to disperse well. The mixture was filtered through a 0.22 μm nylon membrane and washed with *n*-heptane three times. The filtered asphaltene particles were collected, dried under vacuum at 80 ℃ for 1 day, and then used without additional purification.

Preparation of asphaltene oxide

Asphaltene (4.0 g), concentrated sulfuric acid (0.1 L), and a stir bar were added in a 500 mL jacked reaction flask, which was cooled to 0 ℃ using a chiller. $KMnO_4$ (8.0 g) as an oxidant was subsequently slowly added to the flask over 2 h with stirring. The mixture was reacted at 0 ℃ for 15 min and then at 35 ℃ for an additional 3 h. After the reaction, the flask was cooled to 10 ℃, and deionized water (0.8 L) was added extremely slowly to the mixture (CAUTION: this step was found to be exothermic!). The mixture was transferred to a beaker, and then a 35% aqueous solution of H_2O_2 (12.0 mL) was added to the mixture. The resulting black particles were filtered through a 0.22 mm nylon membrane and washed with 1 M HCl (0.8 L) to remove the residue metal impurities. The particles were washed with deionized water until the pH of the filtrate became 6~7. The resulting solids were collected and dried under reduced pressure at 50 ℃ for 1 day. The final product (3.8 g) was obtained as a black powder.

Identification and quantification of carboxylic acid on AO and GO[83]

A 100 mL Schlenk flask was charged with 50.0 mg of AO or GO, 10.0 mL of CH_2Cl_2, and a stir bar under an N_2 atmosphere. The mixture was sonicated in a bath sonicator. After 30 min, 3-cyanobenzyl alcohol (200.0 mg, 1.5 mmol) and 4-(dimethylamino)pyridine (DMAP; 10.0 mg, 0.1 mmol) were added to the flask, and the resulting mixture was cooled to 0 ℃ in an ice bath. A separate flask was purged with nitrogen and then charged with N,N'-dicyclohexylcarbodiimide (DCC; 155.0 mg, 0.8 mmol), and 5.0 mL of CH_2Cl_2 under a positive flow of N_2. The DCC solution was injected dropwise into a flask containing AO or GO at 0 ℃. The combined mixture was reacted at 25 ℃ for 24 h. After the reaction, the resulting particles were filtered through a 0.22 mm nylon membrane and washed with CH_2Cl_2, deionized water, and acetone. The filtered solids were collected and then dried under reduced pressure for 1 day. The final products, which were termed 'modified AO-1' (mAO-1) or 'modified GO-1' (mGO-1), respectively, was obtained as a black powder. To confirm the product, it was taken using FT-IR as well as elemental analysis. A new nitrile stretching frequency at 2225 cm^{-1} was observed in the FT-IR spectrum recorded for the product, and the carbonyl signal measured in the AO starting material (1700 cm^{-1}) shifted to 1650 cm^{-1}.

Identification and quantification of hydroxyl groups on AO and GO

50.0 mg of AO or GO, 10.0 mL of CH_2Cl_2, and a stir bar were added to a 100 mL round bottom flask. The mixture was sonicated in a bath sonicator. After 30 min, sodium acetate (123.0 mg, 1.5 mmol) and 3-cyanophenyl isocyanate (216.2 mg, 1.5 mmol) were subsequently added, and the resulting mixture was reacted at 25 ℃ for 24 h. After the reaction, the resulting particles were filtered through a 0.22 mm nylon membrane and washed with CH_2Cl_2, deionized water, and acetone. The filtered solids were collected and then dried under reduced pressure for 1 day. The final products, which were termed 'modified AO-2' (mAO-2) or 'modified GO-2' (mGO-2), respectively, was obtained as a black powder. To confirm the product, it was taken using FT-IR as well as elemental analysis. The FT-IR spectrum, which is recorded for the product, appeared an attenuated hydroxyl stretching frequency (3400 cm^{-1}) as well as strong absorptions that were assigned to the nitrile (2225 cm^{-1}), amido (3070 cm^{-1}), and carbamyl (1550 cm-1) groups turned out the expected condensation product.

Identification and quantification of epoxide groups on AO and GO[84]

A 100 mL Schlenk flask was purged with nitrogen and then charged with 40.0 mg of AO or GO, 10.0 mL of THF, and a stir bar. The suspension was sonicated for 30 min in a bath sonicator.

Sodium hydride (82.0 mg, 3.4 mmol), malononitrile (220.0 mg, 3.3 mmol), and 30.0 mL of THF were added to a separate 50 mL flask under an atmosphere of N_2. The malononitrile solution was stirred for 10 min in an ice bath. After cooling both mixtures on an ice bath, the malononitrile solution was added dropwise to the AO suspension at 0 ℃. After injection, the mixture was then submerged in an oil bath (60 ℃) and stirred for 24 h. After the reaction, the resulting particles were filtered through a 0.22 mm nylon membrane and washed with CH_2Cl_2, deionized water, and acetone. The filtered solids were collected and then dried under reduced pressure for 1 day. The final product, which was termed 'modified AO-3' (mAO-3) or 'modified GO-3' (mGO-3), respectively, was obtained as a black powder and characterized using FT-IR spectroscopy and elemental analysis. The FT-IR spectrum recorded for the product revealed a signal assigned to a nitrile group (2180 cm^{-1}). Besides, the intensity of the signal assigned to the hydroxyl stretching frequency (3400 cm^{-1}) increased while the signal assigned to the epoxide groups (1230 cm^{-1}) disappeared when compared to the spectrum recorded for the AO starting material.

General etherification procedure

A Teflon-capped 8.0 mL vial was charged with 100.0 mg of benzyl alcohol, 5-20 wt% of AO, and a stir bar. The vial was sealed under an ambient atmosphere with Teflon tape. The vial was then heated to a predetermined temperature (100-150 ℃) for 3-12 h. To monitor the extent of the etherification reaction, aliquots were periodically removed and analyzed by NMR spectroscopy (18-crown-6 was used for the external standard). The conversion was determined by integrating protons assigned to the external standard (δ 3.69 ppm; s, 24H) versus the benzylic protons of benzyl alcohol (δ 4.70 ppm; s, 2H) and benzyl ether (δ 4.57 ppm; s, 4H). The product was not isolated.

General dehydrative polymerization procedure

A Teflon-capped 8.0 mL vial was charged with 500.0 mg of benzyl alcohol, 50.0 mg of AO (10 wt%), and a stir bar. The vial was sealed under an ambient atmosphere with Teflon tape. The vial was submerged in an oil bath (200 ℃) and stirred for 24 h. After cooling to ambient temperature, the resulting product was filtered to remove the catalyst using CH_2Cl_2. The filtrate was concentrated and added dropwise into excess methanol. The precipitate was collected and dried under reduced pressure overnight (66% yield). Spectroscopic data were in accord with literature reports.[51]

General aldol condensation procedure

0.5 mmol of acetophenone, 0.5 mmol of aldehyde, and 50.0 mg of AO were added in a Teflon-lined 8 mL vial. The vial was sealed under an ambient atmosphere with Teflon tape. The vial was submerged in an oil bath (80 ℃) and stirred for 16 h. The resulting mixture was cooled to room temperature and then filtered to remove the catalyst using CH_2Cl_2 as the filtrate. The subsequent collection of the filtrate followed by evaporation of CH_2Cl_2 afforded the crude product, which was further purified using column chromatography (ethyl acetate : *n*-hexane, 1:9 v/v as eluent). Spectroscopic data were in accord with literature values.[97]

General hydration-aldol condensation procedure

A Teflon-capped 8.0 mL vial was charged with phenylacetylene (51.1 mg, 0.5 mmol), 0.5 mmol of aldehydes, 50.0 mg of AO, and a stir bar. The vial was sealed under an ambient atmosphere with Teflon tape. The vial was submerged in an oil bath (100 ℃) and stirred for 16 h. After cooling to ambient temperature, the resulting mixture was filtered to remove the catalyst with the aid of CH_2Cl_2. The residual solvent of the filtrate was evaporated under reduced pressure, and the crude product was purified using column chromatography (silica gel, ethyl acetate : *n*-hexane, 1:9 v/v as eluent). Spectroscopic data were in accord with literature values.[97]

General C–C cross-coupling procedure

Xanthene (91.1 mg, 0.5 mmol), veratrole (138.2 mg, 1.0 mmol), $TsOH{\cdot}H_2O$ (19.0 mg, 1.0×10^{-2} mmol), and AO (20.0 mg) were added to a Teflon-capped 8.0 mL vial with a stir bar. The vial was heated to 100 ℃ for 24 h while being left open to the air. The resulting mixture was cooled to ambient temperature and then filtered to remove the catalyst using CH_2Cl_2. The filtrate was collected, the CH_2Cl_2 was evaporated, and the crude mixture was purified using column chromatography (silica gel, ethyl acetate : *n*-hexane, 1:9 v/v as eluent) to afford the desired product in 63% yield. Spectroscopic and analytical data were in accord with literature values. ^{1}H NMR (400 MHz, $CDCl_3$): δ 7.23-7.19 (t, 2H), δ 7.13-7.11 (d, 2H), δ 7.06-7.00 (d, 2H), δ 6.98-6.96 (t, 2H), δ 6.79-6.78 (d, 2H), δ 6.65 (s, 1H), δ 5.19 (s, 1H), δ 3.84 (s, 3H), δ 3.75 (s, 3H). LR-MS (APCI): Calcd. For $C_{21}H_{18}O_3$ $[M\text{-}H]^+$: 317.12; Found: 317.33.

Microwave-promoted etherification procedure

A Teflon-capped 10.0 mL microwave vial was charged with 100.0 mg of benzyl alcohol, 10 wt% of AO, and a stir bar. The vial was then microwaved at 150 ℃ for 5-30 min. To monitor the extent

of etherification, aliquots were periodically removed and analyzed by NMR spectroscopy against an external standard (18-crown-6). Conversions were determined by integrating protons attributed to the external standard (δ 3.69 ppm; s, 24H) versus the benzylic protons of benzyl alcohol (δ 4.70 ppm; s, 2H) and benzyl ether (δ 4.57 ppm; s, 4H).

Microwave-promoted Fischer indole synthesis procedure

Phenylhydrazine (129.8 mg, 1.2 mmol), cyclohexanone (98.2 mg, 1.0 mmol), AO (100.0 mg), and water (2.0 mL) were added to a Teflon-capped 10.0 mL microwave vial with a stir bar. The vial was then microwaved at 150 ℃ for 1 h. The resulting mixture was cooled to ambient temperature and then filtered to remove the catalyst. After the filtrate was extracted with water and CH_2Cl_2, the organic phase was dried over $MgSO_4$ and then purified using column chromatography (ethyl acetate : *n*-hexane, 1:9 v/v as eluent) to afford the desired product in 62% yield. Spectroscopic and analytical data were in accord with literature values.[98] ^{1}H NMR (400 MHz, $CDCl_3$): δ 7.64 (s, 1H), δ 7.46-7.44 (d, 1H), δ 7.29-7.27 (d, 1H), δ 7.14-7.07 (m, 2H), δ 2.74-2.70 (m, 4H), δ 1.91-1.87 (m, 4H).

Physical Characterization

All Nuclear magnetic resonance (NMR) spectra were recorded on a Bruker Ascend 400 MHz spectrometer at ambient temperature (22.0(±1.0) ℃, unless otherwise noted). Chemical shifts are reported in parts per million (δ). All NMR spectra were recorded in $CDCl_3$, and the residual solvent was referenced to 7.26 ppm. The following abbreviations used for the description of the spectra are s, singlet; d, doublet; t, triplet; q, quartet; m, multiplet; br, broad.

Fourier-transform infrared spectroscopy (FT-IR) were recorded using KBr pellets on a Perkin-Elmer Frontier MIR spectrometer

Elemental analyses were performed using a Thermo Scientific Flash 2000 Organic Elemental Analyzer calibrated with 2,5-bis(5-*tert*-butyl-benzoxazol-2-yl)thiophene (BBOT).

X-ray photoelectron spectroscopy (XPS) data were recorded over a spot size of 500 μm using an Escalab 250Xi (Thermo Fischer Scientific, Waltham, MA, USA) equipped with a monochromated aluminum Kα source (1486.6 eV). All measurements were recorded at an angle normal to the surface using charge compensation via a combined ion/flood fun operating at a current of 50 μA and as ion

voltage of 2 V. Survey spectra were taken at pass energy of 100 eV (10 scans). Calibration of the spectra was conducted by initially recording the gold $4f_{7/2}$ spectrum of a gold foil. The peak position of the gold $4f_{7/2}$ spectrum was then shifted value was applied to all subsequent spectra.

Polystyrene equivalent molecular weights and polydispersity index (*Đ*) values were measured by gel permeation chromatography (GPC) using a Malvern GPCmax Solvent/Sample module. All samples were analyzed using tetrahydrofuran as the eluent at a flow rate of 0.8 mL/min. Detection was performed using a Viscotek VE3580 RI Detector.

Mass spectrometry (MS) data were recorded on a Thermo LCQ Fleet Quadrupole Ion Trap Mass Spectrometer in Atmospheric Pressure Chemical Ionization (APCI) mode (electrospray voltage was 3.5 kV).

Atomic absorption spectroscopy (AAS) measurements were recorded on an Analytik Jena contraAA 800 D.

Inductively coupled plasma optical emission spectroscopy (ICP-OES) measurements were recorded on a Varian 700-ES.

2.5 Acknowledgments

Portions of this chapter were recreated by referring to the reported literature[99] with permission from Hyosic Jung and Christopher W. Bielawski; Asphaltene oxide promotes a broad range of synthetic transformation, *Communications Chemistry*, **2019**, *2*, 113.

The overall design of catalyst and synthesis studies were performed with kind support with Professor Christopher W. Bielawski. Special thanks to Dr. Stanfield. Y. Lee for his assistance with XPS measurement, Mr. Geon-Hui Park for his assistance with MS data, and Dr. Songsu Kang for his assistance with GPC measurements.

Chapter 3: Promoting Variety Synthetic Transformations using Soluble Asphaltene Oxide as Homogeneous Carbocatalyst

3.1 Introduction

As we described previous chapter 2, since transition metal-based catalysts have been pointed out practical drawbacks such as finite resources, increasing costs, and high toxicity, other alternatives have been designed and widely studied to synthesize organic and inorganic compounds. Among these, carbocatalysts have been in the limelight for utilization in diverse synthetic transformations[70, 80, 100]. For example, since the selective oxidation of benzyl alcohol was first introduced under graphene oxide (GO) as a catalyst, GO has been utilized in lots of synthetic chemistry[39], including aldol coupling reactions[75], the oxidation of thiols and sulfides[101], C-H activations/coupling reactions[72-74, 102], aza-Michael additions[103], and others[76]. Moreover, GO was found to promote the polymerization of different monomers through dehydration[51] or cationic mechanisms[52]. Recently, our group successfully synthesized a new class of carbocatalyst from asphaltene precursor, and this asphaltene oxide (AO)[99], synthesized by modified Hummers' method, was shown to afford practical catalytic activities under diverse conditions. Indeed, etherifications, condensations, C-C cross-couplings, and hetero-cyclizations were successfully accelerated by AO as an acid catalyst. Furthermore, AO was demonstrated to facilitate microwave chemistry, where former oxidized carbons were inaccessible[93].

Despite these substantiations of utilizations, GO and AO are accompanied by fundamental and practical limitations. Oxidized carbons, including AO and GO, was generally known to perform a heterogeneous catalyst system[104]. Even though heterogeneity has an advantage of purifications, the catalytically-active sites may undergo deactivations due to its heterogeneous nature, and, as such, catalyst capability may be inherently limited. Highly oxidized GO[105, 106] has been reported to increase performance and material quality to overcome these limitations, but wholly soluble derivatives have remained undiscovered.

We assumed that asphaltene might be converted to homogeneous carbocatalyst by improving the oxidation degree based on these results. An early report inspired our speculation that exposing asphaltene to 70% nitric acid at a high temperature would help remove it from crude oil due to enhanced solubility[67]. Although this procedure was used for oil refinery applications, we hypothesized that the

soluble products function as homogeneous carbocatalysts. Furthermore, the improved solubility was expected to promote catalytic function and provide higher activity than heterogeneous counterparts. This chapter described the synthesis and characterization of soluble asphaltene oxide (sAO) and explained the effectiveness of these substances in promoting synthetic conversion, including relatively complex compounds such as multicomponent reactions and cationic polymerization.

3.2 Result and Discussion

Asphaltene was first washed with n-heptane to get rid of residual oil contaminants, and a modified version of the previously reported oxidation method was applied[67]. Asphaltene was heated to reflux in 60% nitric acid for 24 hours at 120 ℃. After then, the solution was diluted acid concentration with deionized water. The diluted solution was filtered to eliminate insoluble fine particles, and the collecting filtrate was concentrated by heating to 100 ℃ under reduced pressure. The remaining particles were dried under reduced pressure in a vacuum oven at 50 ℃ for 48 h. As shown in Figure 3.1, the products obtained from this procedure were a brown powder and found to be a soluble in methanol (up to 200 mg/mL), ethanol (140 mg/mL), THF (200 mg/mL), DMSO (80 mg/mL), DMF (80 mg/mL) acetone (200 mg/mL), and water (100 mg/mL). Compared to asphaltene oxide (AO) synthesized by using a modified Hummers' method (condition: $KMnO_4$, H_2SO_4, and H_2O_2), sAO has a relatively high oxygen content (13.1 wt%, C/O ratio ~ 6.67 vs. 42.0 wt%, C/O ratio ~ 1.23, respectively; see Table 3.1). FT-IR spectra recorded for materials were similar to those recorded for AO (see Figure 3.2) with strong and wide hydroxyl signals (ν_{O-H} = 3500-2800 cm^{-1}) and strong carbonyl signals ($\nu_{C=O}$ = 1720 cm^{-1}) and epoxide signals (ν_{C-O} = 1240 cm^{-1} and 1050 cm^{-1}). The pH of sAO solution in water (1.0 mg/mL) was measured at 2.7, and, for comparison, the pH of an AO suspension was measured at 3.5 under similar conditions.

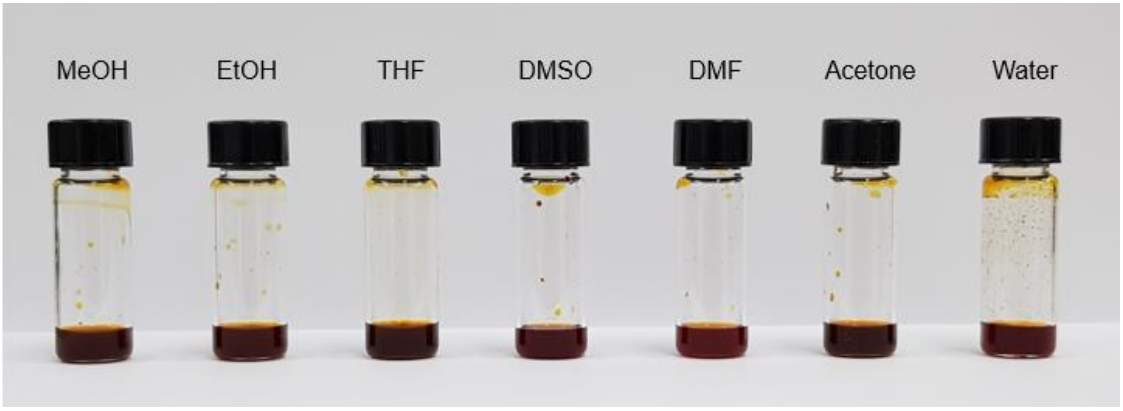

Figure 3.1 photograph of sAO dissolved in various solvents. The concentrations of sAO are as follows: methanol, 200 mg/mL; ethanol, 140 mg/mL; THF, 200 mg/mL; DMSO, 80 mg/mL; DMF, 80 mg/mL; acetone, 200 mg/mL; and water, 100 mg/mL.

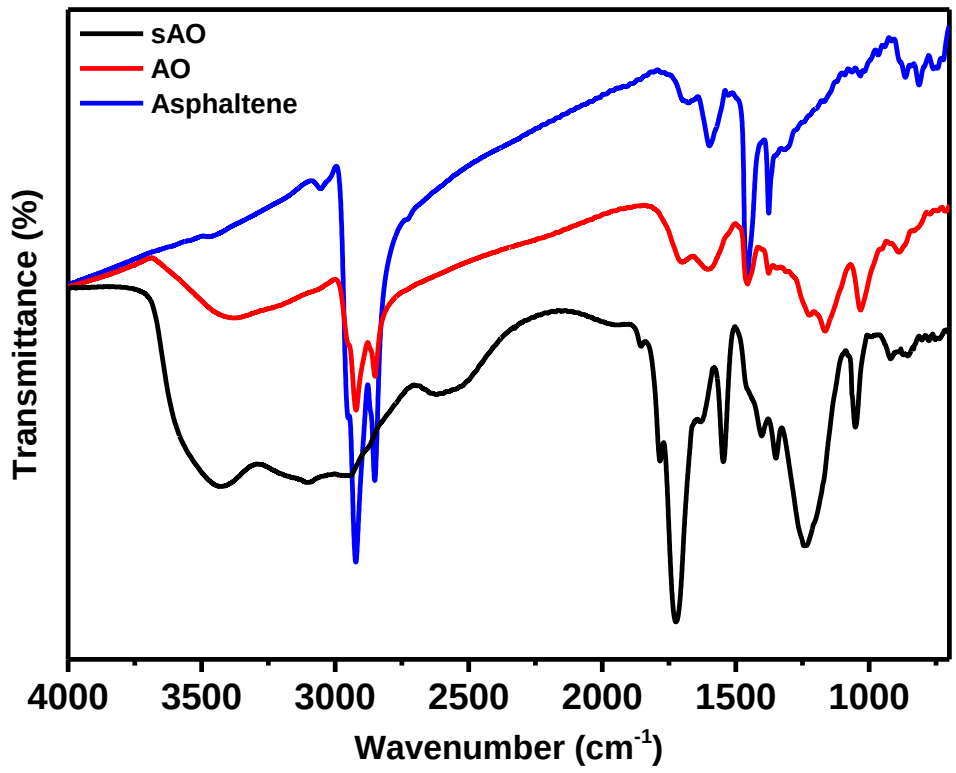

Figure 3.2 FT-IR spectra recorded for asphaltene (blue line), asphaltene oxide (red line), and sAO (black line).

Table 3.1 Elemental analysis data recorded for asphaltene, AO and sAO

	Carbon (wt %)	Hydrogen (wt %)	Nitrogen (wt %)	Sulfur (wt %)	Oxygen (wt %)	Empirical Formula
Asphaltene	81.0	7.9	0.7	6.6	1.4	$C_1H_{1.17}S_{0.03}O_{0.01}$
AO	64.5	6.6	0.6	11.1	13.1	$C_1H_{1.23}S_{0.06}O_{0.15}$
sAO	38.7	4.3	3.3	6.1	42.0	$C_1H_{1.33}N_{0.07}S_{0.06}O_{0.81}$

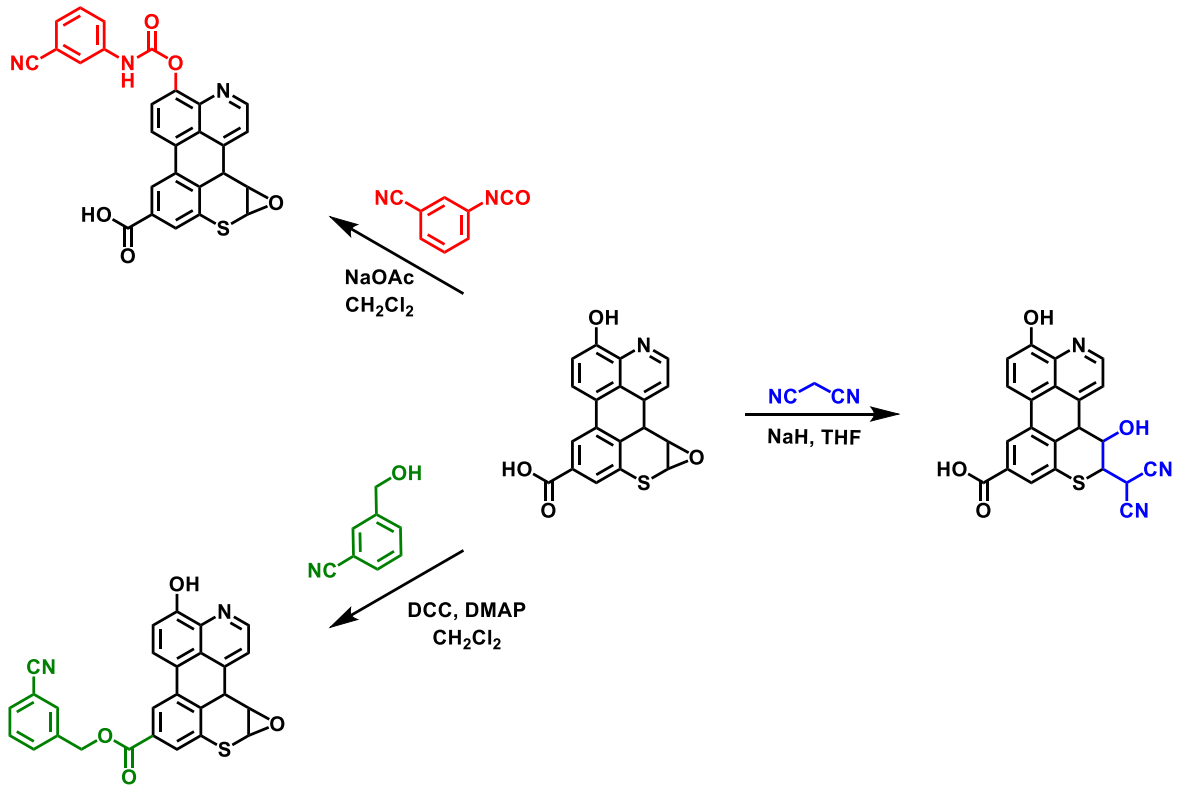

Figure 3.3 Chemical tests that were used to quantify the functional groups displayed on sAO. The starting material shown in the center represents a truncated form sAO and features pendant carboxylic acid, hydroxy, and epoxide groups. By using the reagents shown, the carboxylic acid groups were converted to esters, the hydroxyl groups were converted to carbamates, and epoxide groups were ring-opened. In all cases, the corresponding products feature nitrile groups (CN) that could be quantified using IR spectroscopy and elemental analysis.

As summarized in figure 3.3, a series of chemical tests were arranged to clarify the structure of sAO and quantify oxygen-containing functional groups decorated with materials. A reagent used for chemical tests was designed to react preferentially with carboxylic acid, hydroxyl, or epoxide group and contained nitrogen to facilitate characterization by FT-IR spectroscopy and elemental analysis (see Figure B.3.1 and Table C.3.1). In the treatment of sAO with 3-cyanobenzyl alcohol under Steglich esterification conditions[83], a remarkable nitrile signal ($\nu_{C\equiv N}$ = 2230 cm-1) appeared, and esters were provided as to be partially determined by changes in the bathochromic shift in the $\nu_{C=O}$ signal (from 1720 cm^{-1} to 1630 cm^{-1}). As 3-cyanophenyl isocyanate introduced to sAO, the strength of the signal assigned to the hydroxyl group decreased (ν_{O-H} = 3320 cm^{-1}) and strong signals assigned to nitrile ($\nu_{C\equiv N}$ = 2230cm^{-1}), amido (ν_{N-H} = 3090 cm^{-1}), and carbamyl ($\nu_{C=O}$ = 1590 cm^{-1}) were appeared. Finally, the methodology previously reported to form a C-C bond by ring-opening of epoxide groups in GO[84], sAO was used to treat the bond as a malononitrile under basic conditions. A signal (ν_{C-O} = 1230 cm^{-1}) caused by an epoxide group disappeared in a starting substance, and a new nitrile group was formed at 2180 cm^{-1}. Elemental analysis of the reaction enables the quantification of each nitrogen content, and calculations resulted in a carboxylic acid (5.1 × 10^{-3} mol/g), hydroxyl (5.6 × 10^{-3} mol/g), and epoxide (7.5 × 10^{-3} mol/g). It had been measured that the concentrations of these groups were significantly higher than those measured for AO and GO (see Table C.3.2), which could streamline the relatively high solubility and catalytic activity (vide infra) indicated by sAO.

Further characterization of the material was facilitated because of the relatively high solubility of sAO. The ^{1}H NMR spectrum recorded for the material showed wide signals at δ 8.62–7.41 ppm and δ 2.31-1.00 ppm allocated to the aromatic and alkyl chain protons, respectively (see Figure E.3.1). In the same way, ^{13}C NMR signals were assigned to carbonyl carbons (δ 179.0-176.9 ppm), the aromatic (δ 134.4-129.0 ppm), and the alkyl chain (δ 40.4-16.1 ppm) was also recorded (see Figure E.3.2). As a result of matrix assistance laser desorption/ionization time of flight (MALDI-TOF) mass spectrometry, the molecular weight of sAO was in the range of 500-600 Da (see Figure D.3.1). By estimation, since the oxygen content was relatively high, the substance was revealed to aggregation in the solid-state and formed particles with an average size of ca. 10 nm as determined by AFM (see Figure D.3.2).

Table 3.2 A summary of esterifications that were promoted with sAO[a]

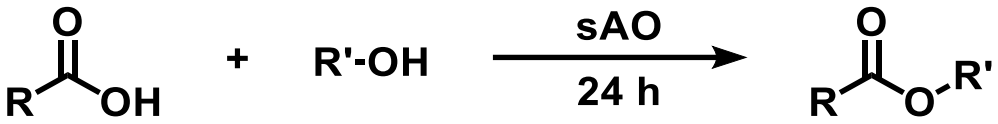

Entry	Carboxylic Acid	Alcohol	Temp. (°C)	Conversion[b] (%)
1	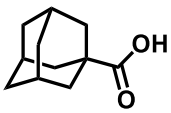	MeOH	50	> 99
2	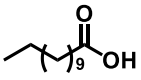	MeOH	50	> 99
3	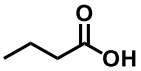	MeOH	50	> 99
4	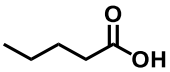	MeOH	50	> 99
5	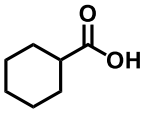	MeOH	50	> 99
6	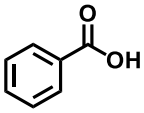	MeOH	50	> 99
7	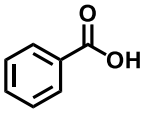	EtOH	70	91
8	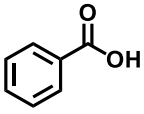	*n*-BuOH	70	96
9	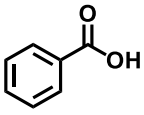	IPA	85	85

[a] Unless otherwise noted, all reactions were performed using 1.0 mmol of carboxylic acid, 1.0 mL of alcohol, and 50 mg of catalyst. [b] Conversion after 24 h was calculated by gas chromatography against a standard (anisole). IPA = isopropyl alcohol.

Initial efforts to use sAO as a carbocatalyst began with esterification chemistry because sAO was acidic. Inorganic acids, such as hydrochloric acid, sulfuric acid, and phosphoric acid, were commonly used to promote such transformation, but these liquid reagents are toxic and volatiles[107]. By comparison, sAO is a relatively manageable solid powder. As summarized in Table 3.2, sAO successfully facilitated the condensation of various types of carboxylic acids and alcohols. Esterification containing carboxylic acid and methyl alcohol as a reagent and solvent quantitatively supplied the corresponding methyl esters, and other alcohols were converted to their respective ester in a yield of up to 96%. Furthermore, intramolecular esterification was explored. As shown in Figure 3.4, 6-hydroxycaproic acid (1.0 mmol) was successfully promoted the ring-closing intramolecular transformation using sAO and obtained a quantitative yield of ε-caprolactone (conditions: 50 mg of sAO and $[6\text{-hydroxycaproic acid}]_0 = 1.0$ M).

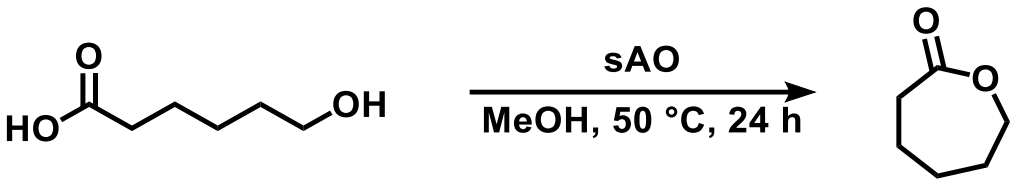

Figure 3.4 Intramolecular condensation of 6-hydroxycaproic acid as catalyzed by sAO.

Previously, we showed that asphaltene based carbocatalyst was superior to graphene analogous in that they could be used in microwave-assisted chemistry[99]. Based on these results, we focused on adapting sAO for microwave-assisted Fischer indole synthesis. Indole derivatives have been adopted for many biological and pharmaceutical applications, and the demand for these compounds continues to increase[96]. As shown in Table 3.3, sAO promotes the condensation of phenylhydrazine and cyclohexanone, and the expected indole product was obtained from an aqueous media. Similarly, other ketone substrates were also performed the expected indole synthesis, and the corresponding indoles were obtained when irradiated with microwave in the presence of sAO.

Table 3.3 A summary of microwave-assisted Fischer Indole syntheses[a]

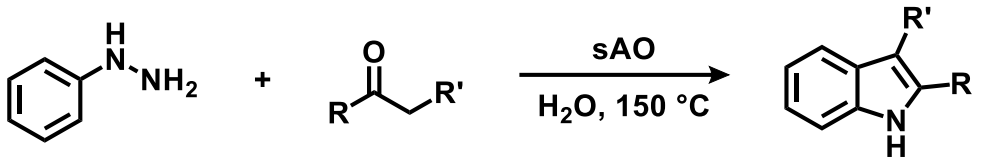

Entry	Ketone	Product	Catalyst (mg)	Time (min)	Yield[b] (%)
1	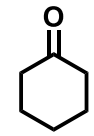	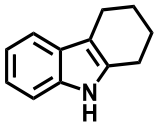	100	30	30
2	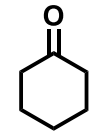	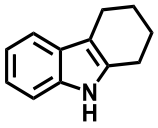	100	60	60
3	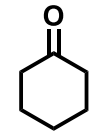	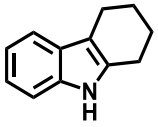	100	90	62
4	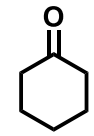	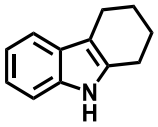	200	60	61
5	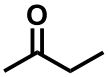	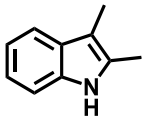	100	60	26
6	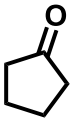	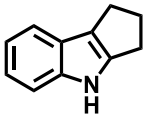	100	60	37
7	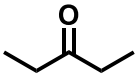	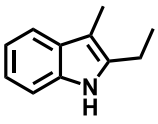	100	60	45

[a] Unless otherwise noted, all reactions were performed using 1.2 mmol of phenylhydrazine, 1.0 mmol of cyclohexanone, 2.0 mL of water as a solvent, and the indicated quantity of catalyst loading at 150 °C in a microwave reactor. [b] Isolated yield after purification using column chromatography.

The characteristic of many carbocatalyst was that they could be easily recycled in the synthesis. Since sAO enables soluble in water, separation of the catalyst from various product mixtures can be conveniently extracted. The aqueous solutions dissolved catalysts were collected after Fischer indole synthesis and successively reused without further purification to clarify the recyclability of sAO. In detail, initial reagents (phenylhydrazine and cyclohexanone) were added to an aqueous catalyst solution ($[sAO]_0$ = 50 mg/mL) and then reacted in a microwave reactor at 150 ℃ for 1 hour. After extracting the resulted indole products with dichloromethane, an aqueous phase containing the catalyst was collected and introduced into a new batch of reagents to be performed again. By using the methodology, the catalyst solution was successfully and repeatedly used over multiple cycles, and condensation was facilitated with minimal loss of catalytic activity. For example, 52% isolated yield of indole product was obtained using a catalytic solution with five consecutive cycles; for comparison, 59% yield was obtained following the first cycle (see Table A.3.1).

Considering that the catalyst activity displayed by sAO was relatively broad, we hypothesized that the material could also promote the multicomponent reaction (MCR). The Biginelli reactions, as a typical example of MCR, have been used to obtain dihydrophyrimidinone (DHPM) and other valuable heterocyclic products[108]. The DHPM derivatives are known as effective calcium channel blockers and have found extensive benefits for therapeutic and pharmacological applications[109]. As summarized in Table 3.4, the biginelli reaction was conducted with benzaldehyde, ethyl acetoacetate, and urea under a variety of catalytic loads (10-50 wt%), temperature (50-100 ℃), and reaction time (5-30 min), but the results were optimized when the reaction was performed in a microwave reactor at 100 ℃ for 5 min in yields of 75% (see Table 3.4, entry 5). For comparison, similar reactions performed in AO provided a 33% yield under other identical conditions. Other benzaldehydes, including electron-rich or electron-deficient functional groups, and urea/thiourea were also used to supply the expected products at good yields (see Table A.3.2).

Table 3.4 A summary of microwave-assisted Biginelli reactions[a]

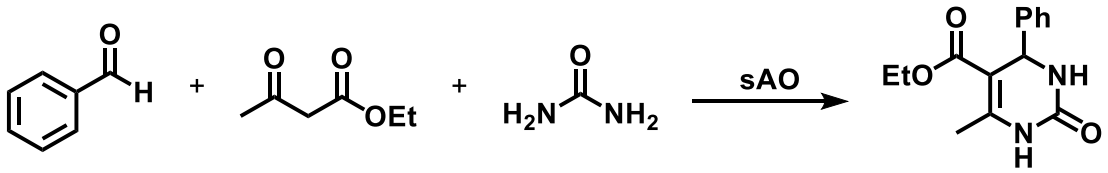

Entry	Cat. Loading (wt%)	Temp. (℃)	Time (min)	Yield[b] (%)
1	10	75	5	13
2	25	75	5	21
3	50	75	5	53
4	50	50	5	7
5	50	100	5	75
6	50	100	15	74
7	50	100	30	75

[a] Unless otherwise noted, all reactions were performed with benzaldehyde (1.0 mmol), ethyl acetoacetate (1.0 mmol), and urea (1.5 mmol) using the indicated catalyst loading. [b] Isolated yield after purification using column chromatography.

Finally, our efforts were directed toward the cationic polymerization to demonstrate the catalytic ability of sAO. Vinyl carbazole and vinyl ether were ideal monomers for such chemistry because nitrogen and oxygen heteroatoms effectively help stabilize the propagating carbocations. As summarized in Table 3.5, it has been revealed that the monomers polymerized when subjecting to sAO (1 wt%) in THF at -20 ℃. The resulted solution was filtered, and the reaction mixture was poured into methanol to promote precipitation, then filtered and isolated. A poly(*n*-butyl vinyl ether) was obtained in quantitative yield and characterized by a number average molecular weight (M_n) of 9.8 kDa and a polydispersity index ($Đ$) of 1.3 as determined by gel permeation chromatography (GPC). Similarly, the 9-vinyl carbazole was quantitatively converted into the corresponding polymer (M_n = 11.1 kDa). Although the poly(N-vinyl carbazole) was shown a $Đ$ value of 5.1, a broad PDI was often observed in

cationic polymerization due to the high reactivity of cation during the propagation step[110]. Additional optimization was achieved reduced distribution and reaction time while maintaining a yield (see Table A.3.3). For comparison, GO has also been used to promote the cationic polymerization[52], but sAO has provided the corresponding polymers in high yields, better control the PDI, and shorter periods.

Table 3.5 A summary of cationic polymerization that was performed with sAO[a]

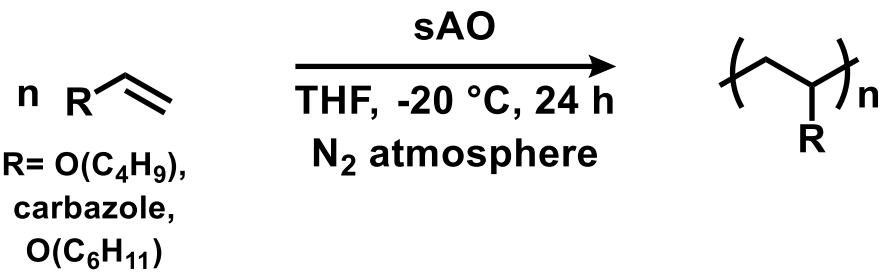

Entry	R	Conc. (mol/L)	Yield[b] (%)	M_n[c] (kDa)	$Đ$[c]
1	-O(C_4H_9)	3	99	9.8	1.3
2	-Cbz	1	99	11.1	5.1
3	-O(C_6H_{11})	3	52	4.5	2.0

[a] The reactions were performed by treating a solution of the monomer in THF with 1 wt% of sAO at -20 °C for 24 h under an atmosphere of N_2. [b] Isolated yield after collection of the precipitate formed upon pouring the reaction mixture into excess methanol. [c] The number-average molecular weight (M_n) and polydispersity index ($Đ$) values were determined by GPC and are reported as their polystyrene equivalents. Cbz = carbazole.

3.3 Conclusions

To sum up this chapter, a novel carbocatalyst was prepared by asphaltene, which was oxidized under harsh conditions. As far as we know, this is the first report on water-soluble carbocatalysts that promote a wide range of synthetic transformations. sAO effectively facilitated esterification, intramolecular and intermolecular condensation, Biginelli reaction, and cationic polymerization. Furthermore, it was successfully used in microwave reactors. Because sAO enables to dissolve in water,

it had been found that it was easy to separate via extraction and recycle. Besides, due to the ability to form the homogeneous phases, sAO exhibited higher catalytic activity than heterogeneous counterparts (e.g., GO or AO). From a broader perspective, asphaltene based catalysts are expected to expand the realization of metal-free catalysts to promote synthetic reactions under heterogeneous and homogeneous conditions, potentially leading to further improvements in catalytic activity and selectively.

3.4 Experimental Section

Chemicals and Materials

All reagents were purchased from Sigma Aldrich Inc., Alfa-Aesar, Tokyo Chemical Inc., or Acros Organics and used as received. Asphaltene (blown asphalt 5-10) was kindly supplied by Korea Petroleum. All solvents were supplied by Daejung Chemical unless otherwise noted.

Unless otherwise noted, all experiments were performed under ambient conditions. All microwave reactions were conducted using an Anton Paar GmbH-Monowave 300 microwave reactor.

The preparation of the asphaltene precursor was done following the procedures outline in Chapter 2.4.

Preparation of soluble asphaltene oxide (sAO)

A 500.0 mL flask was charged with asphaltene (4.0 g), nitric acid (0.1L), and a stir bar. The mixture was heated to reflux at 120 ℃ for 24 h (CAUTION: a brown toxic gas, presumably NO_2 gas, was generated during the reaction. It was quenched using the basic solution). Afterward, the mixture was slowly poured into deionized water (0.5 L). The resulting solution was filtered through a 0.22 μm nylon membrane to remove the unreacted asphaltene particles. The filtrate was collected and distilled under reduced pressure (100 torrs) at 100 ℃. After removing the residual water and nitric acid via distillation, the remaining solid products were collected and dried under vacuum for 2 days. The final product (2.1 g) was obtained as a brown powder.

Identification and quantification of the carboxylic acids on sAO[83]

A 100.0 mL Schlenk flask was charged with 50.0 mg of sAO, 10.0 mL of CH_2Cl_2, and a stir bar under an N_2 atmosphere. The mixture was sonicated in a bath sonicator. After 30 min, 3-cyanobenzyl alcohol (200.0 mg, 1.5 mmol) and 4-(dimethylamino)pyridine (DMAP; 10.0 mg, 0.1 mmol) were added to the flask, and the resulting mixture was cooled to 0 ℃ in an ice bath. A separate flask was purged with nitrogen and then charged with N,N'-dicyclohexylcarbodiimide (DCC; 155.0 mg, 0.8 mmol), and 5.0 mL of CH_2Cl_2 under a positive flow of N_2. The DCC solution was injected dropwise into the flask containing sAO at 0 ℃. The combined mixture was reacted at 25 ℃ for 24 h. After the reaction, the resulting particles were filtered through a 0.22 mm nylon membrane and washed with CH_2Cl_2, deionized water, and acetone. The filtered solids were collected and then dried under reduced pressure for 1 day. The final product was termed 'modified sAO-1' (m-sAO-1) and characterized using FT-IR and elemental analysis. A new nitrile stretching frequency at 2230 cm^{-1} was observed in the FT-IR spectrum recorded for the product, and the carbonyl signal measured in the AO starting material (1720 cm^{-1}) shifted to 1630 cm^{-1}.

Identification and quantification of the hydroxyl groups on sAO

50.0 mg of sAO, 10.0 mL of CH_2Cl_2, and a stir bar were added to a 100.0 mL round bottom flask. The mixture was sonicated in a bath sonicator. After 30 min, sodium acetate (123.0 mg, 1.5 mmol) and 3-cyanophenyl isocyanate (216.2 mg, 1.5 mmol) were subsequently added, and the resulting mixture was reacted at 25 ℃ for 24 h. After the reaction, the resulting particles were filtered through a 0.22 mm nylon membrane and washed with CH_2Cl_2, deionized water, and acetone. The filtered solids were collected and then dried under reduced pressure for 1 day. The final product, termed 'modified sAO-2' (m-sAO-2), was obtained as a black powder. To confirm the product, it was taken using FT-IR as well as elemental analysis. The FT-IR spectrum recorded for the product appeared an attenuated hydroxyl stretching frequency (3320 cm^{-1}) as well as strong absorptions that were assigned to the nitrile (2230 cm^{-1}) and carbamyl (1590 cm-1) groups from the expected condensation product.

Identification and quantification of the epoxide groups on sAO[84]

A 100.0 mL Schlenk flask was purged with nitrogen and then charged with 40.0 mg of sAO, 10.0 mL of THF, and a stir bar. The suspension was sonicated for 30 min in a bath sonicator. Sodium hydride (82.0 mg, 3.4 mmol), malononitrile (220.0 mg, 3.3 mmol), and 30.0 mL of THF were added to a separate 50.0 mL flask under an atmosphere of N_2. The malononitrile solution was stirred for 10 min

in an ice bath. After cooling both mixtures on an ice bath, the malononitrile solution was added dropwise to the sAO suspension at 0 ℃. After injection, the mixture was then submerged in an oil bath (60 ℃) and stirred for 24 h. After the reaction, the resulting particles were filtered through a 0.22 mm nylon membrane and washed with CH_2Cl_2, deionized water, and acetone. The filtered solids were collected and then dried under reduced pressure for 1 day. The final product was termed 'modified sAO-3' (m-sAO-3) and characterized using FT-IR spectroscopy and elemental analysis. The FT-IR spectrum recorded for the product revealed a signal assigned to a nitrile group (2180 cm^{-1}). Besides, when compared to the spectrum recorded for the sAO starting material, the intensity of the signal assigned to the epoxide groups (1230 cm^{-1}) relatively decreased upon inspection of the spectrum recorded for the product.

General esterification procedure

A Teflon-lined 8.0 mL vial was charged with 1.0 mmol of a carboxylic acid, 1.0 mL of alcohol to serve both as a reagent and solvent, sAO (50.0 mg), and a stir bar. The vial was capped under an ambient atmosphere with Teflon tape. The vial was heated to a predetermined temperature (50-85 ℃) for 24 h. After colling to ambient temperature, anisole (1.0 mmol), which was used as an external standard, was added to the resulting mixture. Aliquots were periodically collected and analyzed by GC and GC-MS to calculate the conversion of the reaction. The final products were not isolated.

Representative Fischer indole synthesis procedure

Phenylhydrazine (129.8 mg, 1.2 mmol), cyclohexanone (98.2 mg, 1.0 mmol), sAO (100.0 mg), and water (2.0 mL) were added to a Teflon-capped 10.0 mL microwave vial with a stir bar. The vial was then microwaved at 150 ℃ for 1 h. The resulting mixture was cooled to room temperature, and the product was extracted with CH_2Cl_2 and water. The organic phase was collected and dried over $MgSO_4$. The crude product was purified using column chromatography (silica gel, ethyl acetate : *n*-hexane, 1:9 v/v as eluent) to afford the desired product. Spectroscopic and analytical data were in accord with literature values[98]. ^{1}H NMR (400 MHz, $CDCl_3$): δ 7.64 (s, 1H), 7.46-7.44 (d, 1H), 7.29-7.27 (d, 1H), 7.14-7.07 (m, 2H), 2.74-2.70 (m, 4H), 1.91-1.87 (m, 4H).

Representative Biginelli reaction procedure

A Teflon capped 10.0 mL microwave vial was charged with benzaldehyde (1.0 mmol), ethyl acetoacetate (1.0 mmol), urea (1.5 mmol), sAO (50.0 mg), and a stir bar. The vial was then microwaved

at 100 ℃ for 5 min. The resulting mixture was cooled to room temperature and then extracted with ethyl acetate and water. The organic phase was collected and dried over $MgSO_4$. The crude product was purified using column chromatography (silica gel, ethyl acetate : *n*-hexane, 3:7 v/v as eluent). Spectroscopic and analytical data were in accord with literature values[111-113]. ^{1}H NMR (400 MHz, DMSO-d_6): δ 9.18 (s, 1H), 7.72 (s, 1H), 7.33-7.22 (m, 5H), 5.13-5.12 (d, 1H), 3.99-3.94 (q, 2H), 2.24 (s, 3H), 1.09-1.02 (t, 3H).

General cationic polymerization procedure

A 20.0 mL Schlenk tube was purged with nitrogen and then charged with monomers (1.0 g), sAO (10.0 mg), THF (2.64 – 5.17 mL), and a stir bar at -20 °C. After stirring the reaction mixture at -20 °C for 24 h, it was concentrated and poured into excess methanol. The precipitated solid was collected, dried under vacuum, and then analyzed the molecular weight and polymer structure by GPC and NMR, respectively. Spectroscopic and analytical data were in accord with literature values[114-116].

Physical Characterization

All Nuclear magnetic resonance (NMR) spectra were recorded on a Bruker Ascend 400 MHz spectrometer at ambient temperature (22.0(±1.0) ℃, unless otherwise noted). Chemical shifts are reported in parts per million (δ). NMR spectra were collected in $CDCl_3$, DMSO-d_6, or D_2O, and the residual solvents were referenced to 7.26, 2.50, and 4.79 ppm, respectively. The following abbreviations used for the description of the spectra are s, singlet; d, doublet; t, triplet; q, quartet; m, multiplet; br, broad.

Fourier-transform infrared spectroscopy (FT-IR) were recorded using KBr pellets on a Perkin-Elmer Frontier MIR spectrometer

Elemental analyses were performed using a Thermo Scientific Flash 2000 Organic Elemental Analyzer calibrated with 2,5-bis(5-*tert*-butyl-benzoxazol-2-yl)thiophene (BBOT).

Matrix-assisted Laser Desorption/Ionization (MALDI) spectra were recorded on a Bruker Ultraflex III with 2,5-dihydroxybenzoic acid (DHB) as a matrix. THF solutions of sAO and DHB were combined and then evaporated before mass analysis.

Polystyrene equivalent molecular weights and polydispersity index (*Đ*) values were measured by gel permeation chromatography (GPC) using a Malvern GPCmax Solvent/Sample module. All samples were analyzed using tetrahydrofuran as the eluent at a flow rate of 0.8 mL/min. Detection was performed using a Viscotek VE3580 RI Detector.

Mass spectrometry (MS) data were recorded on a Thermo LCQ Fleet Quadrupole Ion Trap Mass Spectrometer in Atmospheric Pressure Chemical Ionization (APCI) mode (electrospray voltage was 3.5 kV).

Atomic force microscopy measurements were performed using a multimode 8 Nanoscope® V (Bruker). Samples were prepared by dissolving in THF (1.0 mg/mL) and spin-coating onto a silica wafer at 3000 RPM for 1 min.

3.5 Acknowledgments

Portions of this chapter were recreated by referring to the reported literature[117] with permission from Hyosic Jung and Christopher W. Bielawski; Soluble asphaltene oxide: a homogeneous carbocatalyst that promotes synthetic transformation, *RSC Adv*, **2020**, *10*, 15598-15603.

The overall design of catalyst and synthesis studies were performed with kind support with Professor Christopher W. Bielawski. Special thanks to Eun-Jung Han for her assistance with MALDI spectrum, Mr. Geon-Hui Park for his assistance with MS data, and Dr. Songsu Kang for his assistance with GPC measurements.

References

1. Lindström, B.; Pettersson, L. J., A Brief History of Catalysis. *Cattech* **2003,** *7* (4), 130-138.

2. Cartwright, F., The early history of ether. *Anaesthesia* **1960,** *15* (1), 67-69.

3. Wisniak, J., The History of Catalysis. From the Beginning to Nobel Prizes. *Educación Química* **2010,** *21* (1), 60-69.

4. Deltete, R. J., Friedrich Wilhelm Ostwald (1853–1932). In *Philosophy of Chemistry*, Woody, A. I.; Hendry, R. F.; Needham, P., Eds. North-Holland: Amsterdam, 2012; Vol. 6, pp 101-111.

5. Van Houten, J., A Century of Chemical Dynamics Traced through the Nobel Prizes. 1909: Wilhelm Ostwald. *J. Chem. Educ.* **2002,** *79* (2), 146.

6. ICPAC Gold Bood: Http://goldbook.iupac.org/html/C/C00876.html

7. Coperet, C.; Chabanas, M.; Petroff Saint-Arroman, R.; Basset, J. M., Homogeneous and heterogeneous catalysis: bridging the gap through surface organometallic chemistry. *Angew. Chem. Int. Ed.* **2003,** *42* (2), 156-181.

8. Zhou, Q. L., Transition-Metal Catalysis and Organocatalysis: Where Can Progress Be Expected? *Angew. Chem. Int. Ed.* **2016,** *55* (18), 5352-5353.

9. Cui, X. J.; Li, W.; Ryabchuk, P.; Junge, K.; Beller, M., Bridging homogeneous and heterogeneous catalysis by heterogeneous single-metal-site catalysts. *Nat. Catal.* **2018,** *1* (6), 385-397.

10. Stratakis, M.; Garcia, H., Catalysis by supported gold nanoparticles: beyond aerobic oxidative processes. *Chem. Rev.* **2012,** *112* (8), 4469-506.

11. Chinchilla, R.; Najera, C., The Sonogashira reaction: a booming methodology in synthetic organic chemistry. *Chem. Rev.* **2007,** *107* (3), 874-922.

12. Jana, R.; Pathak, T. P.; Sigman, M. S., Advances in transition metal (Pd, Ni, Fe)-catalyzed cross-coupling reactions using alkyl-organometallics as reaction partners. *Chem. Rev.* **2011,** *111* (3), 1417-1492.

13. Punniyamurthy, T.; Velusamy, S.; Iqbal, J., Recent advances in transition metal catalyzed oxidation of organic substrates with molecular oxygen. *Chem. Rev.* **2005,** *105* (6), 2329-2363.

14. Sherry, B. D.; Furstner, A., The promise and challenge of iron-catalyzed cross coupling. *Acc. Chem. Res.* **2008,** *41* (11), 1500-1511.

15. Sabatier P, S. J., New synthesis of methane. *J. Chem. Soc. Abstr.* **1902,** *82* (0), A333.

16. Che, M., Nobel Prize in chemistry 1912 to Sabatier: Organic chemistry or catalysis? *Catal. Today* **2013,** *218*, 162-171.

17. Cecchin, G.; Morini, G.; Piemontesi, F., Ziegler-Natta Catalysts. *Kirk-Othmer Encycl. Chem. Technol.*, **2003,** *26,* 502-554

18. Kryzhanovskii, A. V.; Pvanchev, S. S., Synthesis of linear polyethylene on supported ziegler-natta catalysts. Review. *Polym. Sci. U.S.S.R.* **1990,** *32* (7), 1312-1329.

19. Chauvin, Y., Olefin metathesis: the early days (Nobel Lecture). *Angew. Chem. Int. Ed.* **2006,** *45* (23), 3740-3747.

20. Grubbs, R. H.; Carr, D. D.; Hoppin, C.; Burk, P. L., Consideration of the mechanism of the metal catalyzed olefin metathesis reaction. *J. Am. Chem. Soc.* **1976,** *98* (12), 3478-3483.

21. Grubbs, R. H.; Burk, P. L.; Carr, D. D., Mechanism of the olefin metathesis reaction. *J. Am. Chem. Soc.* **1975,** *97* (11), 3265-3267.

22. Katz, T. J.; Rothchild, R., Mechanism of the olefin metathesis of 2,2'-divinylbiphenyl. *J. Am. Chem. Soc.* **1976,** *98* (9), 2519-2526.

23. Schrock, R. R.; Hoveyda, A. H., Molybdenum and tungsten imido alkylidene complexes as efficient olefin-metathesis catalysts. *Angew. Chem. Int. Ed.* **2003,** *42* (38), 4592-4633.

24. Schrock, R. R.; DePue, R. T.; Feldman, J.; Schaverien, C. J.; Dewan, J. C.; Liu, A. H., Preparation and reactivity of several alkylidene complexes of the type W(CHR')(N-2,6-C6H3-iso-Pr2)(OR)2 and related tungstacyclobutane complexes. Controlling metathesis activity through the choice of alkoxide ligand. *J. Am. Chem. Soc.* **1988,** *110* (5), 1423-1435.

25. Hoveyda, A. H.; Schrock, R. R., Catalytic asymmetric olefin metathesis. *Chemistry* **2001,** *7* (5), 945-950.

26. Roy, D.; Uozumi, Y., Recent Advances in Palladium-Catalyzed Cross-Coupling Reactions at ppm to ppb Molar Catalyst Loadings. *Adv. Synth. Catal.* **2018,** *360* (4), 602-625.

27. Heck, R. F.; Nolley, J. P., Palladium-Catalyzed Vinylic Hydrogen Substitution Reactions with Aryl, Benzyl, and Styryl Halides. *J. Org. Chem.* **1972,** *37* (14), 2320-2322.

28. Negishi, E., A profile of professor Richard F. Heck - Discovery of the Heck reaction. *J. Organomet. Chem.* **1999,** *576* (1-2), Xv-Xvi.

29. Negishi, E.; Van Horn, D. E., Selective carbon-carbon bond formation via transition metal catalysis. 4. A novel approach to cross-coupling exemplified by the nickel-catalyzed reaction of alkenylzirconium derivatives with aryl halides. *J. Am. Chem. Soc.* **1977,** *99* (9), 3168-3170.

30. Miyaura, N.; Suzuki, A., Stereoselective Synthesis of Arylated (E)-Alkenes by the Reaction of Alk-1-Enylboranes with Aryl Halides in the Presence of Palladium Catalyst. *J. Chem. Soc. Chem. Comm.* **1979,** (19), 866-867.

31. Rivera-Utrilla, J.; Bautista-Toledo, I.; Feffo-Garcia, M. A.; Moreno-Castilla, C., Bioadsorption of Pb(II), Cd(II), and Cr(VI) on activated carbon from aqueous solutions. *Carbon* **2003,** *41* (2), 323-330.

32. Nair, D.; Scarpello, J. T.; White, L. S.; dos Santos, L. M. F.; Vankelecom, I. F. J.; Livingston, A. G., Semi-continuous nanofiltration-coupled Heck reactions as a new approach to improve productivity of homogeneous catalysts. *Tetrahedron Lett.* **2001,** *42* (46), 8219-8222.

33. Titirici, M. M.; White, R. J.; Brun, N.; Budarin, V. L.; Su, D. S.; del Monte, F.; Clark, J. H.; MacLachlan, M. J., Sustainable carbon materials. *Chem. Soc. Rev.* **2015,** *44* (1), 250-290.

34. Rideal, E. K.; Wright, W. M., CLXXXIV.—Low temperature oxidation at charcoal surfaces. Part I. The behaviour of charcoal in the absence of promoters. *J. Chem. Soc. Trans.* **1925,** *127* (0), 1347-1357.

35. Lücking, F.; Köser, H.; Jank, M.; Ritter, A., Iron powder, graphite and activated carbon as catalysts for the oxidation of 4-chlorophenol with hydrogen peroxide in aqueous solution. *Water Res.* **1998,** *32* (9), 2607-2614.

36. Fenton, H. J. H., LXXIII.—Oxidation of tartaric acid in presence of iron. *J. Chem. Soc. Trans.* **1894,** *65* (0), 899-910.

37. Zhang, J.; Liu, X.; Blume, R.; Zhang, A.; Schlogl, R.; Su, D. S., Surface-modified carbon nanotubes catalyze oxidative dehydrogenation of n-butane. *Science* **2008,** *322* (5898), 73-77.

38. Li, B.; Xu, Z., A nonmetal catalyst for molecular hydrogen activation with comparable catalytic hydrogenation capability to noble metal catalyst. *J. Am. Chem. Soc.* **2009,** *131* (45), 16380-16382.

39. Dreyer, D. R.; Jia, H. P.; Bielawski, C. W., Graphene oxide: a convenient carbocatalyst for facilitating oxidation and hydration reactions. *Angew. Chem. Int. Ed.* **2010,** *49* (38), 6813-6816.

40. Su, C.; Acik, M.; Takai, K.; Lu, J.; Hao, S. J.; Zheng, Y.; Wu, P.; Bao, Q.; Enoki, T.; Chabal, Y. J.; Loh, K. P., Probing the catalytic activity of porous graphene oxide and the origin of this behaviour. *Nat. Commun.* **2012,** *3* (1), 1298.

41. Long, Y.; Zhang, C. C.; Wang, X. X.; Gao, J. P.; Wang, W.; Liu, Y., Oxidation of SO2 to SO3 catalyzed by graphene oxide foams. *J. Mater. Chem.* **2011,** *21* (36), 13934-13941.

42. Tang, S.; Cao, Z., Site-dependent catalytic activity of graphene oxides towards oxidative dehydrogenation of propane. *Phys. Chem. Chem. Phys.* **2012,** *14* (48), 16558-16565.

43. Primo, A.; Neatu, F.; Florea, M.; Parvulescu, V.; Garcia, H., Graphenes in the absence of metals as carbocatalysts for selective acetylene hydrogenation and alkene hydrogenation. *Nat. Commun.* **2014,** *5*, 5291.

44. Vijay Kumar, A.; Rama Rao, K., Recyclable graphite oxide catalyzed Friedel–Crafts addition of indoles to α,β-unsaturated ketones. *Tetrahedron Lett.* **2011,** *52* (40), 5188-5191.

45. Wang, Y. H.; Sang, R.; Zheng, Y.; Guo, L.; Guan, M.; Wu, Y., Graphene oxide: An efficient recyclable solid acid for the synthesis of bis(indolyl)methanes from aldehydes and indoles in water. *Catal. Commun.* **2017,** *89*, 138-142.

46. Khalili, D.; Lavian, S.; Moayyed, M., Graphene oxide as a catalyst for one-pot sequential aldol coupling/aza-Michael addition of amines to chalcones through in situ generation of Michael acceptors under neat conditions. *Tetrahedron Lett.* **2020,** *61* (6), 151470.

47. Tan, L.; Wang, B.; Feng, H. X., Comparative studies of graphene oxide and reduced graphene oxide as carbocatalysts for polymerization of 3-aminophenylboronic acid. *Rsc. Adv.* **2013,** *3* (8), 2561-2565.

48. Ebajo, V. D., Jr.; Santos, C. R. L.; Alea, G. V.; Lin, Y. A.; Chen, C. H., Regenerable Acidity of Graphene Oxide in Promoting Multicomponent Organic Synthesis. *Sci. Rep.* **2019,** *9* (1), 15579.

49. Khodabakhshi, S.; Karami, B., Graphene oxide nanosheets as metal-free catalysts in the three-component reactions based on aryl glyoxals to generate novel pyranocoumarins. *New J. Chem.* **2014,** *38* (8), 3586-3590.

50. Ahmad, M. S.; He, H.; Nishina, Y., Selective Hydrogenation by Carbocatalyst: The Role of Radicals. *Org. Lett.* **2019,** *21* (20), 8164-8168.

51. Dreyer, D. R.; Jarvis, K. A.; Ferreira, P. J.; Bielawski, C. W., Graphite Oxide as a Dehydrative Polymerization Catalyst: A One-Step Synthesis of Carbon-Reinforced Poly(phenylene methylene) Composites. *Macromolecules* **2011,** *44* (19), 7659-7667.

52. Dreyer, D. R.; Bielawski, C. W., Graphite Oxide as an Olefin Polymerization Carbocatalyst: Applications in Electrochemical Double Layer Capacitors. *Adv. Funct. Mater.* **2012,** *22* (15), 3247-3253.

53. Mullins, O. C., The asphaltenes. *Annu. Rev. Anal. Chem.* **2011,** *4* (1), 393-418.

54. Fakher, S.; Ahdaya, M.; Elturki, M.; Imqam, A., Critical review of asphaltene properties and factors impacting its stability in crude oil. *J. Pet. Explor. Prod. Technol.* **2019,** *10* (3), 1183-1200.

55. Sheu, E. Y., Petroleum AsphalteneProperties, Characterization, and Issues. *Energy & Fuels* **2002,** *16* (1), 74-82.

56. Speight, J. G., The chemical and physical structure of petroleum: effects on recovery operations. *J. Pet. Sci. Technol.* **1999,** *22* (1-3), 3-15.

57. Dickie, J. P.; Yen, T. F., Macrostructures of the asphaltic fractions by various instrumental methods. *Anal. Chem.* **1967,** *39* (14), 1847-1852.

58. Mullins, O. C., The Modified Yen Model. *Energy & Fuels* **2010,** *24* (4), 2179-2207.

59. Schuler, B.; Meyer, G.; Pena, D.; Mullins, O. C.; Gross, L., Unraveling the Molecular Structures of Asphaltenes by Atomic Force Microscopy. *J. Am. Chem. Soc.* **2015,** *137* (31), 9870-9876.

60. Andersen, S. I., Effect of Precipitation Temperature on the Composition of N-Heptane Asphaltenes. *Fuel. Sci. Techn. Int.* **1994,** *12* (1), 51-74.

61. Miller, J. T.; Fisher, R. B.; Thiyagarajan, P.; Winans, R. E.; Hunt, J. E., Subfractionation and characterization of Mayan asphaltene. *Energy & Fuels* **1998,** *12* (6), 1290-1298.

62. Groenzin, H.; Mullins, O. C., Asphaltene Molecular Size and Structure. *J. Phys. Chem. A* **1999,** *103* (50), 11237-11245.

63. Groenzin, H.; Mullins, O. C., Molecular size and structure of asphaltenes from various sources. *Energy & Fuels* **2000,** *14* (3), 677-684.

64. Buenrostro-Gonzalez, E.; Groenzin, H.; Lira-Galeana, C.; Mullins, O. C., The overriding chemical principles that define asphaltenes. *Energy & Fuels* **2001,** *15* (4), 972-978.

65. Groenzin, H.; Mullins, O. C.; Eser, S.; Mathews, J.; Yang, M. G.; Jones, D., Molecular size of asphaltene solubility fractions. *Energy & Fuels* **2003,** *17* (2), 498-503.

66. Badre, S.; Goncalves, C. C.; Norinaga, K.; Gustavson, G.; Mullins, O. C., Molecular size and weight of asphaltene and asphaltene solubility fractions from coals, crude oils and bitumen. *Fuel* **2006,** *85* (1), 1-11.

67. Moschopedis, S. E.; Speight, J. G., Water-Soluble Derivatives of Athabasca-Asphaltenes. *Fuel* **1971,** *50* (1), 34-40.

68. Choi, S.; Byun, D. H.; Lee, K.; Kim, J. D.; Nho, N. S., Asphaltene precipitation with partially oxidized asphaltene from water/heavy crude oil emulsion. *J. Pet. Sci. Technol.* **2016,** *146*, 21-29.

69. Choi, S.; Choi, S. Q.; Kim, J. D.; Nho, N. S., Partially Oxidized Asphaltene as a Bitumen Viscosity Reducer. *Energy & Fuels* **2017,** *31* (9), 9240-9246.

70. Dreyer, D. R.; Bielawski, C. W., Carbocatalysis: Heterogeneous carbons finding utility in synthetic chemistry. *Chem. Sci.* **2011,** *2* (7), 1233-1240.

71. Alkhazov, T. G.; Lisovskii, A. E.; Gulakhmedova, T. K., Oxidative Dehydrogenation of Ethylbenzene over a Charcoal Catalyst. *React. Kinet. Catal. Lett.***1979,** *12* (2), 189-193.

72. Wu, H.; Su, C.; Tandiana, R.; Liu, C.; Qiu, C.; Bao, Y.; Wu, J.; Xu, Y.; Lu, J.; Fan, D.; Loh, K. P., Graphene-Oxide-Catalyzed Direct CH-CH-Type Cross-Coupling: The Intrinsic Catalytic Activities of Zigzag Edges. *Angew. Chem. Int. Ed.* **2018,** *57* (34), 10848-10853.

73. Morioku, K.; Morimoto, N.; Takeuchi, Y.; Nishina, Y., Concurrent Formation of Carbon-Carbon Bonds and Functionalized Graphene by Oxidative Carbon-Hydrogen Coupling Reaction. *Sci. Rep.* **2016,** *6*, 25824.

74. Ahmad, M. S.; Nishina, Y., Graphene-based carbocatalysts for carbon-carbon bond formation. *Nanoscale* **2020,** *12* (23), 12210-12227.

75. Jia, H. P.; Dreyer, D. R.; Bielawski, C. W., Graphite Oxide as an Auto-Tandem Oxidation-Hydration-Aldol Coupling Catalyst. *Adv. Synth. Catal.* **2011,** *353* (4), 528-532.

76. Hu, F.; Patel, M.; Luo, F.; Flach, C.; Mendelsohn, R.; Garfunkel, E.; He, H.; Szostak, M., Graphene-Catalyzed Direct Friedel-Crafts Alkylation Reactions: Mechanism, Selectivity, and Synthetic Utility. *J. Am. Chem. Soc.* **2015,** *137* (45), 14473-14480.

77. Dhakshinamoorthy, A.; Alvaro, M.; Puche, M.; Fornes, V.; Garcia, H., Graphene Oxide as Catalyst for the Acetalization of Aldehydes at Room Temperature. *Chemcatchem* **2012,** *4* (12), 2026-2030.

78. Dreyer, D. R.; Todd, A. D.; Bielawski, C. W., Harnessing the chemistry of graphene oxide. *Chem. Soc. Rev.* **2014,** *43* (15), 5288-5301.

79. Kudin, K. N.; Ozbas, B.; Schniepp, H. C.; Prud'homme, R. K.; Aksay, I. A.; Car, R., Raman spectra of graphite oxide and functionalized graphene sheets. *Nano. Lett.* **2008,** *8* (1), 36-41.

80. Su, C.; Loh, K. P., Carbocatalysts: graphene oxide and its derivatives. *Acc. Chem. Res.* **2013,** *46* (10), 2275-2285.

81. Hummers, W. S.; Offeman, R. E., Preparation of Graphitic Oxide. *J. Am. Chem. Soc.* **1958,** *80* (6), 1339.

82. Yakubov, M. R.; Milordov, D. V.; Yakubova, S. G.; Borisov, D. N.; Ivanov, V. T.; Sinyashin, K. O., Concentrations of vanadium and nickel and their ratio in heavy oil asphaltenes. *Pet. Chem.* **2016,** *56* (1), 16-20.

83. Neises, B.; Steglich, W., Simple Method for the Esterification of Carboxylic Acids. *Angew. Chem. Int. Ed.* **1978,** *17* (7), 522-524.

84. Collins, W. R.; Schmois, E.; Swager, T. M., Graphene oxide as an electrophile for carbon nucleophiles. *Chem. Commun.* **2011,** *47* (31), 8790-8792.

85. Dimiev, A. M.; Alemany, L. B.; Tour, J. M., Graphene oxide. Origin of acidity, its instability in water, and a new dynamic structural model. *ACS Nano* **2013,** *7* (1), 576-588.

86. Dhakshinamoorthy, A.; Alvaro, M.; Concepcion, P.; Fornes, V.; Garcia, H., Graphene oxide as an acid catalyst for the room temperature ring opening of epoxides. *Chem. Commun. (Camb)* **2012,** *48* (44), 5443-5445.

87. Aponte, J. C.; Verastegui, M.; Malaga, E.; Zimic, M.; Quiliano, M.; Vaisberg, A. J.; Gilman, R. H.; Hammond, G. B., Synthesis, cytotoxicity, and anti-Trypanosoma cruzi activity of new chalcones. *J. Med. Chem.* **2008,** *51* (19), 6230-6234.

88. Shen, G.; Zhao, L.; Wang, Y.; Xia, W.; Yang, M.; Zhang, T., Palladium–copper catalyzed C(sp3)–C(sp2) bond C–H activation cross-coupling reaction: selective arylation to synthesize 9-aryl-9H-xanthene and 9,9-diaryl-xanthene derivatives. *Rsc. Adv.* **2016,** *6* (88), 84748-84751.

89. Schweitzer-Chaput, B.; Sud, A.; Pinter, A.; Dehn, S.; Schulze, P.; Klussmann, M., Synergistic effect of ketone and hydroperoxide in Bronsted acid catalyzed oxidative coupling reactions. *Angew. Chem. Int. Ed.* **2013,** *52* (50), 13228-13232.

90. Navalon, S.; Dhakshinamoorthy, A.; Alvaro, M.; Antonietti, M.; Garcia, H., Active sites on graphene-based materials as metal-free catalysts. *Chem. Soc. Rev.* **2017,** *46* (15), 4501-4529.

91. Chen, W. F.; Yan, L. F.; Bangal, P. R., Preparation of graphene by the rapid and mild thermal reduction of graphene oxide induced by microwaves. *Carbon* **2010,** *48* (4), 1146-1152.

92. Chiu, P. L.; Mastrogiovanni, D. D.; Wei, D.; Louis, C.; Jeong, M.; Yu, G.; Saad, P.; Flach, C. R.; Mendelsohn, R.; Garfunkel, E.; He, H., Microwave- and nitronium ion-enabled rapid and direct production of highly conductive low-oxygen graphene. *J. Am. Chem. Soc.* **2012,** *134* (13), 5850-5856.

93. Shulga, Y. M.; Baskakov, S. A.; Knerelman, E. I.; Davidova, G. I.; Badamshina, E. R.; Shulga, N. Y.; Skryleva, E. A.; Agapov, A. L.; Voylov, D. N.; Sokolov, A. P.; Martynenko, V. M., Carbon nanomaterial produced by microwave exfoliation of graphite oxide: new insights. *Rsc. Adv.* **2014,** *4* (2), 587-592.

94. Dallinger, D.; Kappe, C. O., Microwave-assisted synthesis in water as solvent. *Chem. Rev.* **2007,** *107* (6), 2563-2591.

95. Zhu, Y. W.; Murali, S.; Stoller, M. D.; Velamakanni, A.; Piner, R. D.; Ruoff, R. S., Microwave assisted exfoliation and reduction of graphite oxide for ultracapacitors. *Carbon* **2010,** *48* (7), 2118-2122.

96. Mohammadi Ziarani, G.; Moradi, R.; Ahmadi, T.; Lashgari, N., Recent advances in the application of indoles in multicomponent reactions. *Rsc. Adv.* **2018,** *8* (22), 12069-12103.

97. Dai, W.; Lv, Y.; Wang, L.; Shang, S.; Chen, B.; Li, G.; Gao, S., Highly efficient oxidation of alcohols catalyzed by a porphyrin-inspired manganese complex. *Chem. Commun. (Camb)* **2015,** *51* (56), 11268-11271.

98. Xu, D. Q.; Wu, J.; Luo, S. P.; Zhang, J. X.; Wu, J. Y.; Du, X. H.; Xu, Z. Y., Fischer indole synthesis catalyzed by novel SO3H-functionalized ionic liquids in water. *Green Chem.* **2009,** *11* (8), 1239-1246.

99. Jung, H.; Bielawski, C. W., Asphaltene oxide promotes a broad range of synthetic transformations. *Commun. Chem.* **2019,** *2* (1), 113.

100. Julkapli, N. M.; Bagheri, S., Graphene supported heterogeneous catalysts: An overview. *Int. J. Hydrogen Energy* **2015,** *40* (2), 948-979.

101. Dreyer, D. R.; Jia, H. P.; Todd, A. D.; Geng, J.; Bielawski, C. W., Graphite oxide: a selective and highly efficient oxidant of thiols and sulfides. *Org. Biomol. Chem.* **2011,** *9* (21), 7292-7295.

102. Gao, Y.; Tang, P.; Zhou, H.; Zhang, W.; Yang, H.; Yan, N.; Hu, G.; Mei, D.; Wang, J.; Ma, D., Graphene Oxide Catalyzed C−H Bond Activation: The Importance of Oxygen Functional Groups for Biaryl Construction. *Angew. Chem. Int. Ed.* **2016,** *55* (9), 3124-3128.

103. Verma, S.; Mungse, H. P.; Kumar, N.; Choudhary, S.; Jain, S. L.; Sain, B.; Khatri, O. P., Graphene oxide: an efficient and reusable carbocatalyst for aza-Michael addition of amines to activated alkenes. *Chem. Commun. (Camb)* **2011,** *47* (47), 12673-12675.

104. Rodríguez-reinoso, F., The role of carbon materials in heterogeneous catalysis. *Carbon* **1998,** *36* (3), 159-175.

105. Chen, C. H.; Hu, S.; Shih, J. F.; Yang, C. Y.; Luo, Y. W.; Jhang, R. H.; Chiang, C. M.; Hung, Y. J., Effective Synthesis of Highly Oxidized Graphene Oxide That Enables Wafer-scale Nanopatterning: Preformed Acidic Oxidizing Medium Approach. *Sci. Rep.* **2017,** *7* (1), 3908.

106. Park, J.; Kim, Y. S.; Sung, S. J.; Kim, T.; Park, C. R., Highly dispersible edge-selectively oxidized graphene with improved electrical performance. *Nanoscale* **2017,** *9* (4), 1699-1708.

107. Liu, Y. J.; Lotero, E.; Goodwin, J. G., Effect of water on sulfuric acid catalyzed esterification. *J. Mol. Catal. A: Chem.* **2006,** *245* (1-2), 132-140.

108. Nagarajaiah, H.; Mukhopadhyay, A.; Moorthy, J. N., Biginelli reaction: an overview. *Tetrahedron Lett.* **2016,** *57* (47), 5135-5149.

109. Matos, L. H. S.; Masson, F. T.; Simeoni, L. A.; Homem-de-Mello, M., Biological activity of dihydropyrimidinone (DHPM) derivatives: A systematic review. *Eur. J. Med. Chem.* **2018,** *143*, 1779-1789.

110. Lin, C. H.; Xiang, J. S.; Matyjaszewski, K., Living Cationic Polymerization of Styrene in the Presence of Tetrabutylammonium Salts. *Macromolecules* **1993,** *26* (11), 2785-2790.

111. Abbaspour-Gilandeh, E.; Azimi, S. C.; Mohammadi-Barkchai, A., Li(glycine)(CF3SO3) as an effective and recoverable catalyst for the preparation of 3,4-dihydropyrimidine-2-(1H)-one under solvent-free conditions. *Rsc. Adv.* **2014,** *4* (97), 54854-54863.

112. Jetti, S. R.; Upadhyaya, A.; Jain, S., 3,4-Hydropyrimidin-2-(1H)one derivatives: solid silica-based sulfonic acid catalyzed microwave-assisted synthesis and their biological evaluation as antihypertensive and calcium channel blocking agents. *Med. Chem. Res.* **2014,** *23* (10), 4356-4366.

113. Savanur, H. M.; Kalkhambkar, R. G.; Aridoss, G.; Laali, K. K., [bmim(SO 3 H)][OTf]/[bmim][X] and Zn(NTf 2) 2 /[bmim][X] (X = PF 6 and BF 4); efficient catalytic systems for the synthesis of tetrahydropyrimidin-ones (-thiones) via the Biginelli reaction. *Tetrahedron Lett.* **2016,** *57* (27-28), 3029-3035.

114. Guo, H. Q.; Kajiwara, A.; Morishima, Y.; Kamachi, M.; Schnabel, W., Polymerization of n-butyl vinyl ether photoinitiated by the initiator system poly(methyl phenyl silane)/N-ethoxy-2-methylpyridinium iodide/ZnI2/benzaldehyde. *Polym. J.* **1997,** *29* (5), 446-449.

115. Hazra, D. K.; Chatterjee, R., In situ solid state polymerization and characterization of poly (N-vinylcarbazole) encapsulated Keggin type polyoxometalate nanocomposite. *J. Mol. Struct.* **2013,** *1045*, 139-144.

116. Zhou, Y. H.; Faust, R.; Richard, R.; Schwarz, M., Syntheses and characterization of poly(cyclohexyl vinyl ether-stat-vinyl alcohol)-b-polyisobutylene-b-poly(cyclohexyl vinyl ether-stat-vinyl alcohol) triblock copolymers and their application as coatings to deliver paclitaxel from coronary stents. *Macromolecules* **2005,** *38* (20), 8183-8191.

117. Jung, H.; Bielawski, C. W., Soluble asphaltene oxide: a homogeneous carbocatalyst that promotes synthetic transformations. *Rsc. Adv.* **2020,** *10* (26), 15598-15603.

Acknowledgments

Dear Christopher W. Bielawski (Ph.D. advisor),

Since the winter of 2013, 7 years have passed since I got to know you and worked with you. First of all, I would like to thank you for all the time that has led and motivated me during my Ph.D. I remember your words that we met for the first time. At that time, I told you, “If I can participate in your lab, I can do everything, even chores like cleaning or mopping.”. However, you told me, “No, you do not need to do. All you have to do is enjoy chemistry!”. You have taught me how to enjoy chemistry. With your support, I could successfully finish my Ph.D. course, and I was able to take the first step in the world of chemistry and took a step closer as a chemist. Following your teaching, I will continue to enjoy and challenge chemistry. I really appreciate you!

Sincerely yours

Hyosic Jung

Dear all committee members

I do really appreciate all of my committee members (Prof. Jong-Beom Baek, Prof. Sung You Hong, Prof. Young S. Park, and Prof. Hyeon Suk Shin) for taking your time to attend my Ph.D. defense presentation and giving much helpful feedback and advisors about my research project. Thanks to your support, I successfully finished my research projects and had a chance to look up my project from a different perspective. I appreciate all of the committee members again.

Sincerely yours

Hyosic Jung

Dear group members

Thank you for all of the things during my Ph.D. course. I could not count how much I have received from you guys. I would not have completed my Ph.D. course without you guys. I have not to doubt that all CWB group members will achieve everything you have ever wanted and become great chemists. I really missed you and all of our memories in the CWB lab. Thank you so much!

Sincerely yours

Hyosic

Dear Kyungha Kim (Girlfriend and partner)

Since we had met in 2019, we are walking out looking at the same goal. Even though we are studying different science fields, we are moving forward together thanks to your sincere concern and encouragement. You are the best luck and blessing to me. I was not good at expressing it, but I relied on you a lot and gained strength during my Ph.D. Thank you for being with me until now, even though there have been many happy and hard times. Let us walk together, relying on each other like we are now. I love you so much!

사랑하는 부모님에게

지난 제 모든 인생에서 부모님의 따뜻한 사랑과 지원이 없었다면 아마 저는 지금 이 자리에 서 있을 수도 없었을 거예요. 제가 무엇을 하든 묵묵히 믿고 끊임없이 지원을 아끼지 않으셨던 부모님의 희생 덕분에 제가 화학 분야에서 박사라는 결과를 얻게 되었습니다. 기쁠 때는 저보다도 더욱 기뻐해 주시고 슬플 때나 힘들 때는 뒤에서 묵묵히 받아 주시고 포기하지 않게 다시 한번 일어날 힘을 주시던 우리 부모님. 항상 고마운 마음을 가지고 있으면서도 표현을 잘 못 한다는 핑계로 단 한 번도 제 마음을 제대로 전달해 본 적이 없는 거 같아요. 정말 이 글을 빌어서 너무 감사드리고 이젠 제가 떳떳이 사회로 나가서 부모님을 기쁘게 그리고 꽃길만 걷게 해드릴 게요. 엄마 아빠 사랑합니다.

아들 정효식 올림.

Appendix A: Supplementary of Table

Table of Contents

Table A.2.1 Summary of optimization experiments[a]

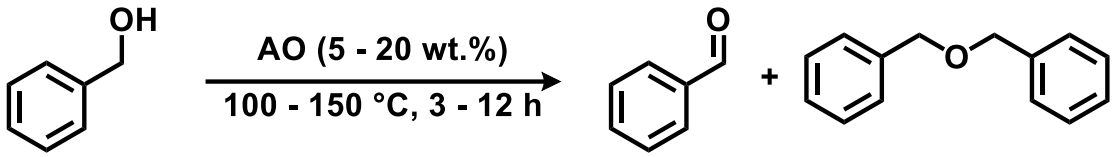

Temperature (℃)	Time (h)	5 wt%		10 wt%		20 wt%	
		PhCHO (%)	Ether (%)	PhCHO (%)	Ether (%)	PhCHO (%)	Ether (%)
100	3	0	10	0	17	0	24
	6	0	17	0	29	0	41
	12	0	24	0	39	2	52
120	3	0	41	0	60	1	68
	6	0	49	0	69	1	75
	12	0	59	0	78	3	60
150	3	6	61	9	82	7	73
	6	10	64	11	75	9	44
	12	12	64	15	78	13	19

[a] All reactions were performed under the following conditions: benzyl alcohol as substrate (neat), 5–20 wt% of AO (indicated), 100-150 ℃ (indicated), 3-12 h (indicated). The conversion of benzyl alcohol to benzyl ether or benzaldehyde (indicated) was calculated by ^{1}H NMR spectroscopy against an external standard (18-crown-6).

Table A.2.2 Summary of etherification reactions[a]

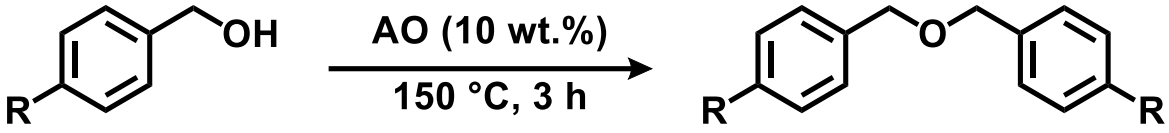

Entry	R	^{1}H NMR Chemical Shift of the Respective Benzylic Protons (δ)	Conversion[b] (%)
1	H	4.59	82
2	OMe	--	-
3[c]	NO_2	4.72	26
4[c]	Cl	4.51	56
5[d]	Me	4.50	70

[a] Unless otherwise noted, the reactions were performed under the following conditions: benzyl alcohol or derivative (neat), 10 wt% catalyst, 150 ℃, 3 h. [b] Conversion to the corresponding benzyl ether was calculated by ^{1}H NMR spectroscopy against an external standard (18-crown-6). [c] Reaction was performed at 150 ℃ for 6 h. [d] Reaction was performed at 100 ℃ for 1 h.

Table A.2.3 Assessment of the recyclability of AO[a]

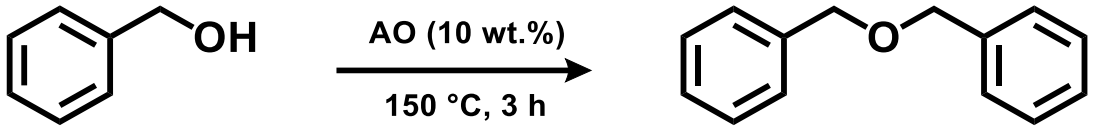

Entry	Conversion[b] (%)	Recovered Catalyst (%)
1st cycle	80	> 99
2nd cycle	82	86
3rd cycle	75	97
4th cycle	68	94
5th cycle	70	> 99

[a] The reactions were performed under the following conditions: benzyl alcohol (neat), 10 wt% catalyst, 150 ℃, 3 h. [b] Conversion to benzyl ether was calculated by ^{1}H NMR spectroscopy against an external standard (18-crown-6).

Table A.2.4 Summary of polymerizations that were performed with AO[a]

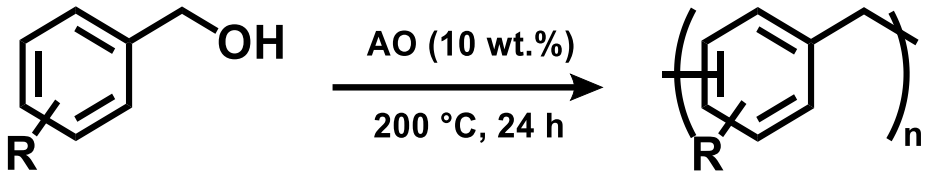

Entry	R	Yield[b] (%)	M_n[c] (Da)	$Đ$[c]
1	H	66	733	3.2
2	3-OMe	60	973	2.1
3	4-OMe	53	1148	1.8

[a] The reactions were performed by treating 0.5 g of benzyl alcohol or a derivative with 5.0×10^{-2} g (10 wt%) of AO at 200 ℃ for 24 h. [b] The products were isolated by filtration after precipitation from MeOH. [c] The number-average molecular weight (M_n) and polydispersity index ($Đ$) were determined by GPC and are reported as their polystyrene equivalents.

Table A.2.5 Hydration of phenylacetylene with AO[a]

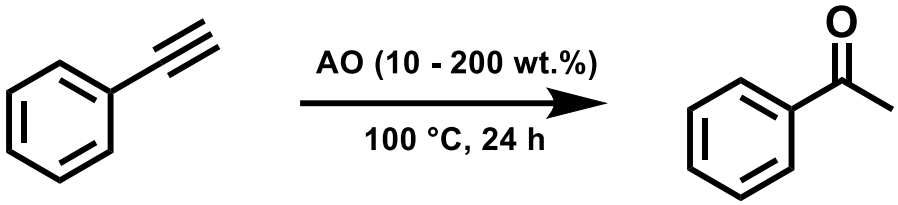

Entry	Loading (wt%)	Yield[b] (%)
1	200	86
2	100	65
3	50	27
4	10	5

[a] All reactions were performed under the following conditions: phenylacetylene (50.0 mg, 0.5 mmol), 10–200 wt% catalyst, 100 ℃, and 24 h [b] Conversion to acetophenone was calculated by ^{1}H NMR spectroscopy against an external standard (18-crown-6).

Table A.2.6 Summary of comparative cross-coupling reactions[a]

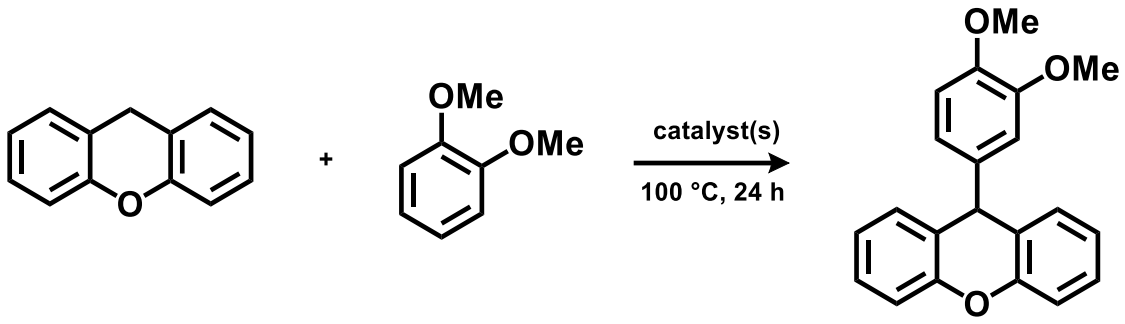

Entry	$TsOH \cdot H_2O$ ($\times 10^{-2}$ mmol)	Catalyst (total wt / oxygen wt)	Yield[b] (%)
1	1.0	AO (20.0 mg / 2.6 mg)	63
2[d]	1.0	GO (6.2 mg / 2.6 mg)	27
3[c]	--	AO (20.0 mg / 2.6 mg)	40
4[c][d]	--	GO (6.2 mg / 2.6 mg)	16

[a] Unless otherwise noted, all reactions were performed with xanthene (0.5 mmol), veratrole (1.0 mmol), AO or GO as a catalyst (20.0 mg), and $TsOH \cdot H_2O$ (1.0×10^{-2} mmol) as a co-catalyst at 100 ℃ for 24 h. [b] All products were purified using column chromatography. [c] Reaction was performed without a co-catalyst. [d] The loadings of the catalyst (AO and GO) were normalized to their respective oxygen contents.

Table A.2.7 Summary of optimization reactions that were performed in a microwave reactor[a]

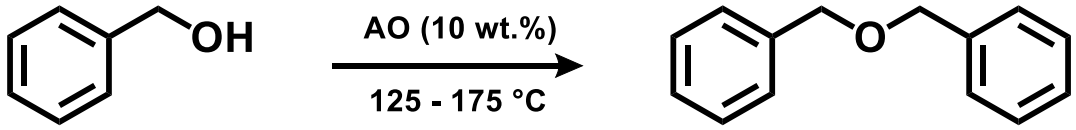

Entry	Temperature (℃)	Time (min)	Conversion[b] (%)
1	150	5	65
2	150	15	90
3	150	30	88
4	125	15	54
5	175	15	51

[a] All reactions were performed in a microwave reactor using the following conditions: benzyl alcohol (neat), 10 wt% AO, 125–175 ℃ (indicated), 5-30 min (indicated). [b] Conversion to the benzyl ether was calculated by ^{1}H NMR spectroscopy against an external standard (18-crown-6).

Table A.2.8 Summary of microwave enhanced condensation reactions[a]

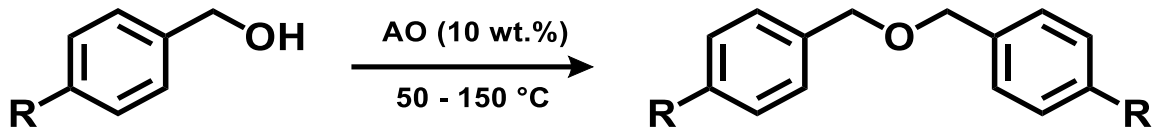

Entry	R	Temp (℃)	Time (min)	Benzylic Protons Peak in NMR (δ)	Conversion[b] (%)
1	H	150	10	4.59	90
2	OMe	50	60	4.46	80
3	NO_2	150	60	4.72	32
4	Cl	150	30	4.51	81
5	Me	100	30	4.50	84

[a] All reactions were performed in a microwave reactor using the following conditions: benzyl alcohol derivative (neat), 10 wt% AO, 50-150 ℃ (indicated), 10-60 min (indicated). [b] Conversion to the corresponding benzyl ether was calculated by ^{1}H NMR spectroscopy against an external standard (18-crown-6).

Table A.2.9 Assessment of the recyclability of AO under microwave reactions[a]

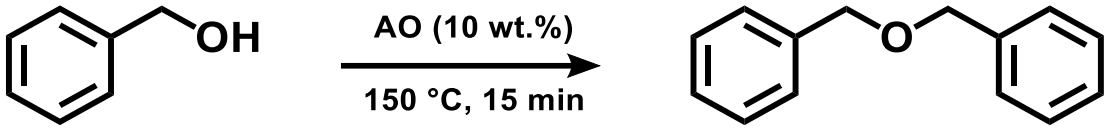

Cycle	Conversion[b] (%)	Oxygen[c] (wt%)	Recovery (%)
Starting Material	--	13.1	--
1	86	9.3	99
2	78	7.0	97
3	76	6.4	99
4	74	4.5	94
5	59	4.2	94

[a] All reactions were performed in a microwave reactor using the following conditions: benzyl alcohol as a substrate (neat), 10 wt% catalyst, 150 ℃, 15 min. [b] Conversion of benzyl alcohol to benzyl ether was calculated using ^{1}H NMR spectroscopy against an external standard (18-crown-6). [c] The weight percent of oxygen in the starting material or recovered catalyst was determined by elemental analysis.

Table A.3.1 A summary of a series of experiments designed to assess the recyclability of sAO[a]

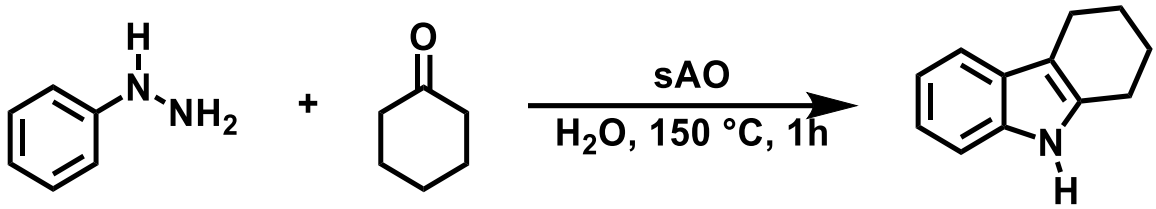

Entry	Yield[b] (%)
1st cycle	59
2nd cycle	53
3rd cycle	57
4th cycle	53
5th cycle	52

[a] All reactions were performed using phenylhydrazine (1.2 mmol), cyclohexanone (1.0 mmol), sAO (100 mg), and water (2.0 mL) at 150 ℃ for 1 h in a microwave reactor. [b] Isolated yield after purification using column chromatography.

Table A.3.2 A summary of the scope of substrates that was explored for the Biginelli reactions described in the main text[a]

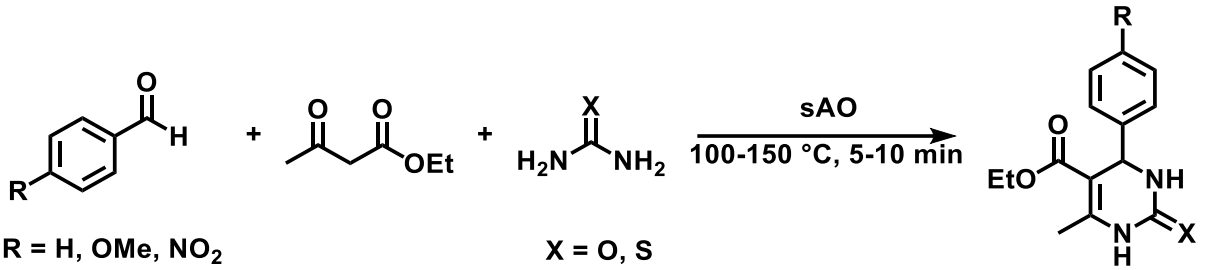

R = H, OMe, NO_2 X = O, S

Entry	R	X	Time (min)	Yield[b] (%)
1	H	O	5	75
2	OMe	O	5	72
3	NO_2	O	5	69
4	H	S	10	61
5	OMe	S	10	69
6[c]	NO_2	S	10	64

[a] All reactions were performed with aldehydes (1.0 mmol), ethyl acetoacetate (1.0 mmol), and urea (1.5 mmol) using sAO (50.0 mg) at 100 °C in a microwave reactor. [b] Isolated yield after purification using column chromatography. [c] The reaction was performed with aldehyde (1.0 mmol), ethyl acetoacetate (5.0 mmol), thiourea (1.5 mmol) and sAO (50.0 mg) at 150 °C for 10 min.

Table A.3.3 Optimization of the polymerization of N-vinylcarbazole[a]

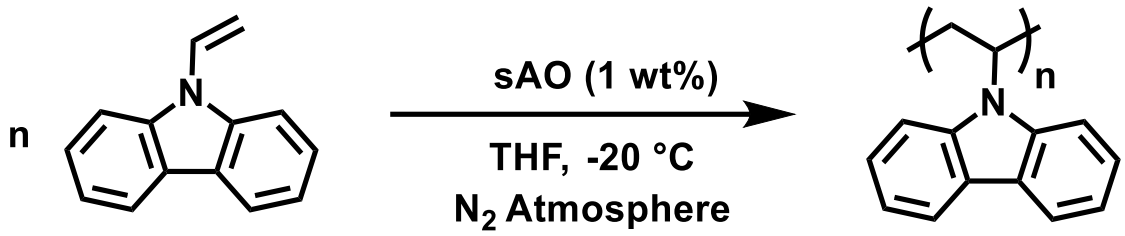

Entry	Time (h)	Yield[b] (%)	M_n[c] (Da)	$Đ$[c]
1	24	99	11.1	5.1
2	4	99	9.5	5.0
3	2	96	9.1	4.1
4	1	96	8.8	4.4
5	0.167 (10 min)	94	9.0	4.3

[a] The reactions were performed by treating a solution of N-vinylcarbazole in THF (1 mol/L) with 1 wt% of sAO at -20 °C under an atmosphere of N_2. [b] Isolated yield after collection of the precipitate formed upon pouring the reaction mixture into excess methanol. [c] The number-average molecular weight (M_n) and polydispersity index ($Đ$) were determined by GPC and are reported as their polystyrene equivalents.

Appendix B: FT-IR Spectra

Table of Contents

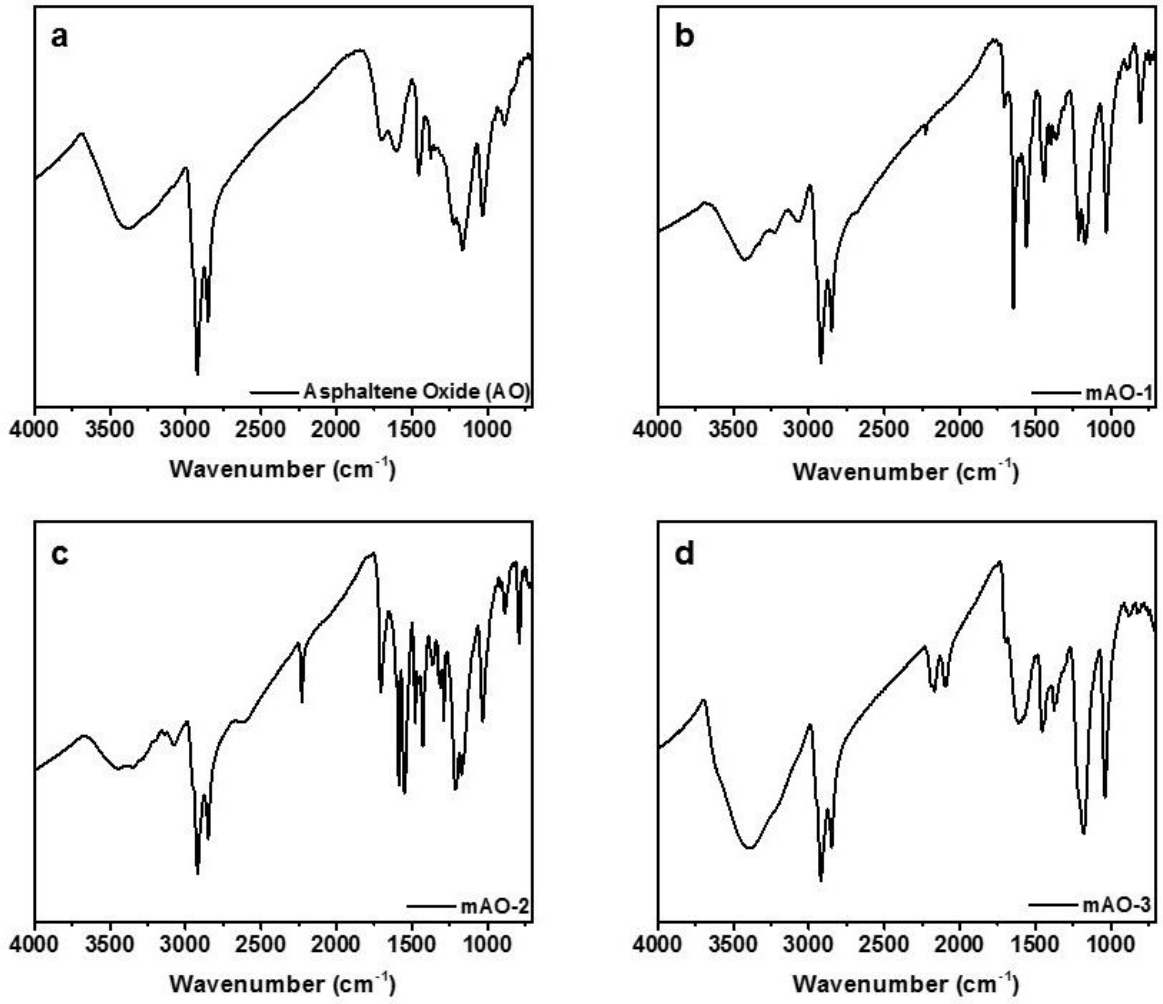

Table B.2.1 FT-IR spectra recorded for (a) AO, (b) mAO-1 as prepared by treating AO with 3-cyanobenzyl alcohol under Steglich esterification conditions, (c) mAO-2 as prepared by treating AO with 3-cyanophenyl isocyanate, and (d) mAO-3 as prepared by treating AO with malononitrile under basic conditions.

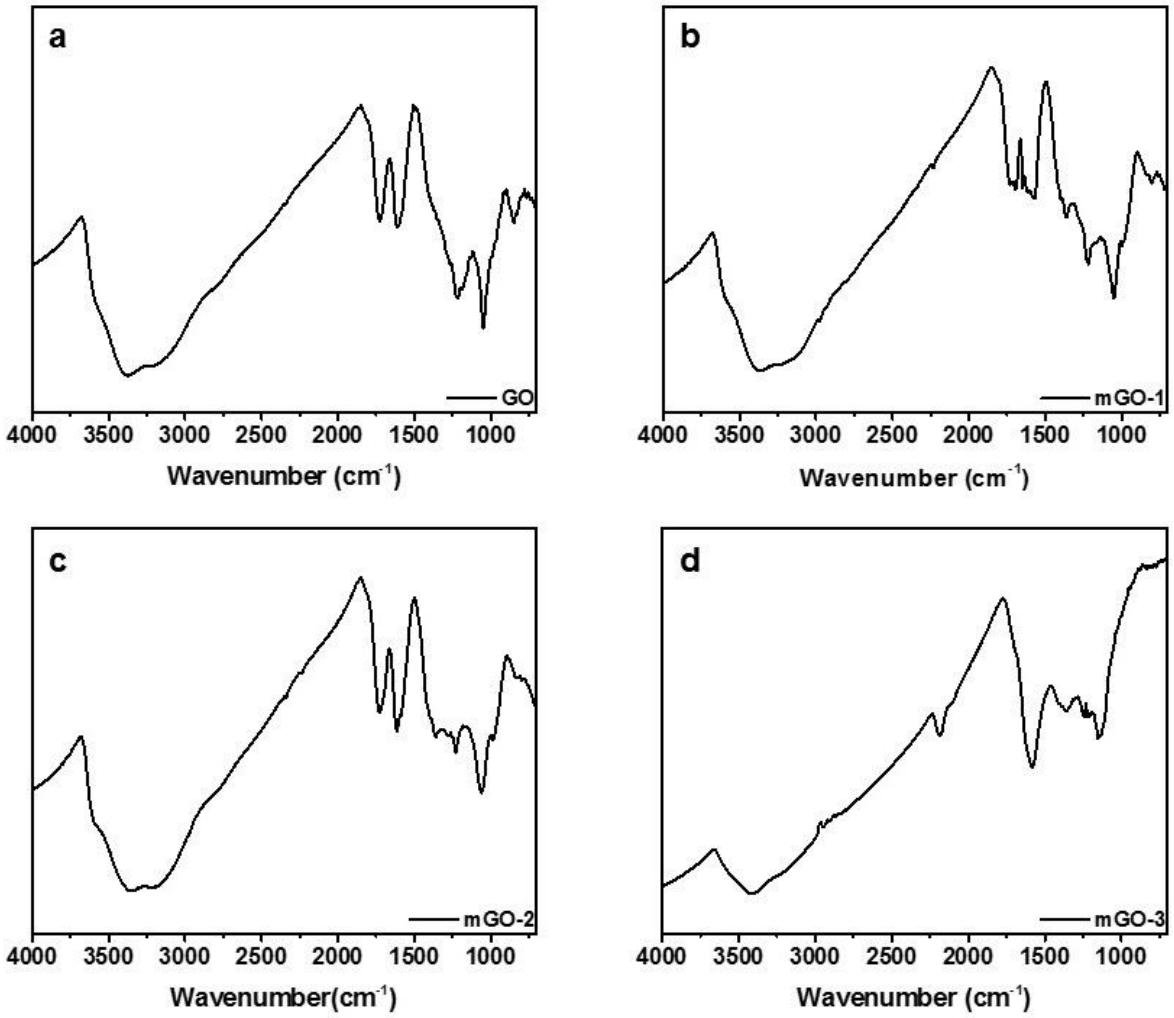

Table B.2.2 FT-IR spectra recorded for (a) GO, (b) mGO-1 as prepared by treating GO with 3-cyanobenzyl alcohol under Steglich esterification conditions, (c) mGO-2 as prepared by treating GO with 3-cyanophenyl isocyanate, and (d) mGO-3 as prepared by treating GO with malononitrile under basic conditions.

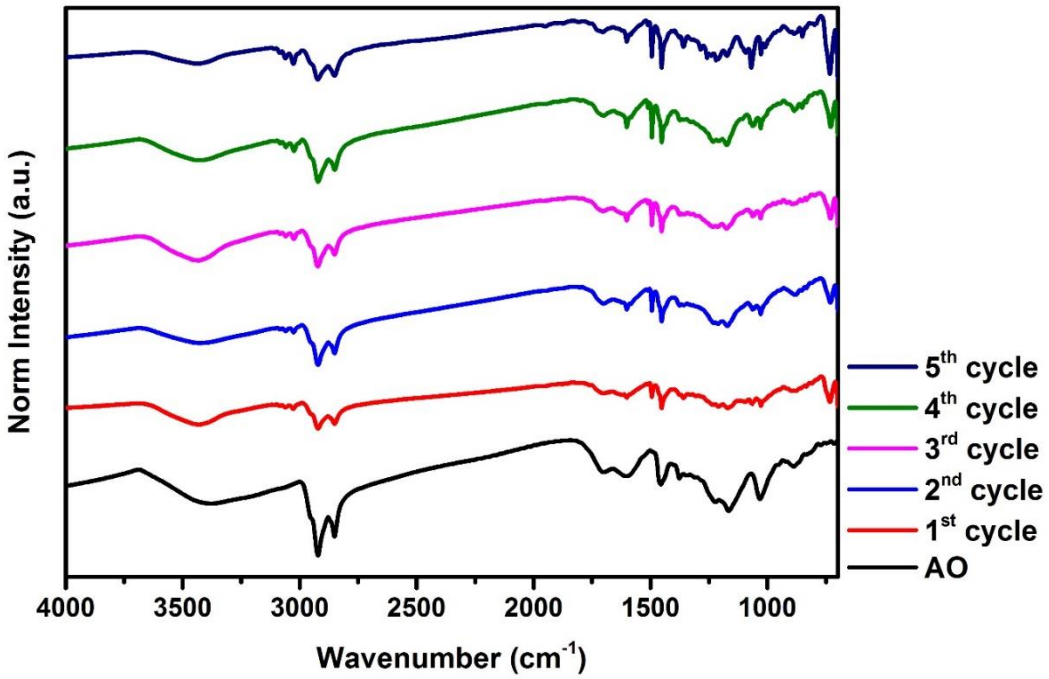

Table B.2.3 FT-IR spectra recorded for AO as a starting material and after being recovered from a series of etherification reactions.

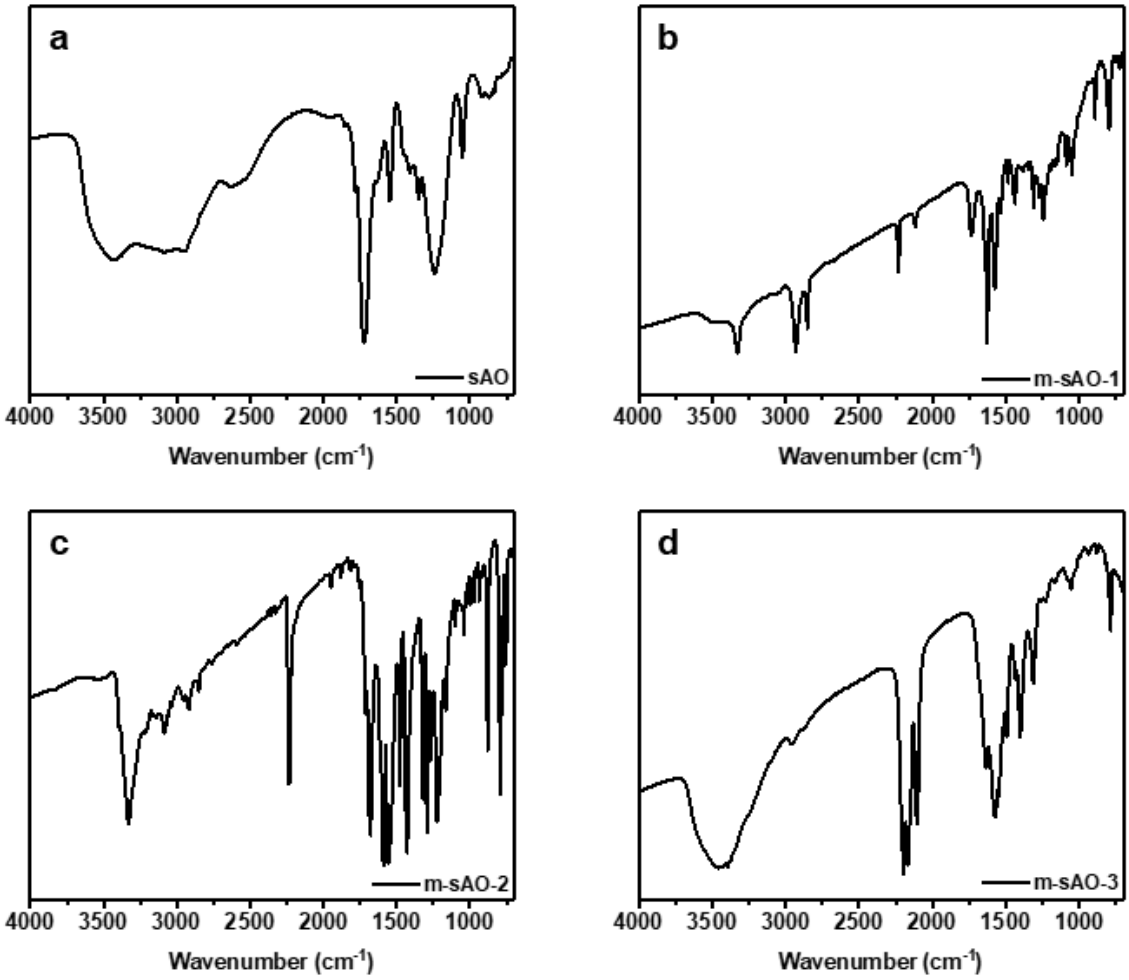

Table B.3.1 FT-IR spectra recorded for (a) sAO, (b) m-sAO-1 as prepared by treating sAO with 3-cyanobenzyl alcohol under Steglich esterification conditions, (c) m-sAO-2 as prepared by treating sAO with 3-cyanophenyl isocyanate, and (d) m-sAO-3 as prepared by treating sAO with malononitrile under basic conditions.

Appendix C: Elemental analysis and quantification data

Table of Contents

Table C.2.1 Elemental analysis data recorded for asphaltene and asphaltene oxide (AO)

	Carbon (wt%)	Hydrogen (wt%)	Nitrogen (wt%)	Sulfur (wt%)	Oxygen (wt%)	Empirical Formula
Asphaltene	81.0	7.9	0.7	6.6	1.4	$C_{1.00}H_{1.17}S_{0.03}O_{0.01}$
Asphaltene Oxide (AO)	64.5	6.6	0.6	11.1	13.1	$C_{1.00}H_{1.23}S_{0.06}O_{0.15}$

Table C.2.2 Summary of elemental data recorded for the modified AOs

	Carbon (wt%)	Hydrogen (wt%)	Nitrogen (wt%)	Sulfur (wt%)	Oxygen (wt%)	Empirical Formula
AO	64.5	6.6	0.6	11.1	13.1	$C_{1.00}H_{1.23}S_{0.06}O_{0.15}$
mAO-1	69.4	6.4	3.8	6.1	9.2	$C_{1.00}H_{1.14}N_{0.05}S_{0.03}O_{0.09}$
mAO-2	67.7	5.8	4.5	6.7	8.9	$C_{1.00}H_{1.02}N_{0.05}S_{0.03}O_{0.10}$
mAO-3	62.5	5.9	2.1	6.7	12.5	$C_{1.00}H_{1.12}N_{0.02}S_{0.04}O_{0.14}$

Table C.2.3 Summary of elemental data recorded for the modified GOs

	Carbon (wt%)	Hydrogen (wt%)	Nitrogen (wt%)	Sulfur (wt%)	Oxygen (wt%)	Empirical Formula
GO	49.1	2.1	0.0	1.2	42.5	$C_{1.00}H_{0.52}S_{0.01}O_{0.65}$
mGO-1	52.9	2.6	0.5	0.4	36.4	$C_{1.00}H_{0.59}N_{0.008}S_{0.003}O_{0.52}$
mGO-2	48.8	2.3	0.3	0.5	36.8	$C_{1.00}H_{0.57}N_{0.005}S_{0.004}O_{0.57}$
mGO-3	47.1	2.4	3.3	0.3	30.5	$C_{1.00}H_{0.61}N_{0.06}S_{0.002}O_{0.49}$

Table C.2.4 Elemental analysis data recorded for AO as a starting material and after being isolated from a series of etherification reactions (see also Table A.2.3)

Cycle	Carbon (wt%)	Hydrogen (wt%)	Nitrogen (wt%)	Sulfur (wt%)	Oxygen (wt%)	Empirical Formula
AO	64.5	6.6	0.6	11.1	13.1	$C_{1.00}H_{1.23}S_{0.06}O_{0.15}$
1	73.1	6.4	0.4	7.0	8.5	$C_{1.00}H_{1.05}S_{0.036}O_{0.09}$
2	70.2	6.2	0.4	7.3	9.9	$C_{1.00}H_{1.05}S_{0.039}O_{0.10}$
3	73.6	6.3	0.4	6.8	8.1	$C_{1.00}H_{1.02}S_{0.034}O_{0.08}$
4	74.4	6.3	0.4	6.5	8.5	$C_{1.00}H_{1.01}S_{0.033}O_{0.08}$
5	78.5	6.5	0.3	4.2	7.7	$C_{1.00}H_{0.98}S_{0.020}O_{0.07}$

Table C.3.1 Summary of elemental data recorded for the modified sAOs

Entry	Carbon (wt%)	Hydrogen (wt%)	Nitrogen (wt%)	Sulfur (wt%)	Oxygen (wt%)	Empirical Formula
AO	40.1	4.4	3.1	6.6	39.5	$C_{1.00}H_{1.30}N_{0.07}S_{0.06}O_{0.73}$
m-sAO-1	68.1	6.8	10.3	0	11.7	$C_{1.00}H_{1.20}N_{0.13}O_{0.13}$
m-sAO-2	66.3	4.4	18.8	0	7.5	$C_{1.00}H_{0.80}N_{0.24}O_{0.08}$
m-sAO-3	43.0	3.4	24.2	0	12.5	$C_{1.00}H_{0.95}N_{0.48}O_{0.22}$

Table C.3.2 Summary of functional group quantification data recorded for sAO, AO, and GO. The calculations were based on the elemental analysis data (see Figure B.2.2, Figure B.2.3, and Figure B.3.1).

Functional Group	sAO (mol/g)	AO (mol/g)	GO (mol/g)
COOH	$> 5.1 \times 10^{-3}$	$> 2.3 \times 10^{-3}$	$> 3.6 \times 10^{-4}$
OH	$> 5.6 \times 10^{-3}$	$> 1.4 \times 10^{-3}$	$> 1.1 \times 10^{-4}$
epoxide	$> 7.5 \times 10^{-3}$	$> 5.4 \times 10^{-4}$	$> 1.2 \times 10^{-3}$

Appendix D: MALDI-TOF and AFM images

Table of Contents

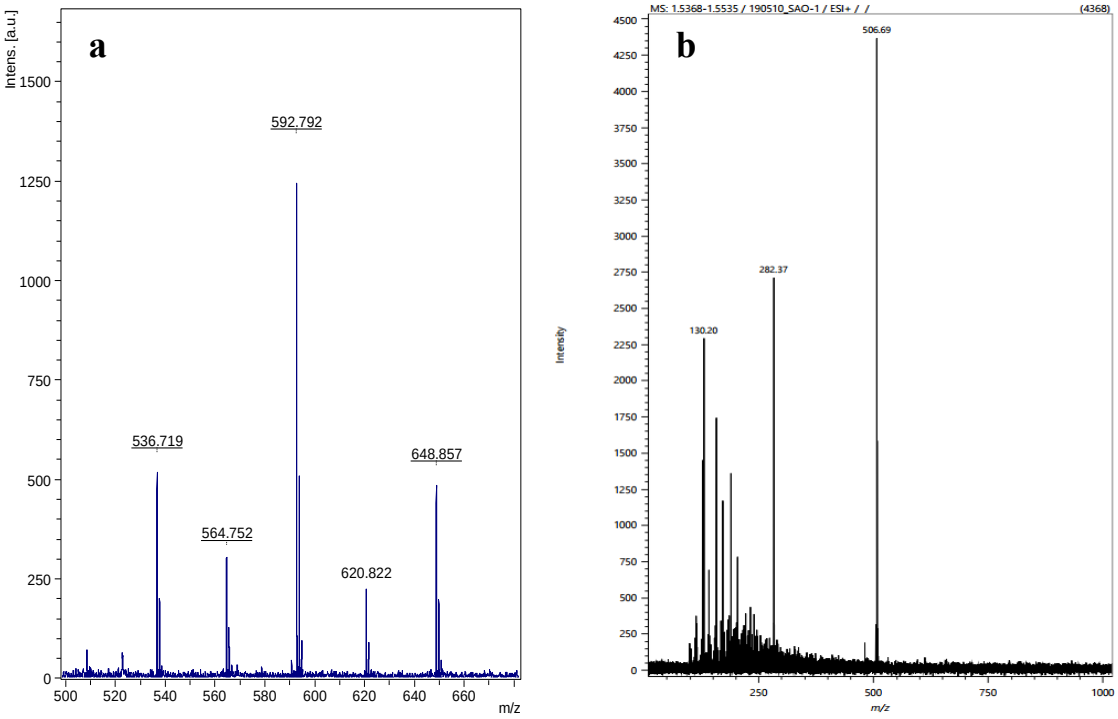

Table D.3.1 (a) MALDI-TOF data recorded for sAO. (b) ESI MS data recorded for sAO in the positive mode.

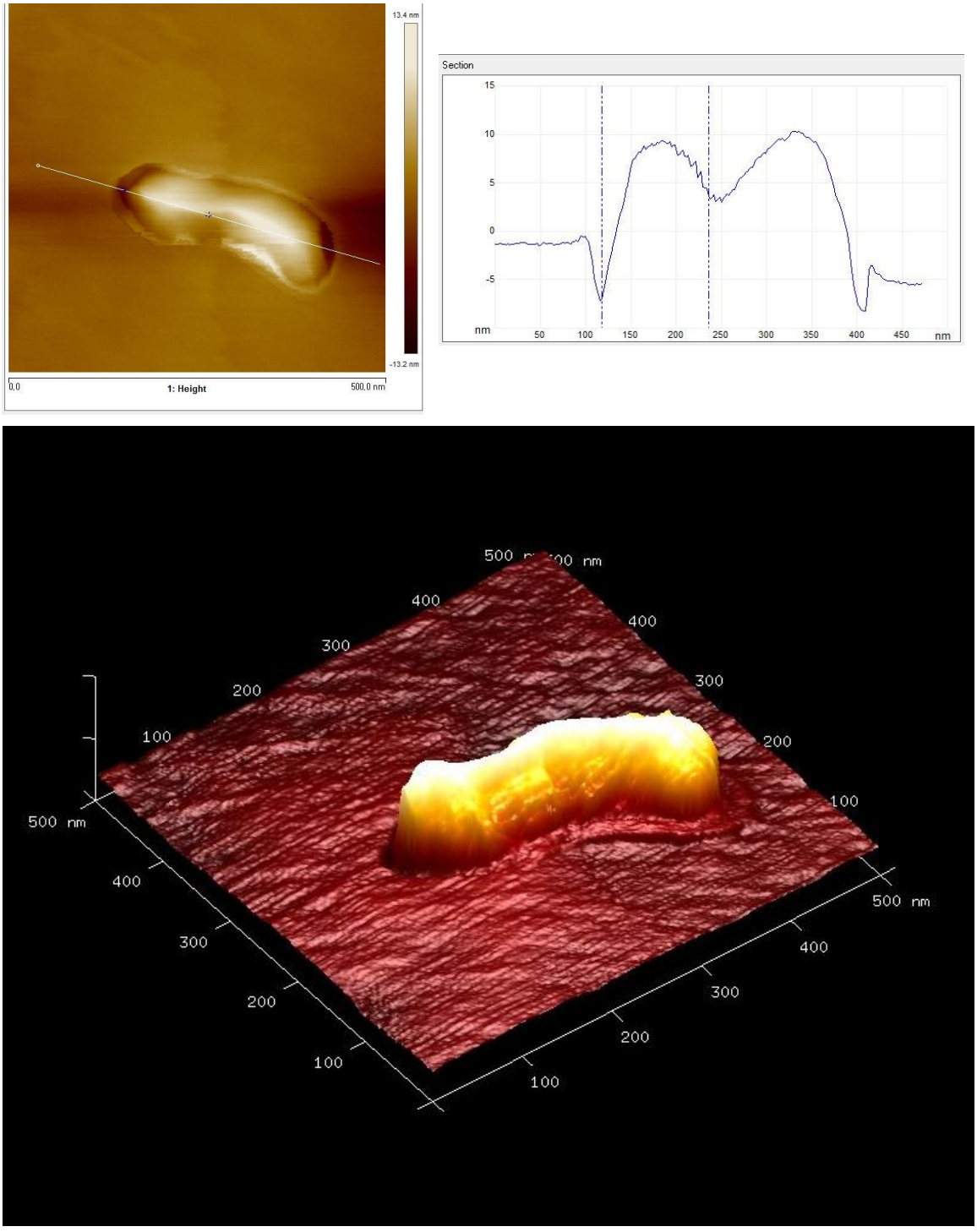

Table D.3.2 AFM images recorded for sAO on silica. Conditions used to create films: 1 mg/mL in THF; spinning rate = 3000 rpm for 1 min. Images were collected in the tapping mode using non-contact tips with a spring constant of 6 N m^{-1} and tip radii of ≤ 8 nm (Bruker RTESP-150).

Appendix E: NMR Spectra

Table of Contents

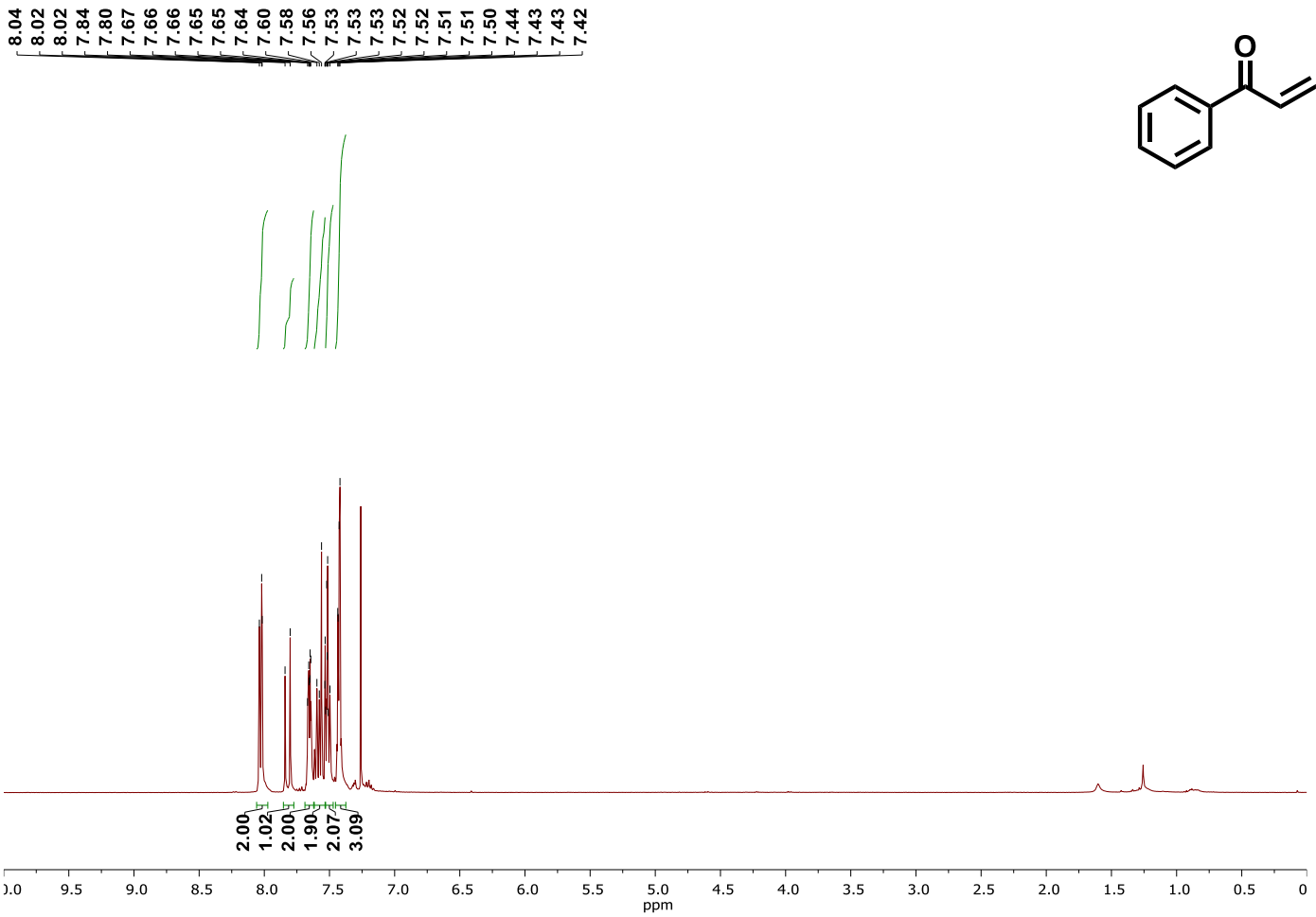

Figure E.2.1 ^{1}H NMR (400 MHz, $CDCl_3$) spectrum recorded for chalcone.

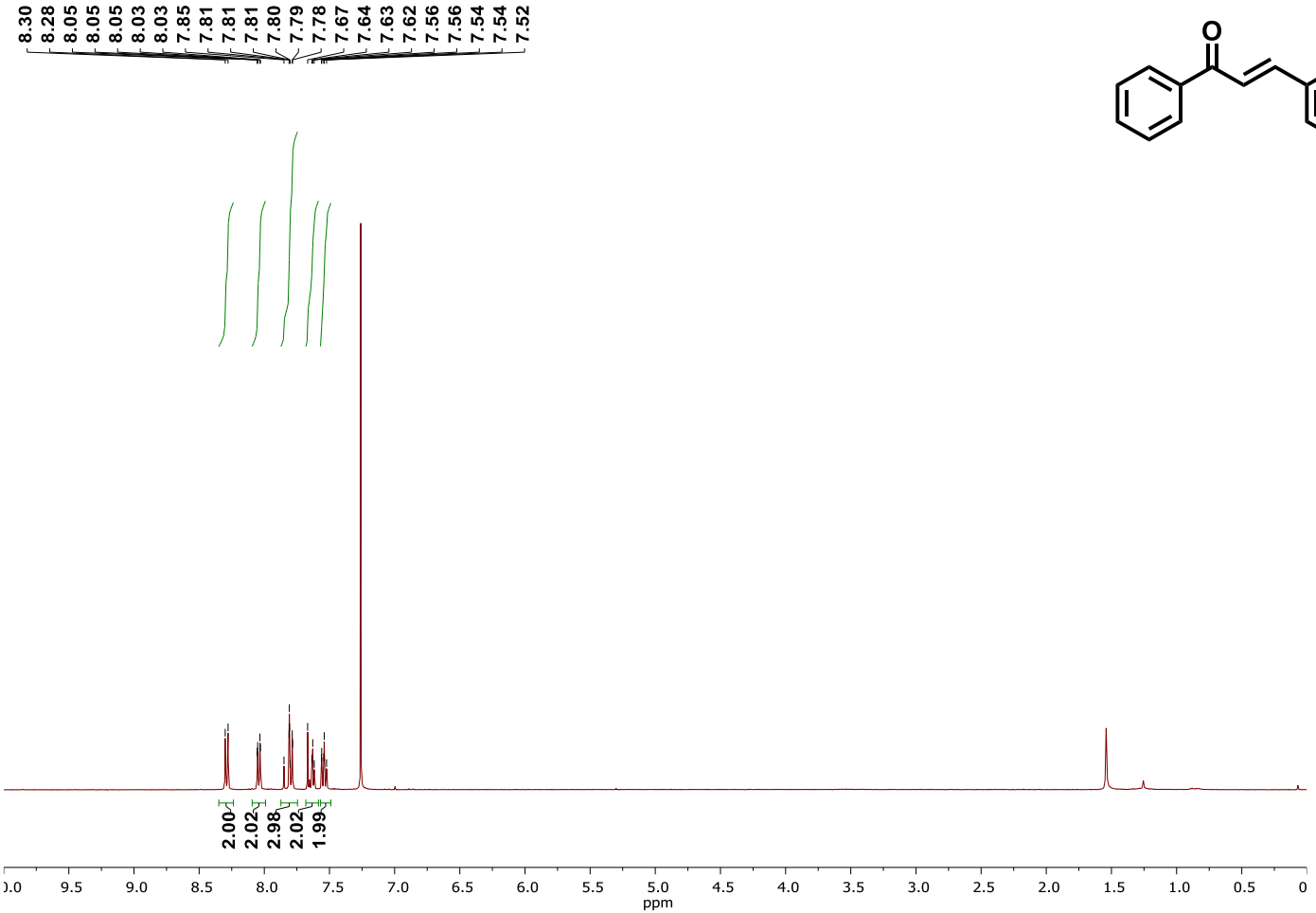

Figure E.2.2 ^{1}H NMR (400 MHz, $CDCl_3$) spectrum recorded for 4-nitrochalcone.

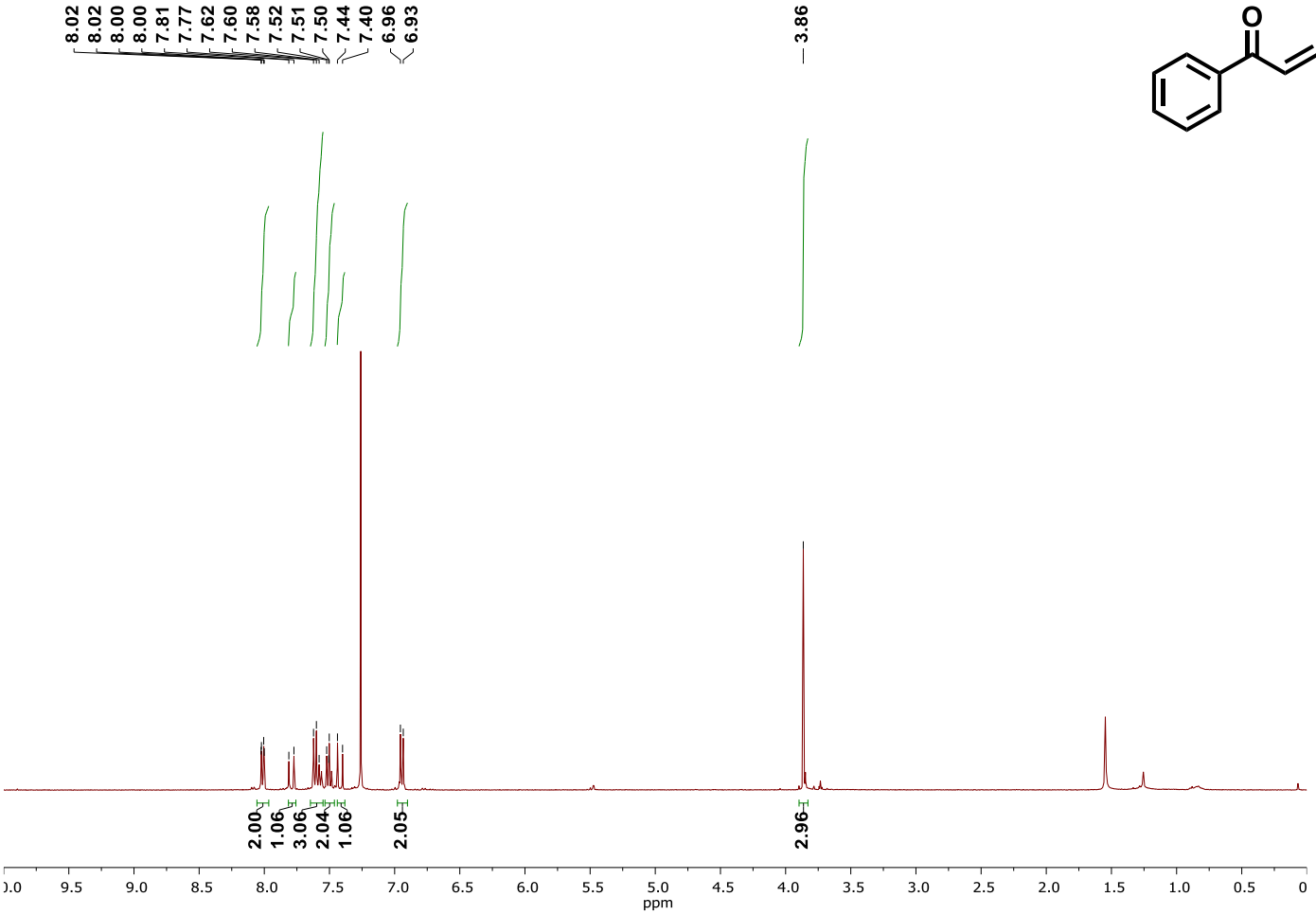

Figure E.2.3 ^{1}H NMR (400 MHz, $CDCl_3$) spectrum recorded for 4-methoxychalcone.

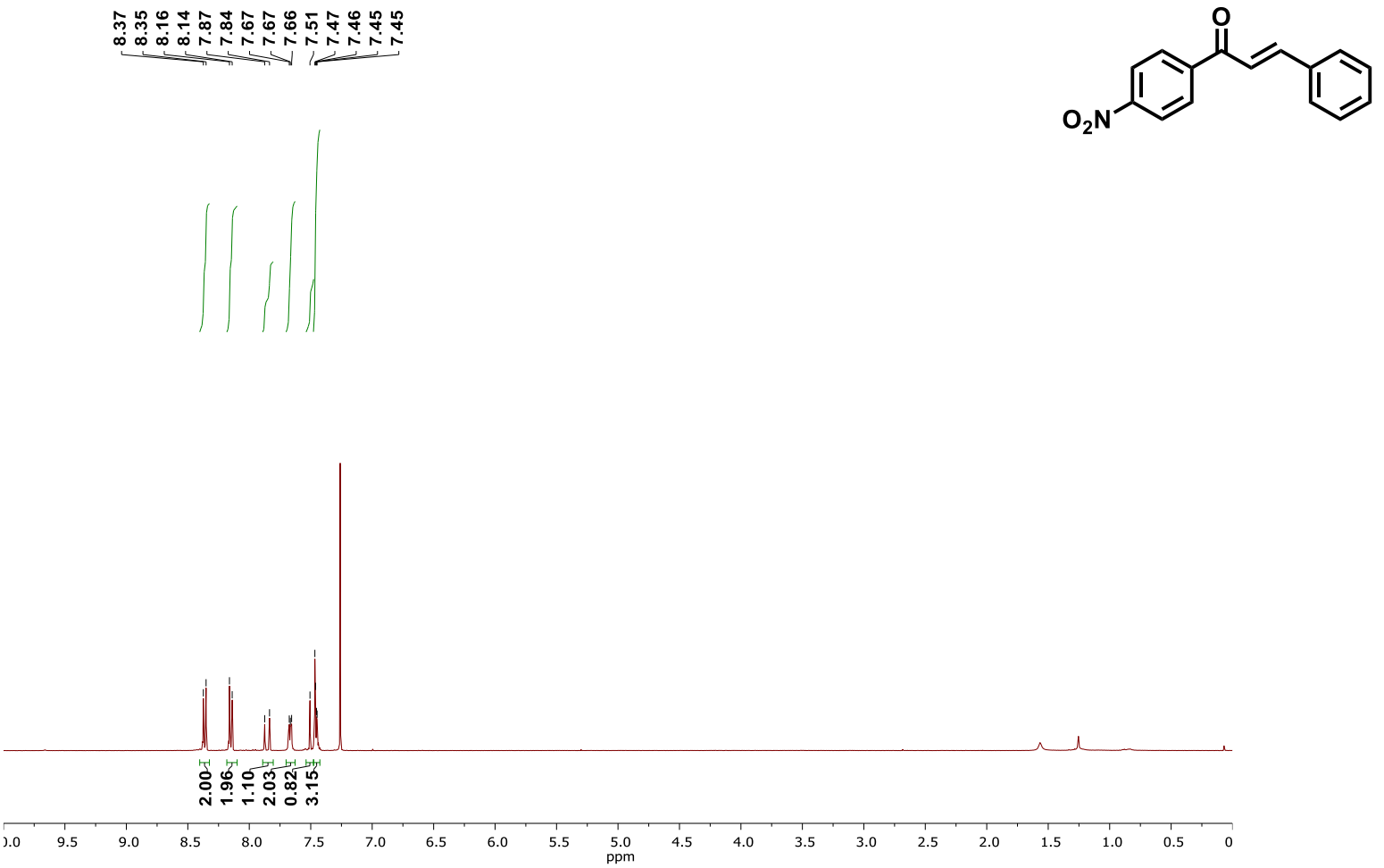

Figure E.2.4 ^{1}H NMR (400 MHz, $CDCl_3$) spectrum recorded for 4'-nitrochalcone.

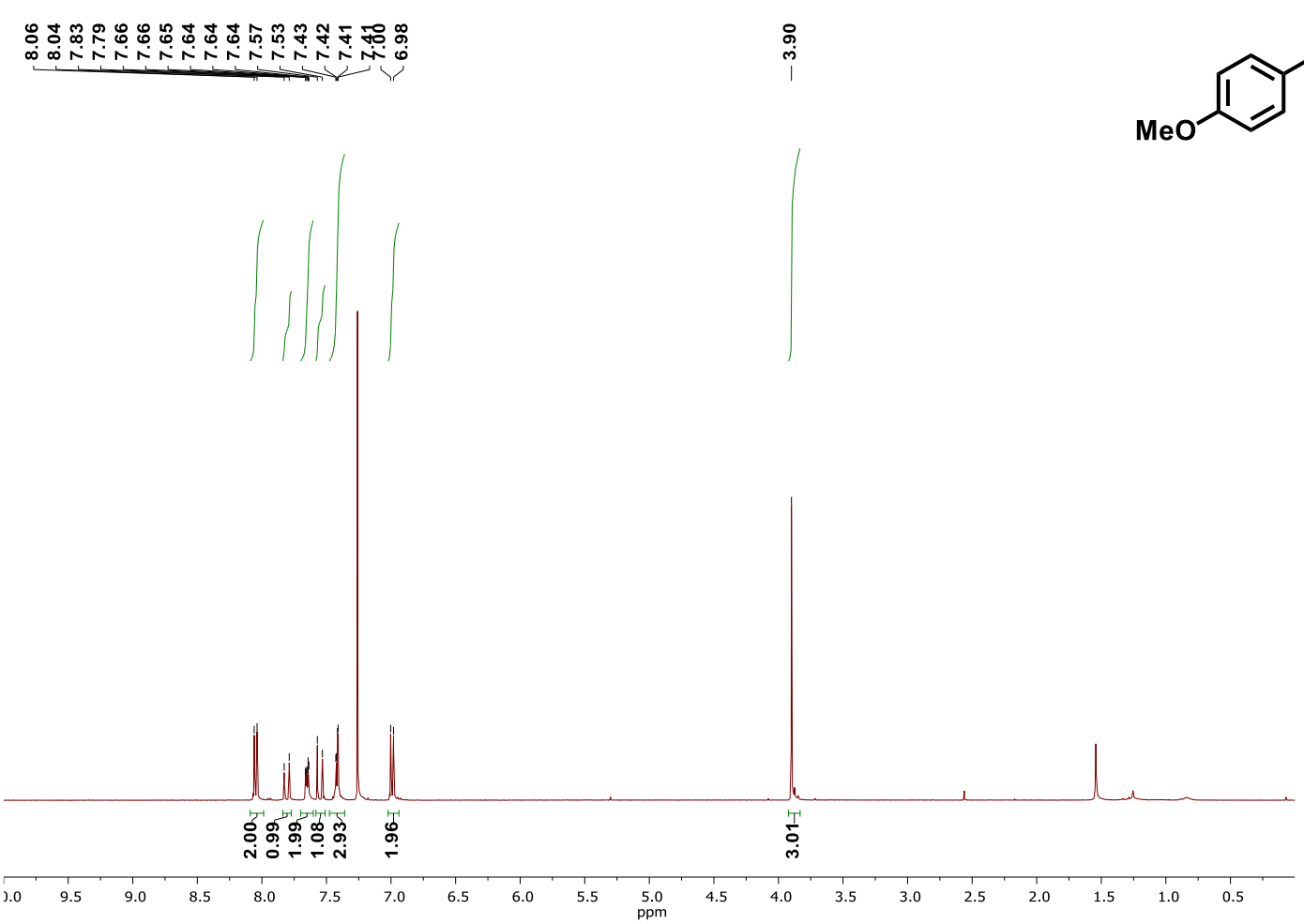

Figure E.2.5 ^{1}H NMR (400 MHz, $CDCl_3$) spectrum recorded for 4'-methoxychalcone.

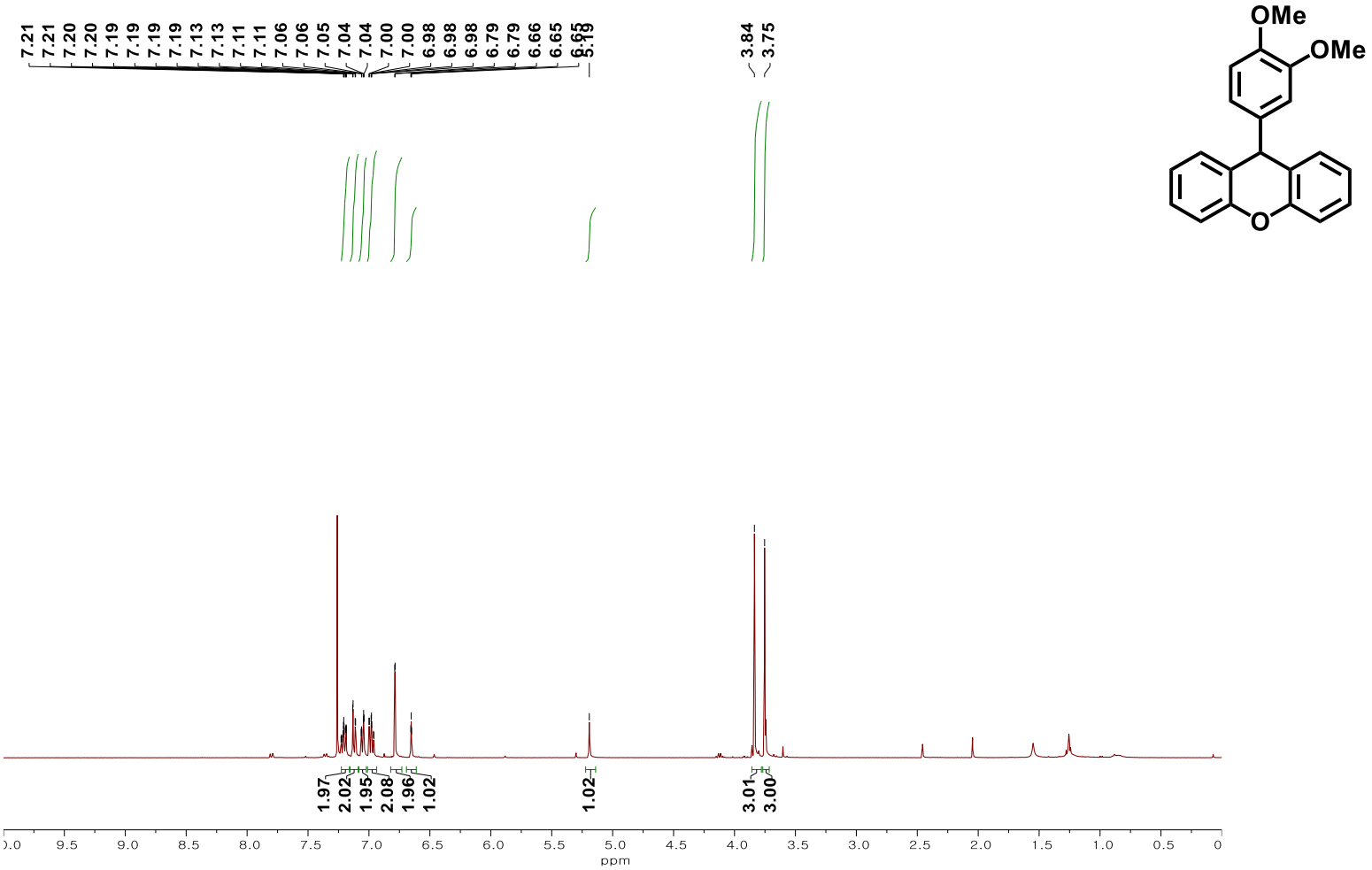

Figure E.2.6 ^{1}H NMR (400 MHz, $CDCl_3$) spectrum recorded for 9-(3,4-dimethoxyphenyl)-9H-xanthene.

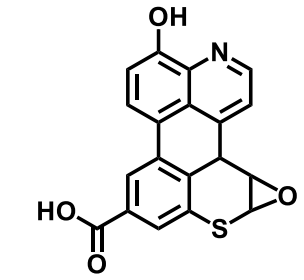

Proposed sAO structure

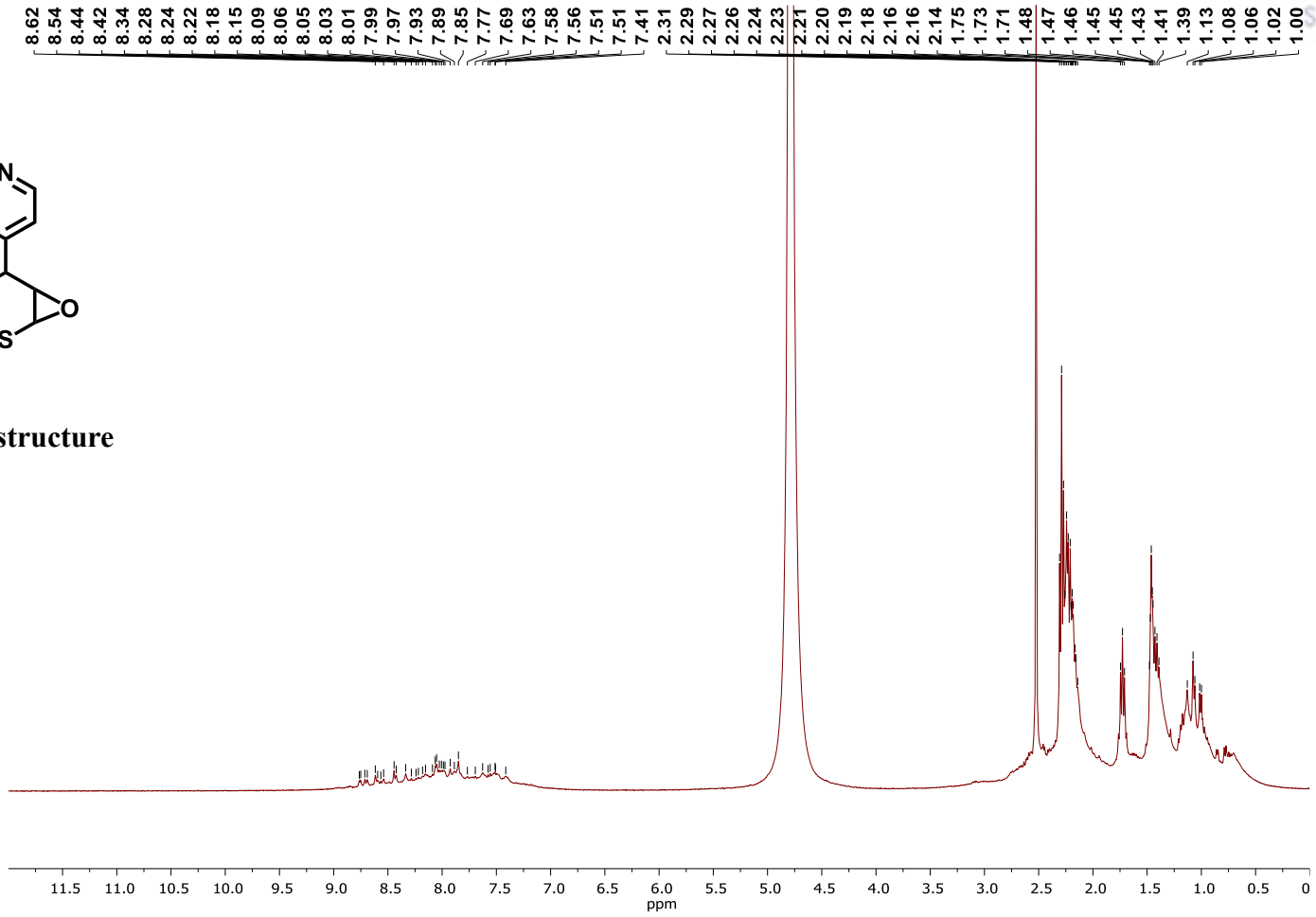

Figure E.3.1 ^{1}H NMR (400 MHz, D_2O) spectrum recorded for soluble asphaltene oxide (sAO).

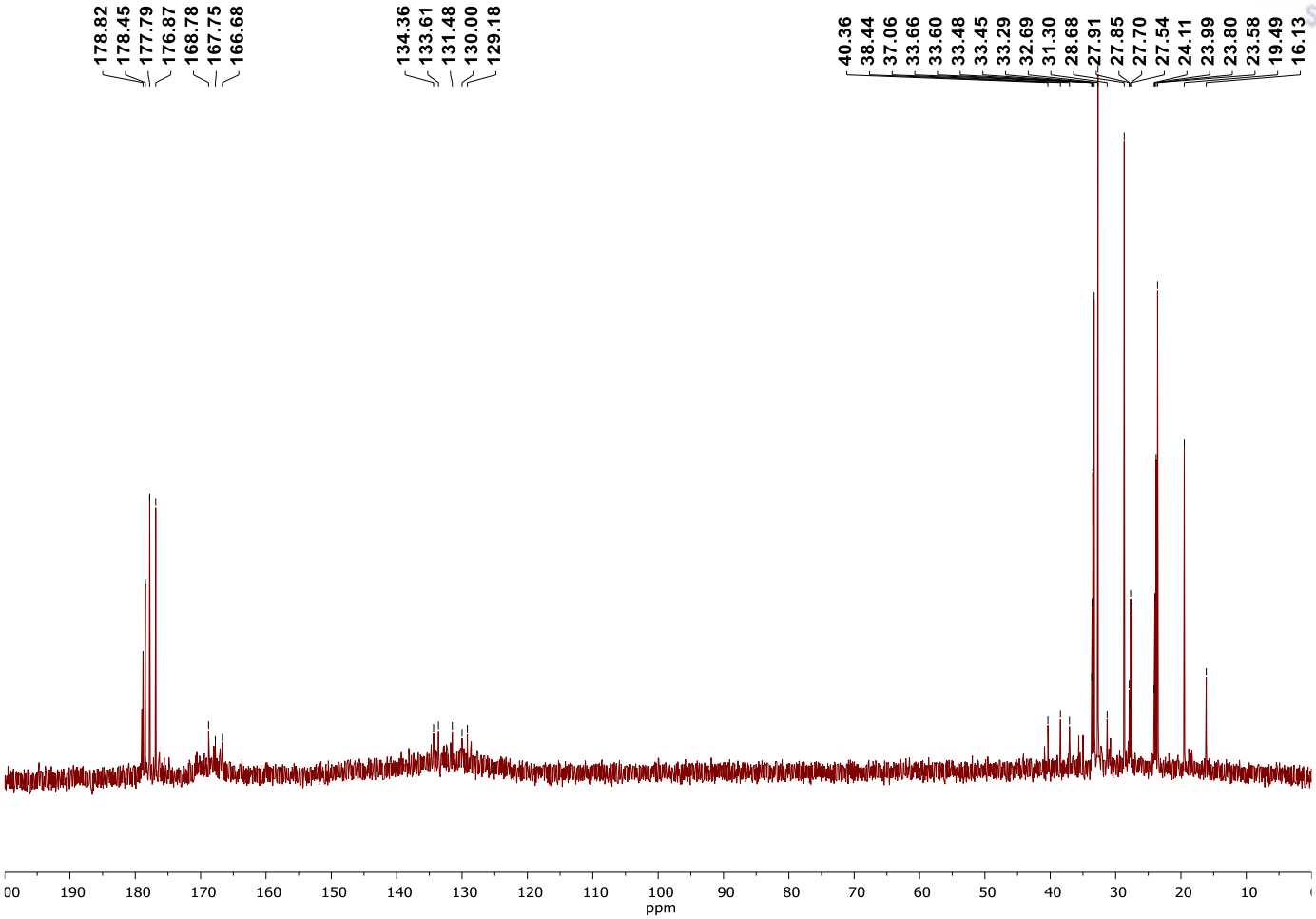

Figure E.3.2 ^{13}C NMR (400 MHz, D_2O) spectrum recorded for soluble asphaltene oxide (sAO).

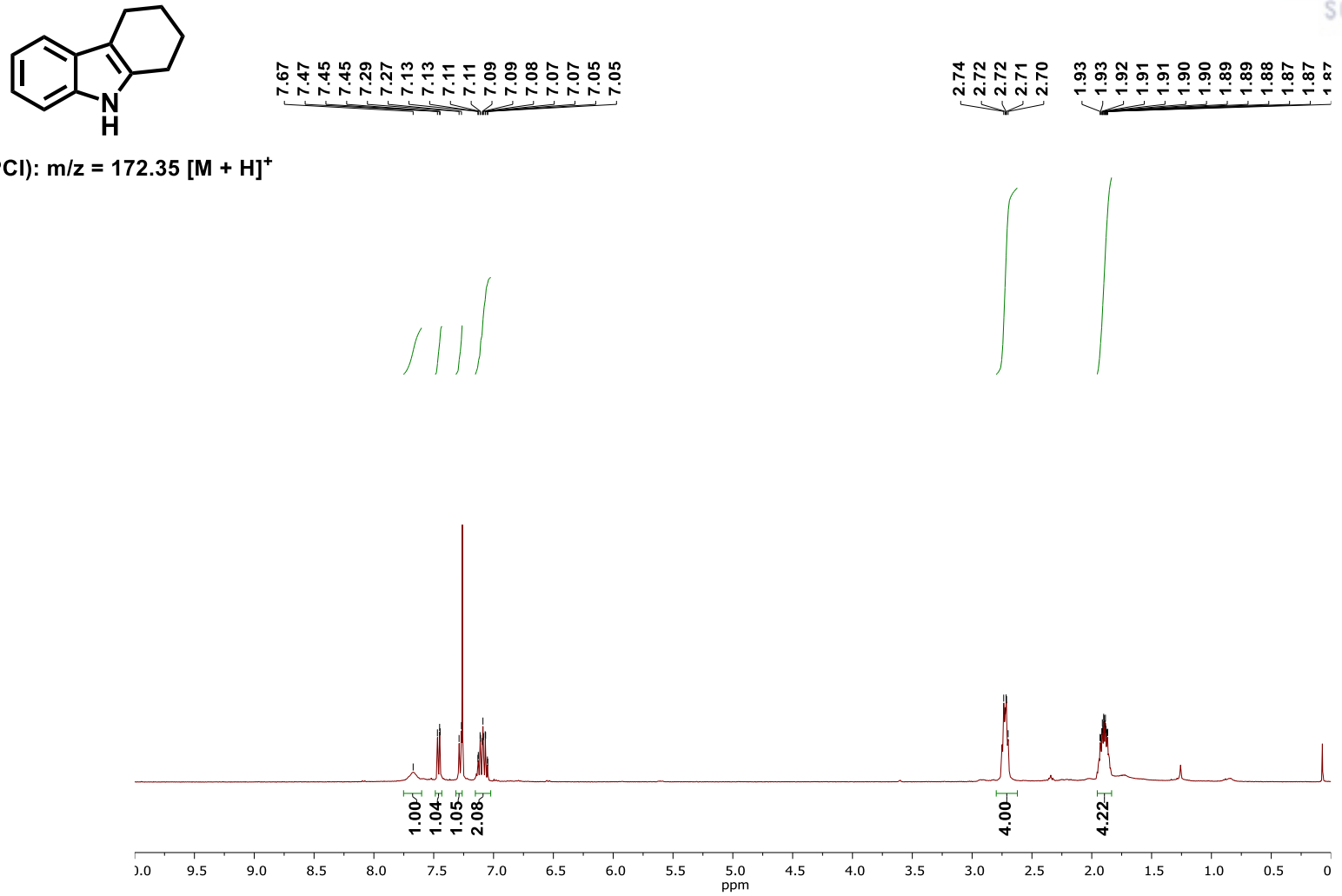

Figure E.3.3 ^{1}H NMR (400 MHz, $CDCl_3$) spectrum recorded for 1,2,3,4-tetrahydrocarbazole.

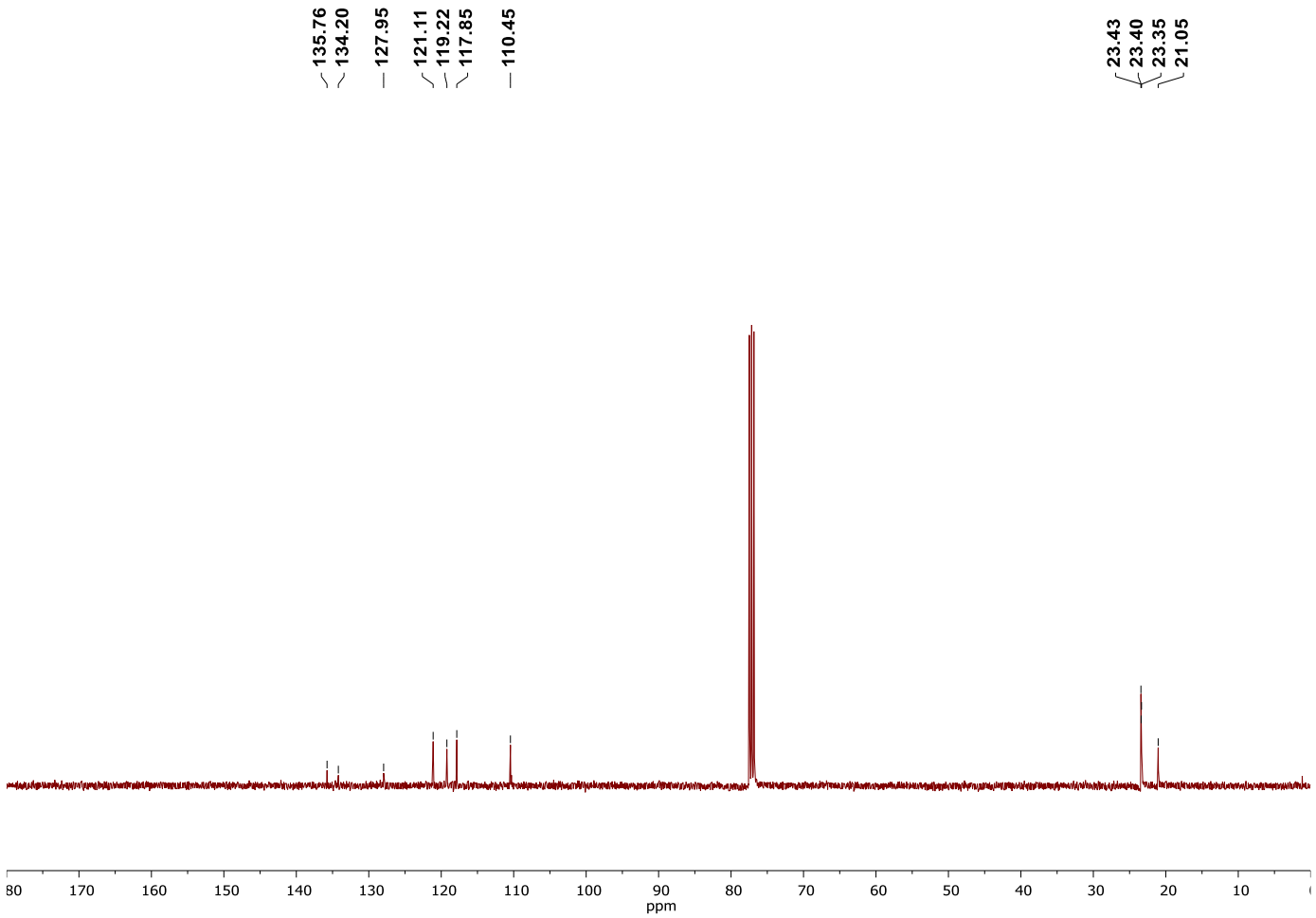

Figure E.3.4 ^{13}C NMR (400 MHz, $CDCl_3$) spectrum recorded for 1,2,3,4-tetrahydrocarbazole.

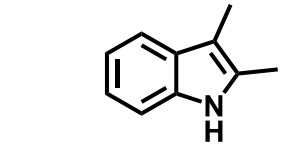

MS(APCI): m/z = 146.27 $[M + H]^+$

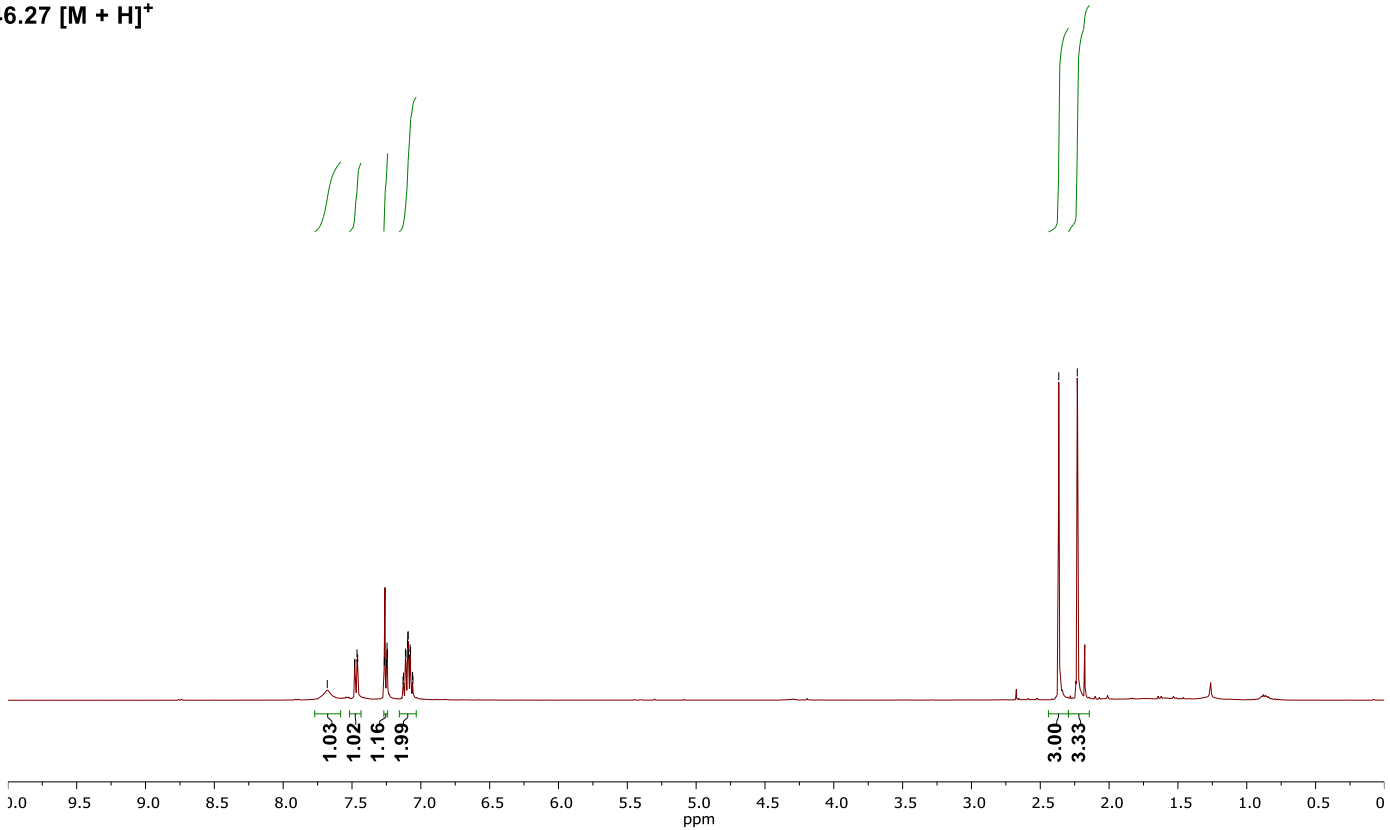

Figure E.3.5 ^{1}H NMR (400 MHz, $CDCl_3$) spectrum recorded for Table 3.3, Entry 5.

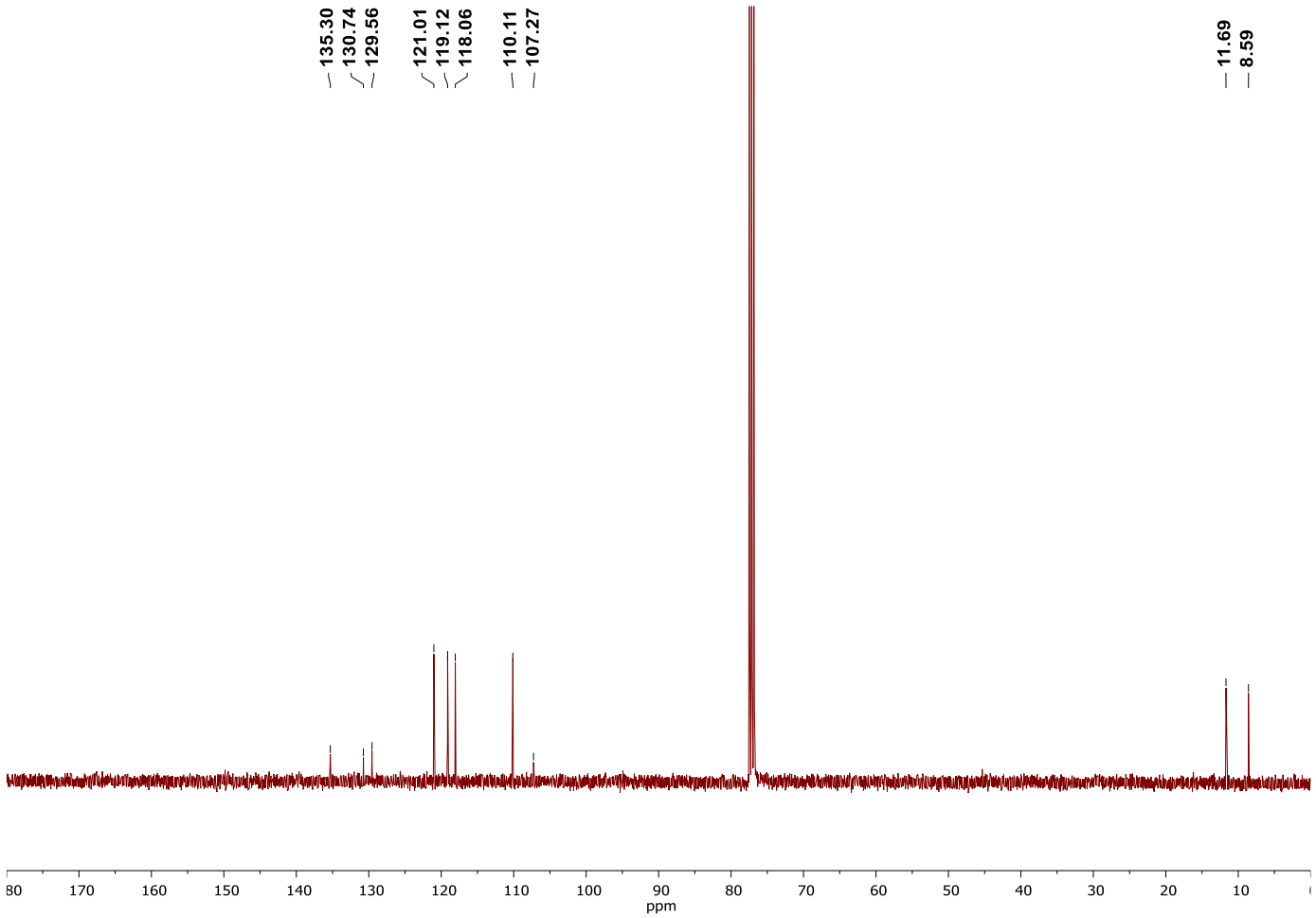

Figure E.3.6 ^{13}C NMR (400 MHz, $CDCl_3$) spectrum recorded for Table 3.3, Entry 5.

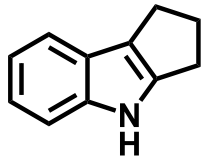

MS(APCI): m/z = 158.22 $[M + H]^+$

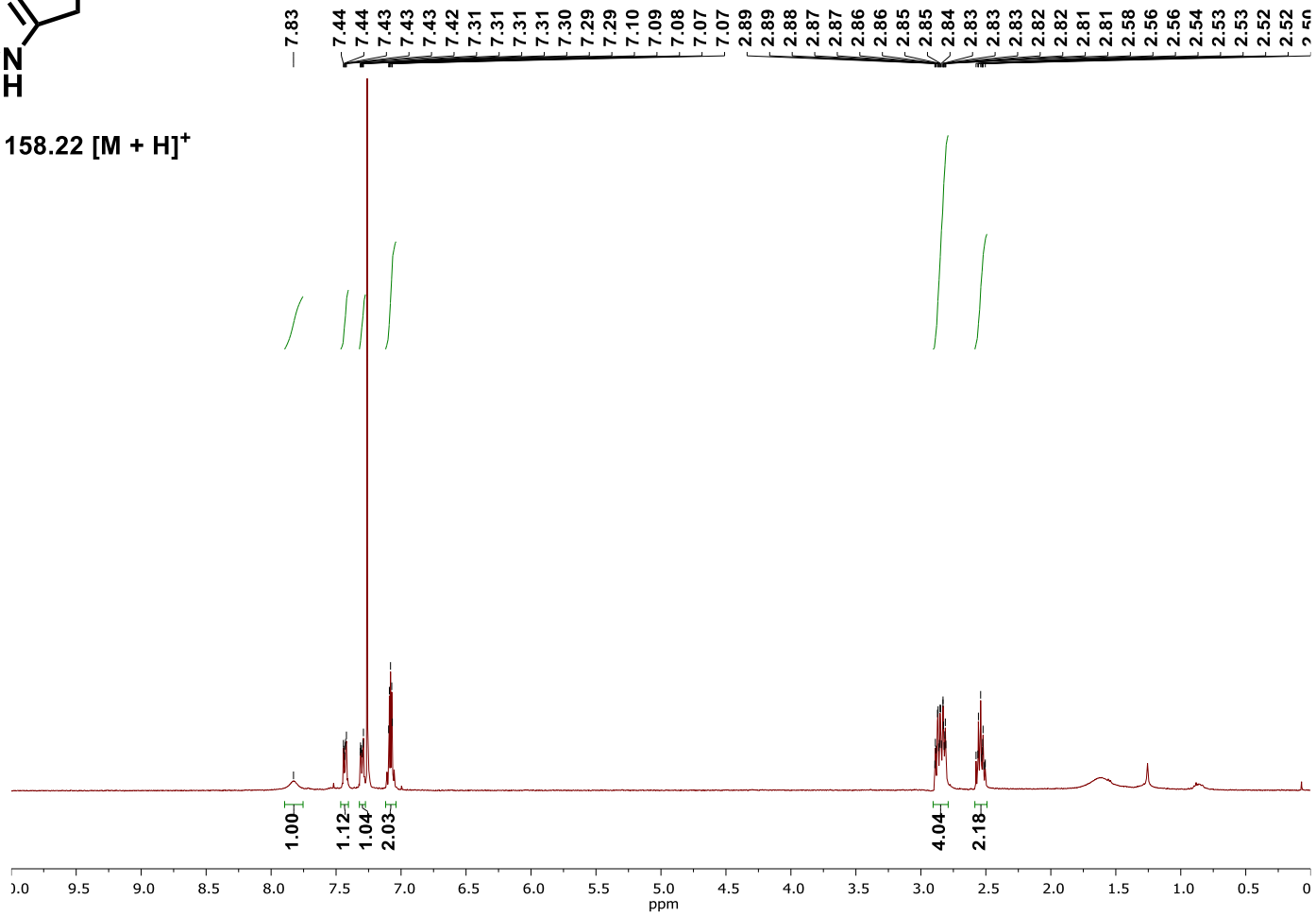

Figure E.3.7 ^{1}H NMR (400 MHz, $CDCl_3$) spectrum recorded for Table 3.3, Entry 6.

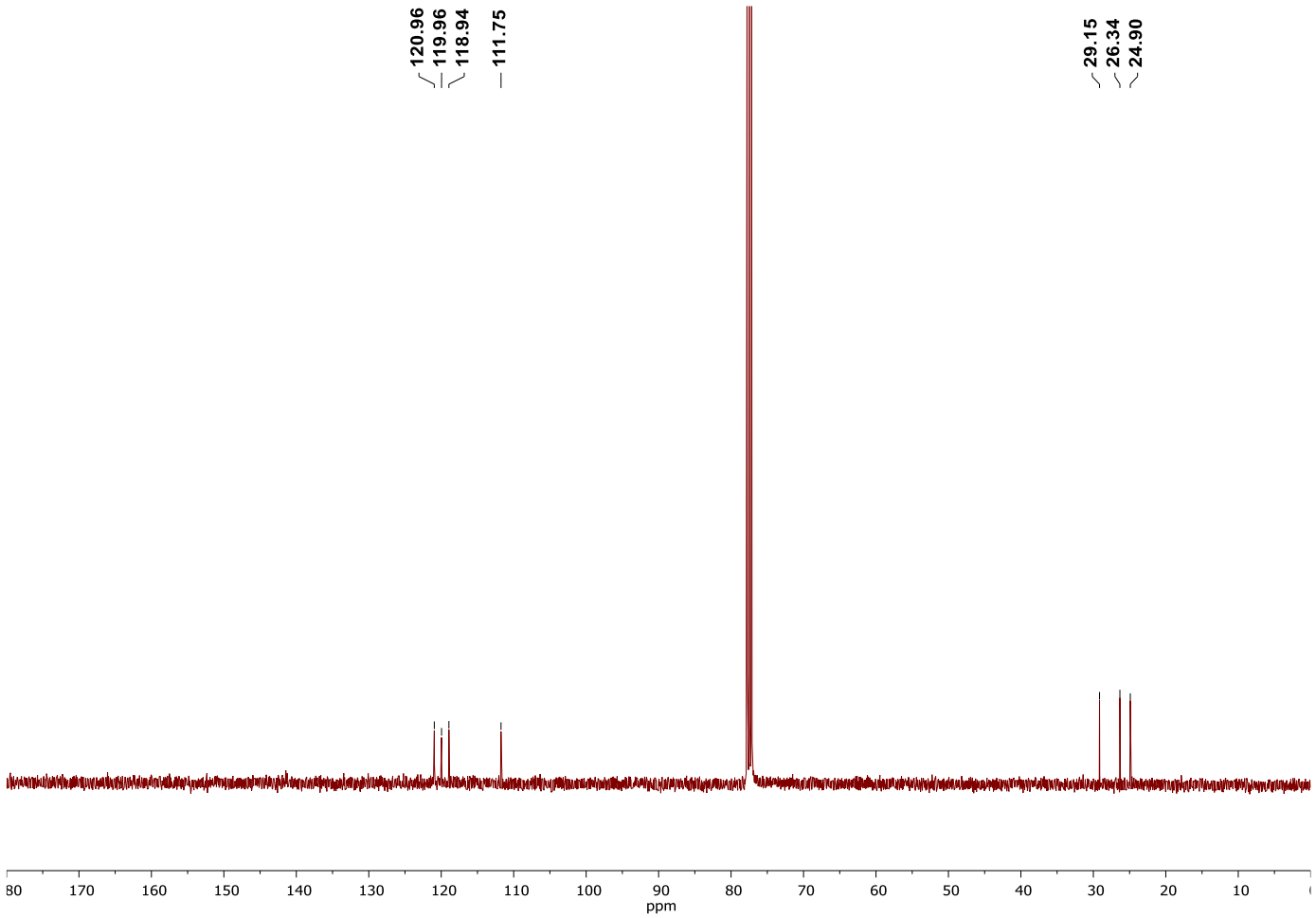

Figure E.3.8 ^{13}C NMR (400 MHz, $CDCl_3$) spectrum recorded for Table 3.3, Entry 6.

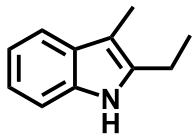

MS(APCI): m/z = 160.35 $[M + H]^+$

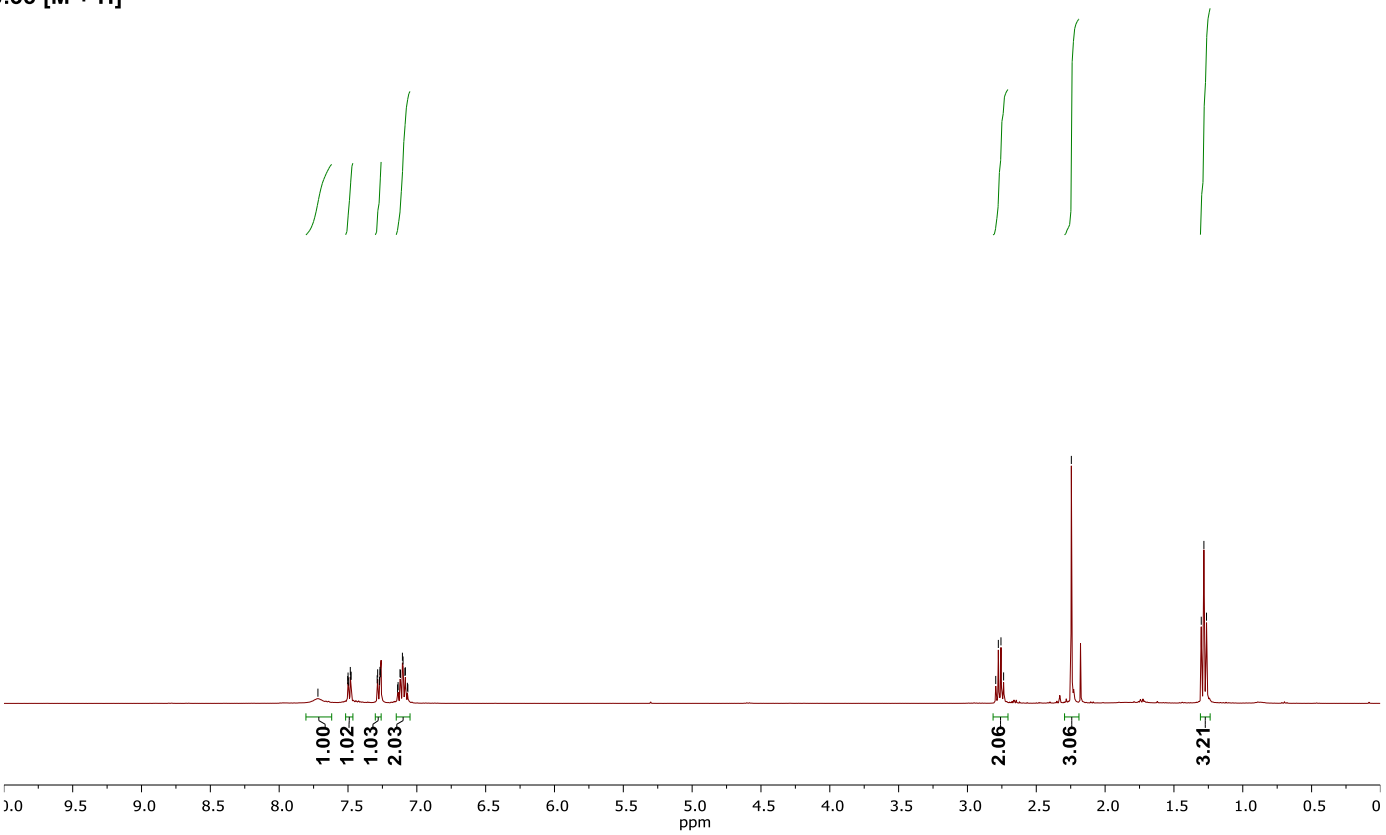

Figure E.3.9 ^{1}H NMR (400 MHz, $CDCl_3$) spectrum recorded for Table 3.3, Entry 7.

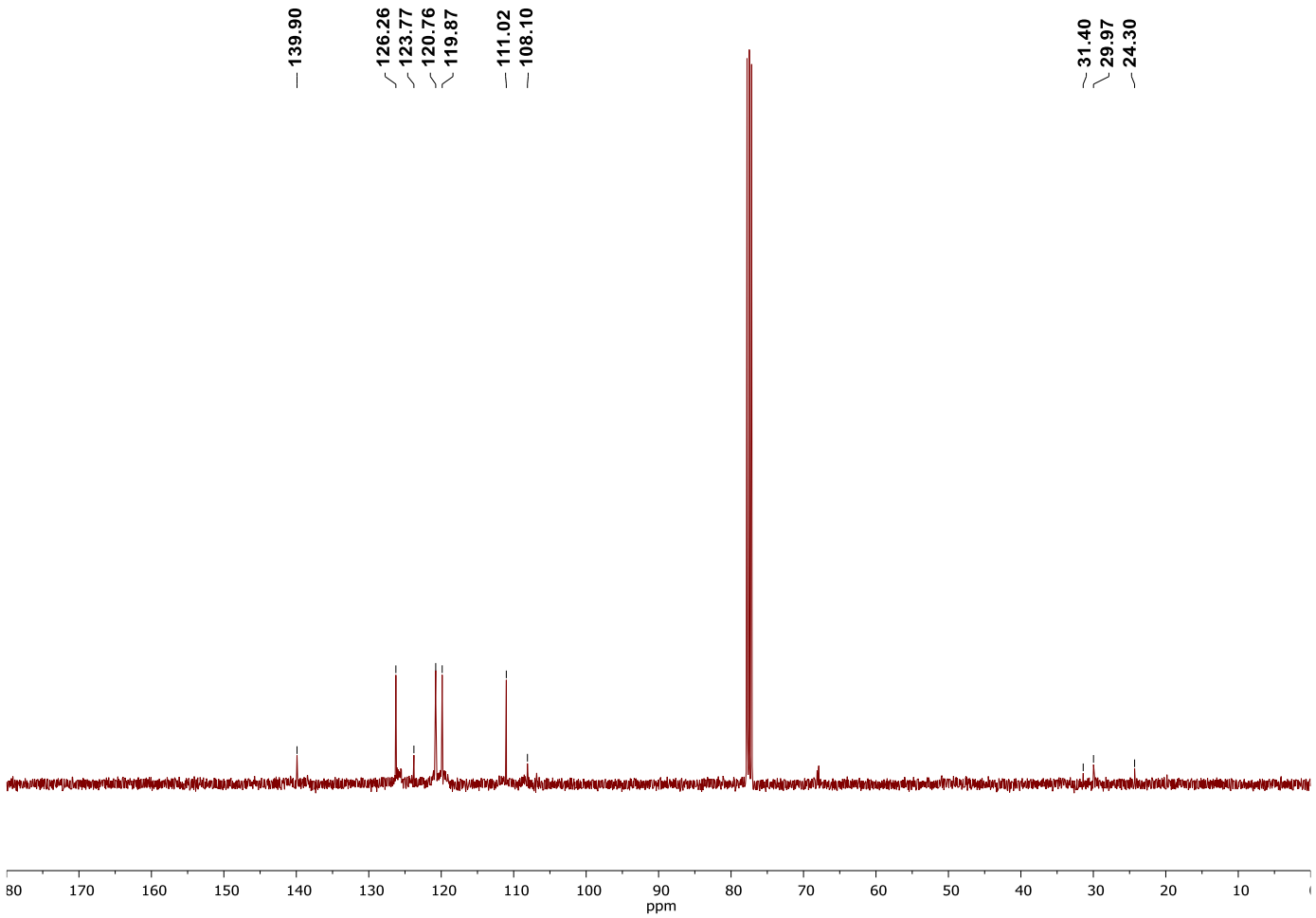

Figure E.3.10 ^{13}C NMR (400 MHz, $CDCl_3$) spectrum recorded for Table 3.3, Entry 7.

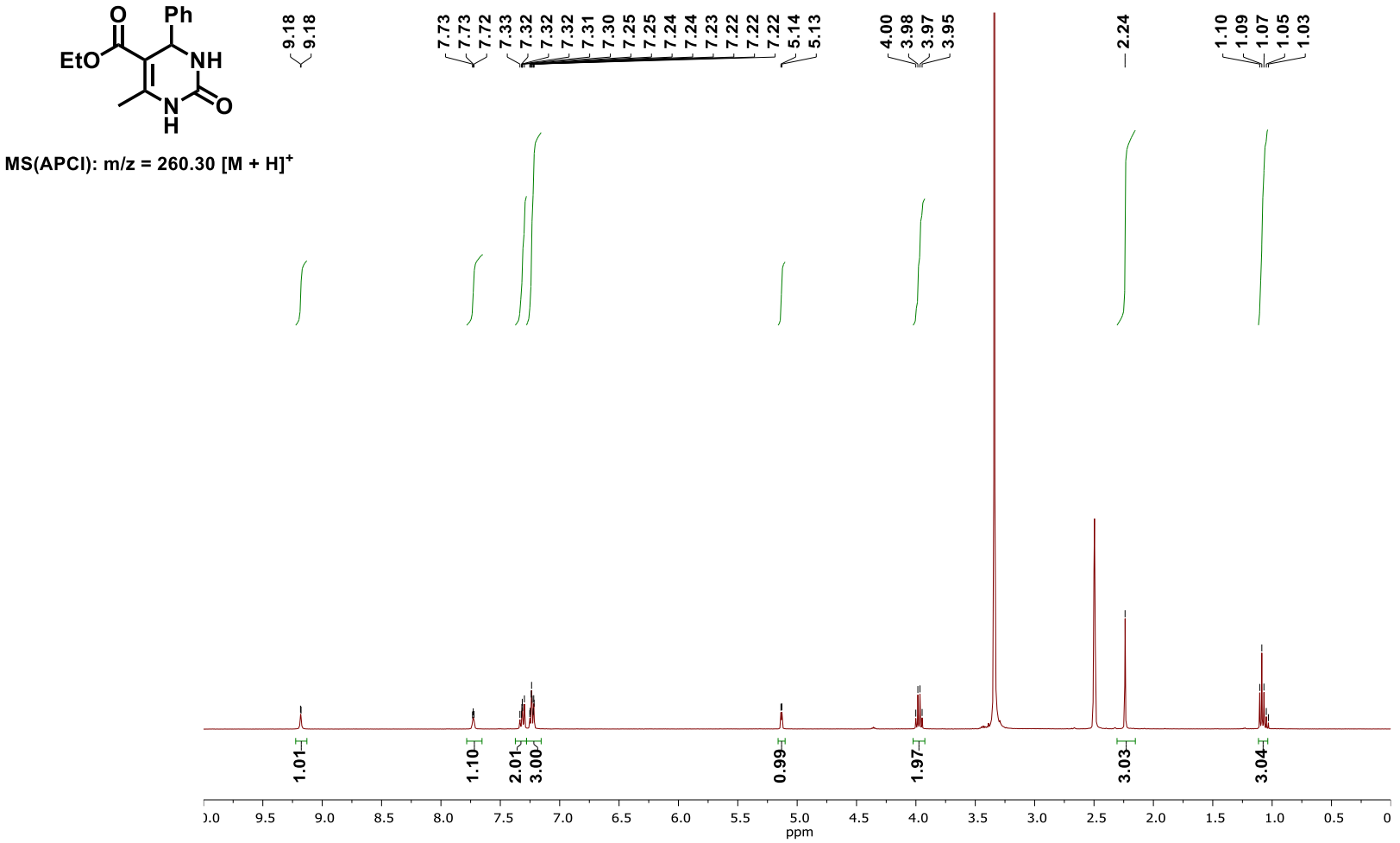

Figure E.3.11 ^{1}H NMR (400 MHz, DMSO-d_6) spectrum recorded for Table A.3.2, Entry 1.

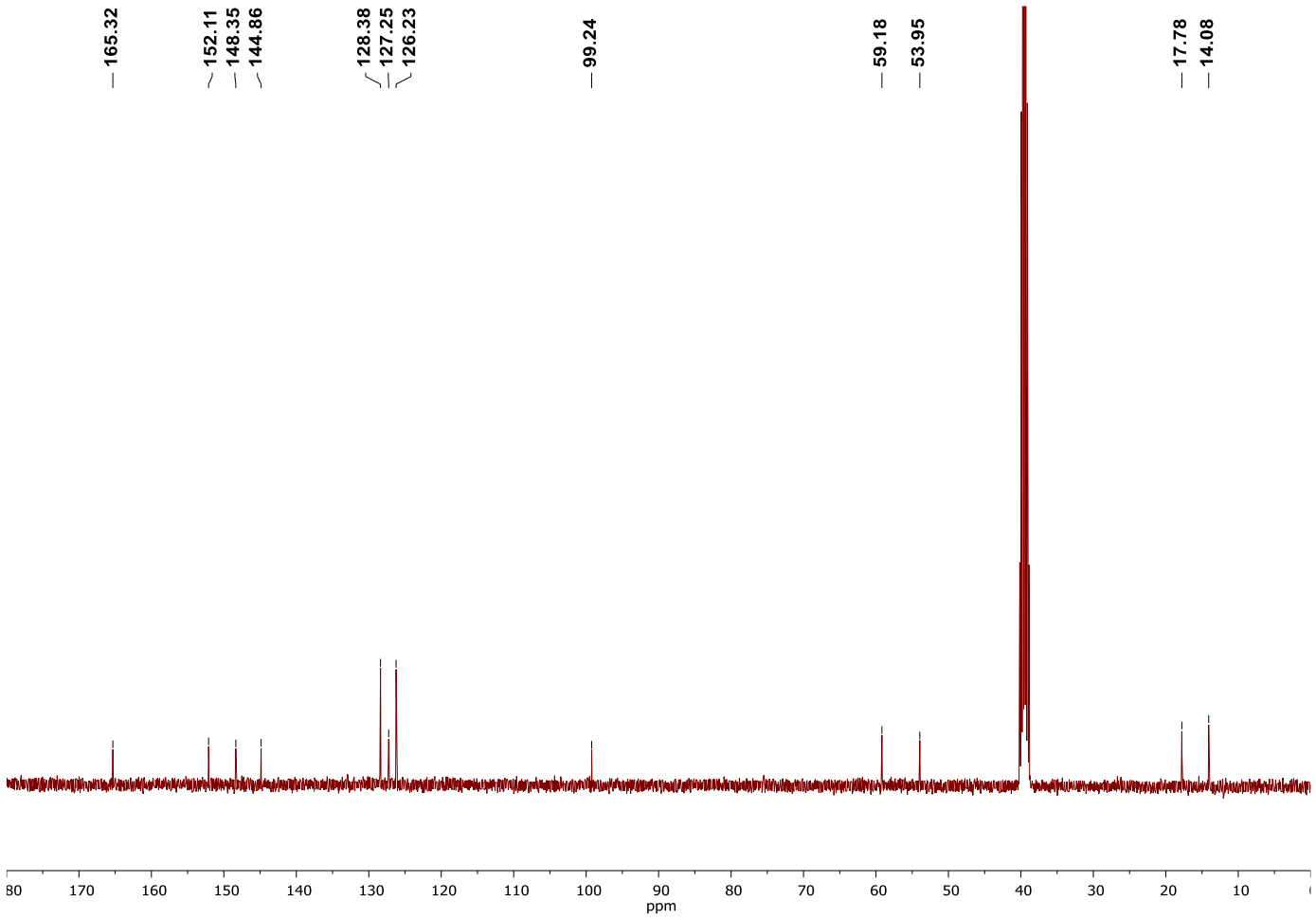

Figure E.3.12 ^{13}C NMR (400 MHz, DMSO-d_6) spectrum recorded for Table A.3.2, Entry 1.

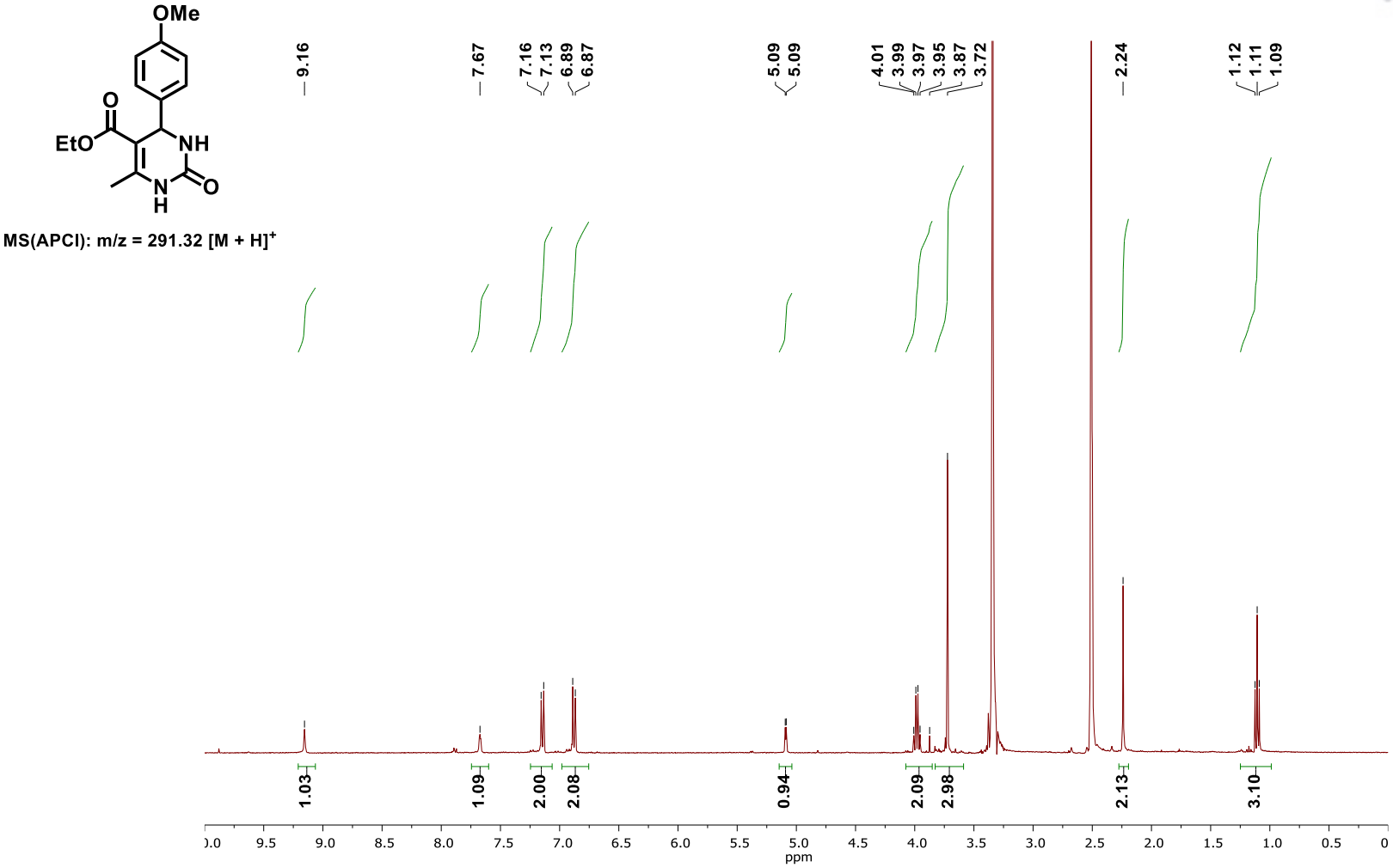

Figure E.3.13 ^{1}H NMR (400 MHz, DMSO-d_6) spectrum recorded for Table A.3.2, Entry 2.

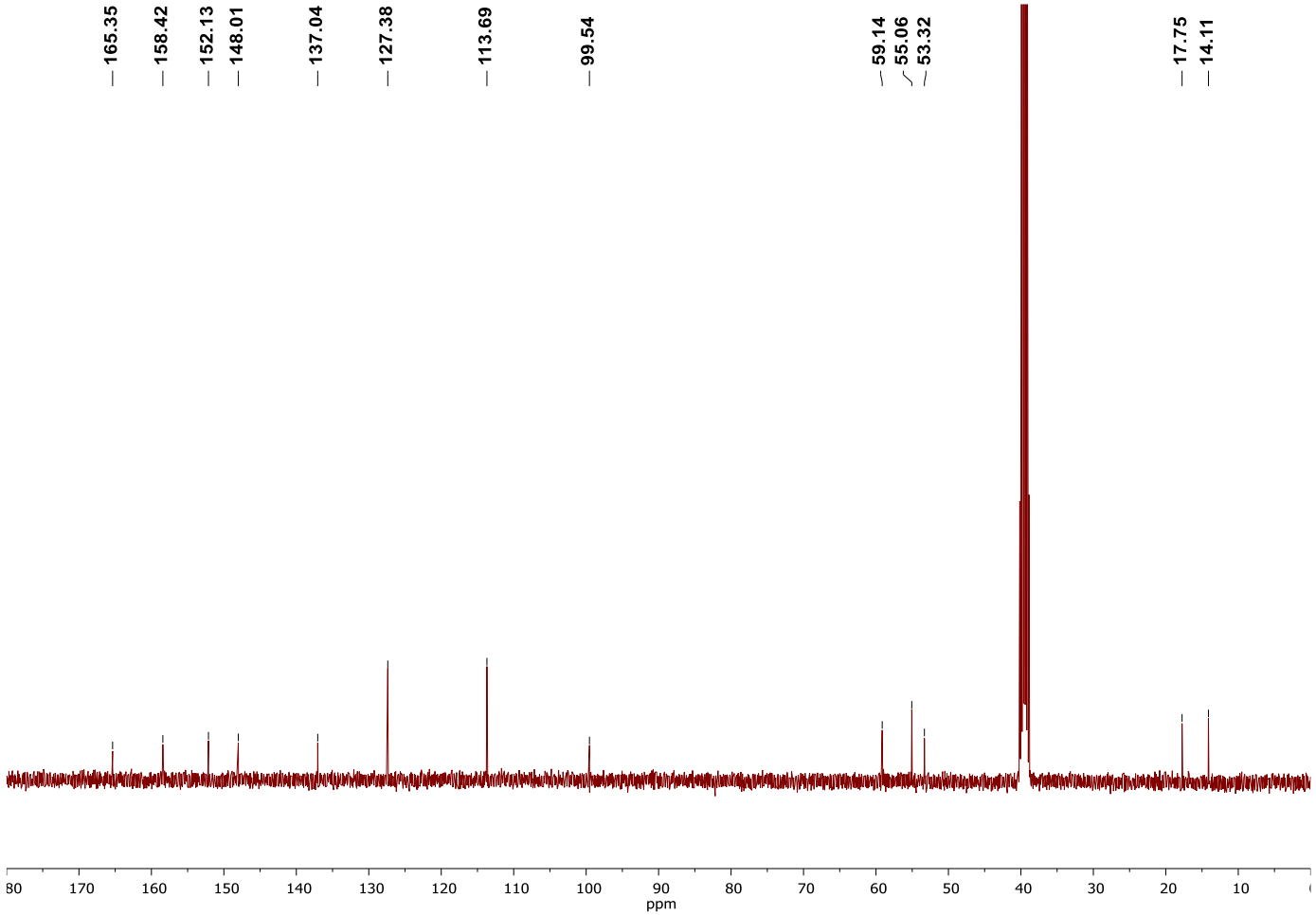

Figure E.3.14 ^{13}C NMR (400 MHz, DMSO-d_6) spectrum recorded for Table A.3.2, Entry 2.

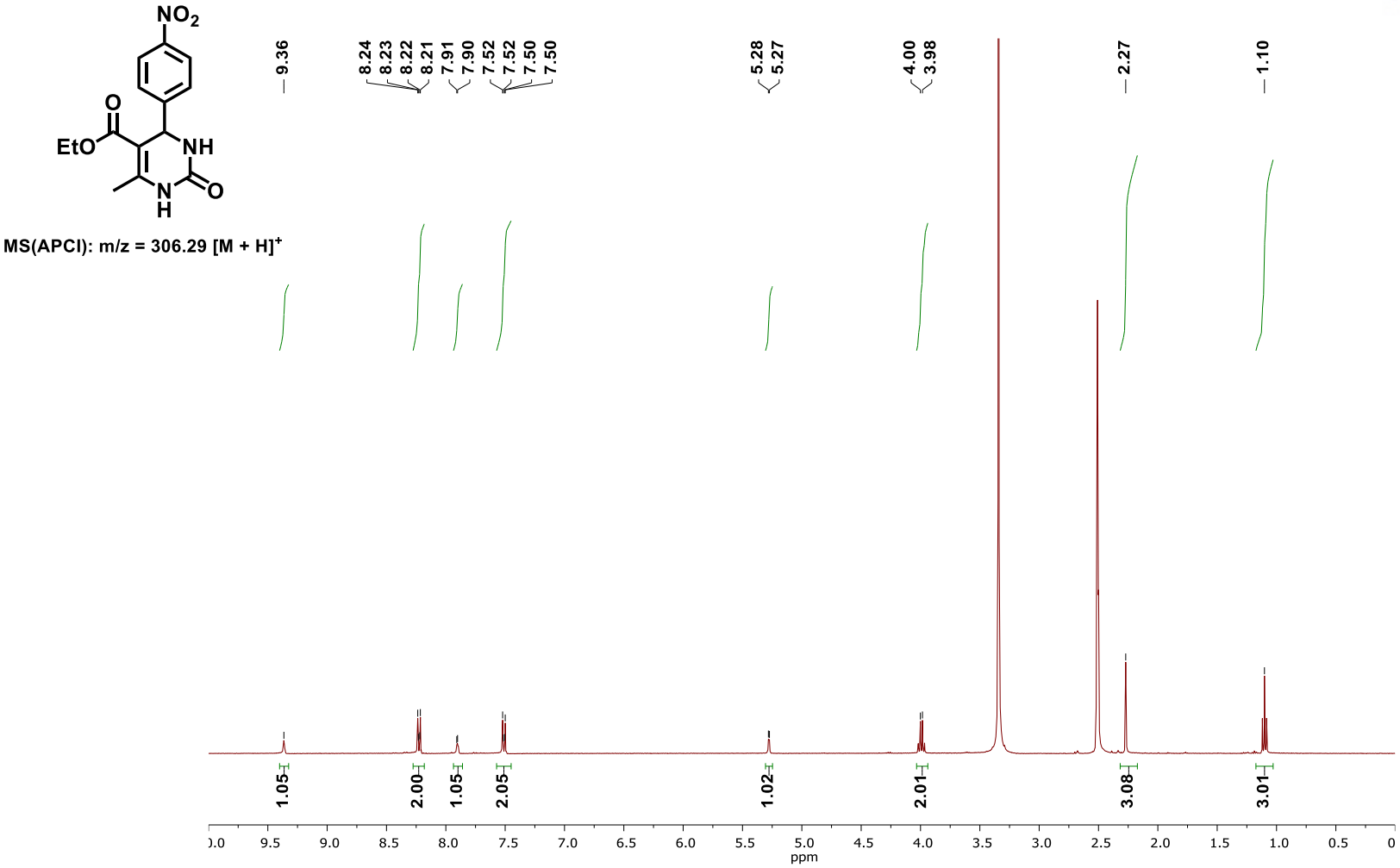

Figure E.3.15 ^{1}H NMR (400 MHz, DMSO-d_6) spectrum recorded for Table A.3.2, Entry 3.

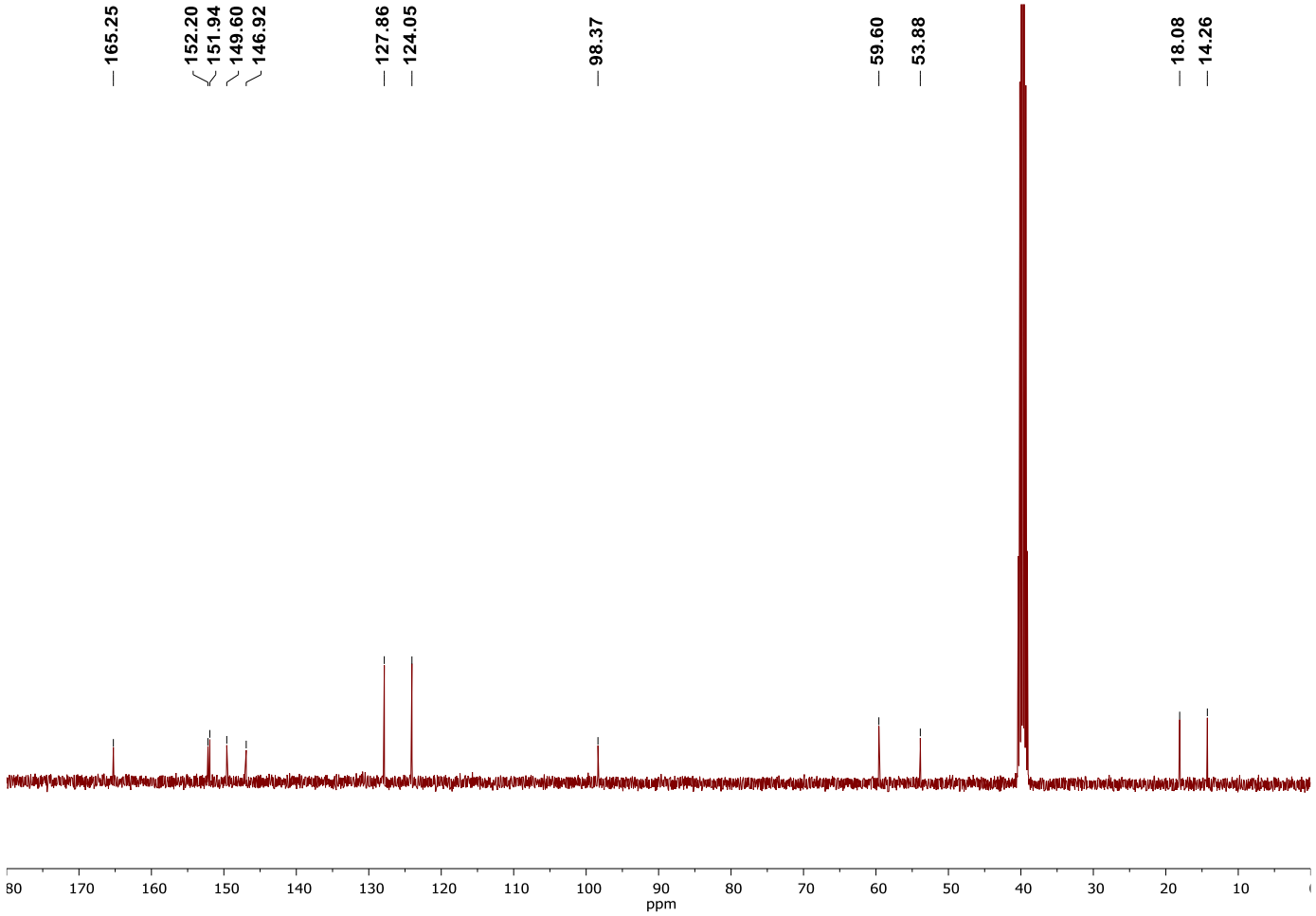

Figure E.3.16 ^{13}C NMR (400 MHz, DMSO-d_6) spectrum recorded for Table A.3.2, Entry 3.

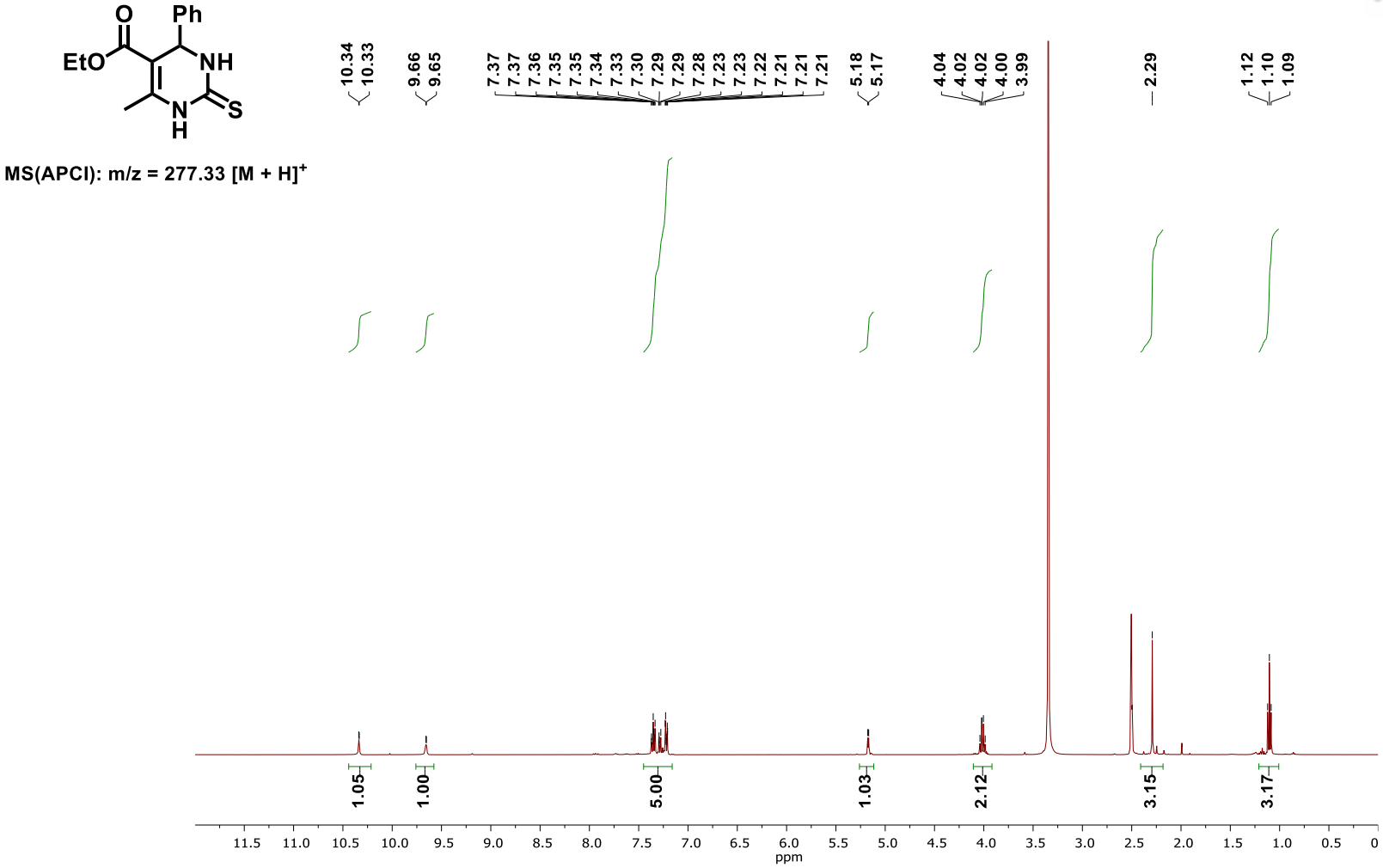

Figure E.3.17 ^{1}H NMR (400 MHz, DMSO-d_6) spectrum recorded for Table A.3.2, Entry 4.

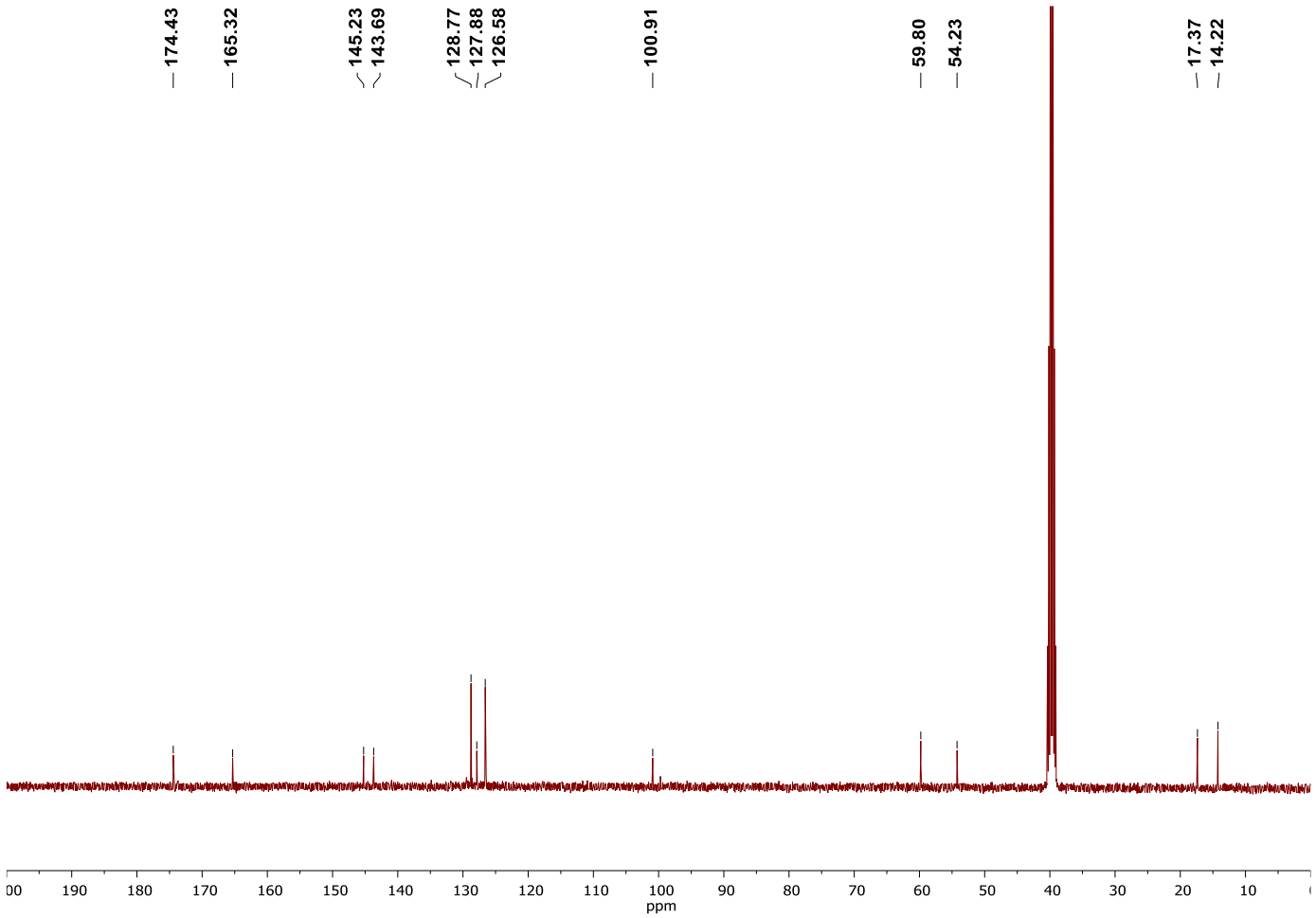

Figure E.3.18 ^{13}C NMR (400 MHz, DMSO-d_6) spectrum recorded for Table A.3.2, Entry 4.

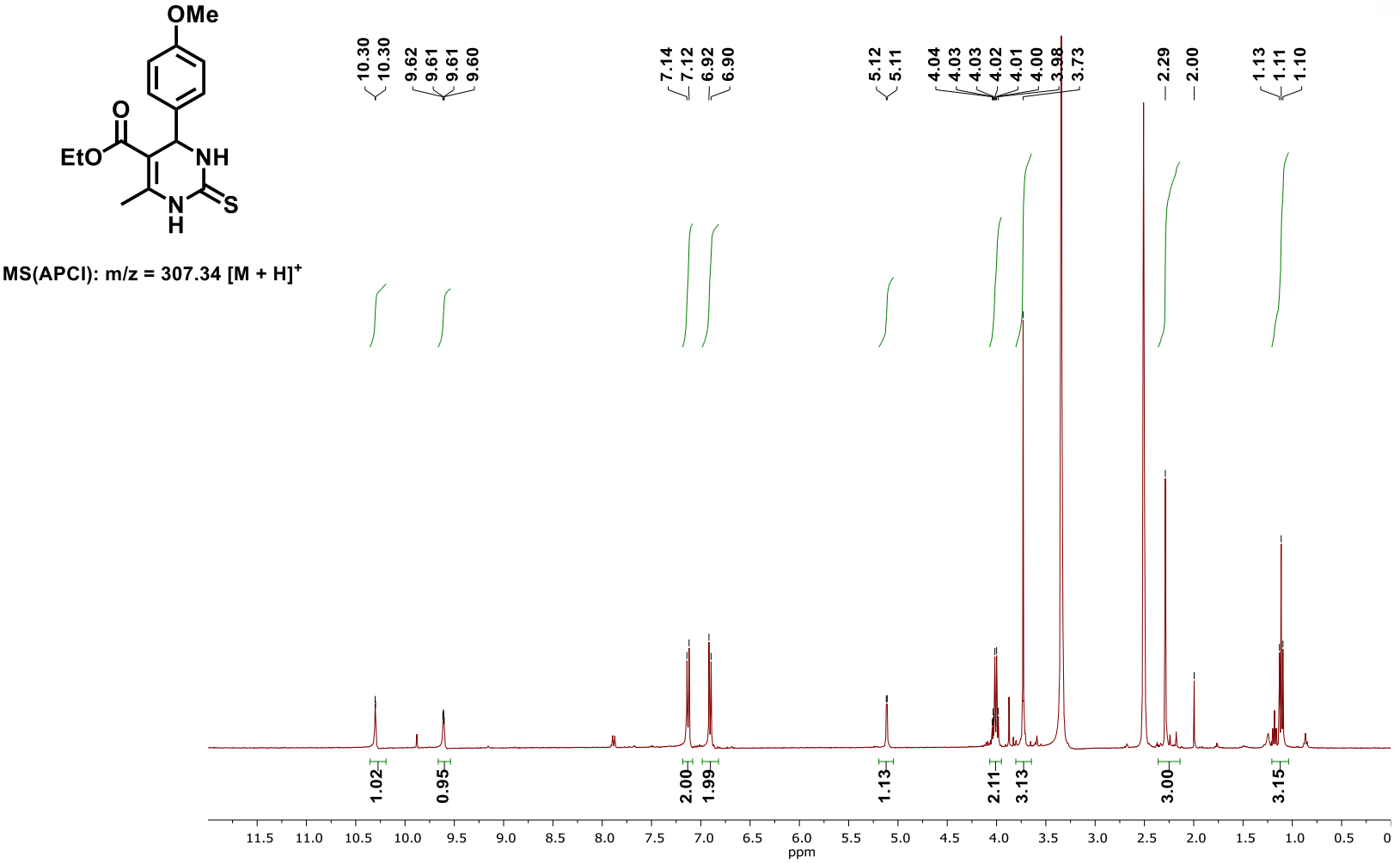

Figure E.3.19 ^{1}H NMR (400 MHz, DMSO-d_6) spectrum recorded for Table A.3.2, Entry 5.

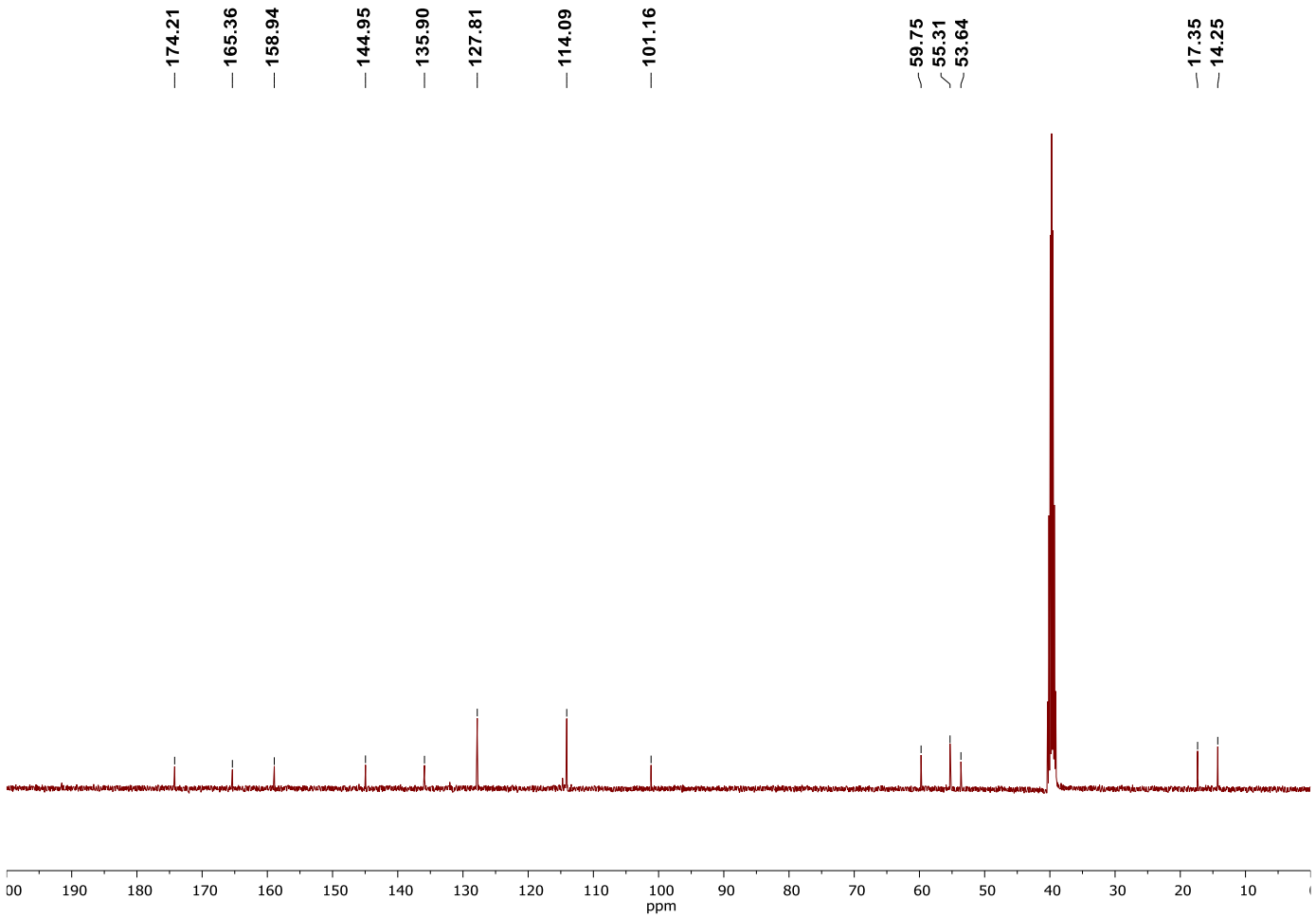

Figure E.3.20 ^{13}C NMR (400 MHz, DMSO-d_6) spectrum recorded for Table A.3.2, Entry 5.

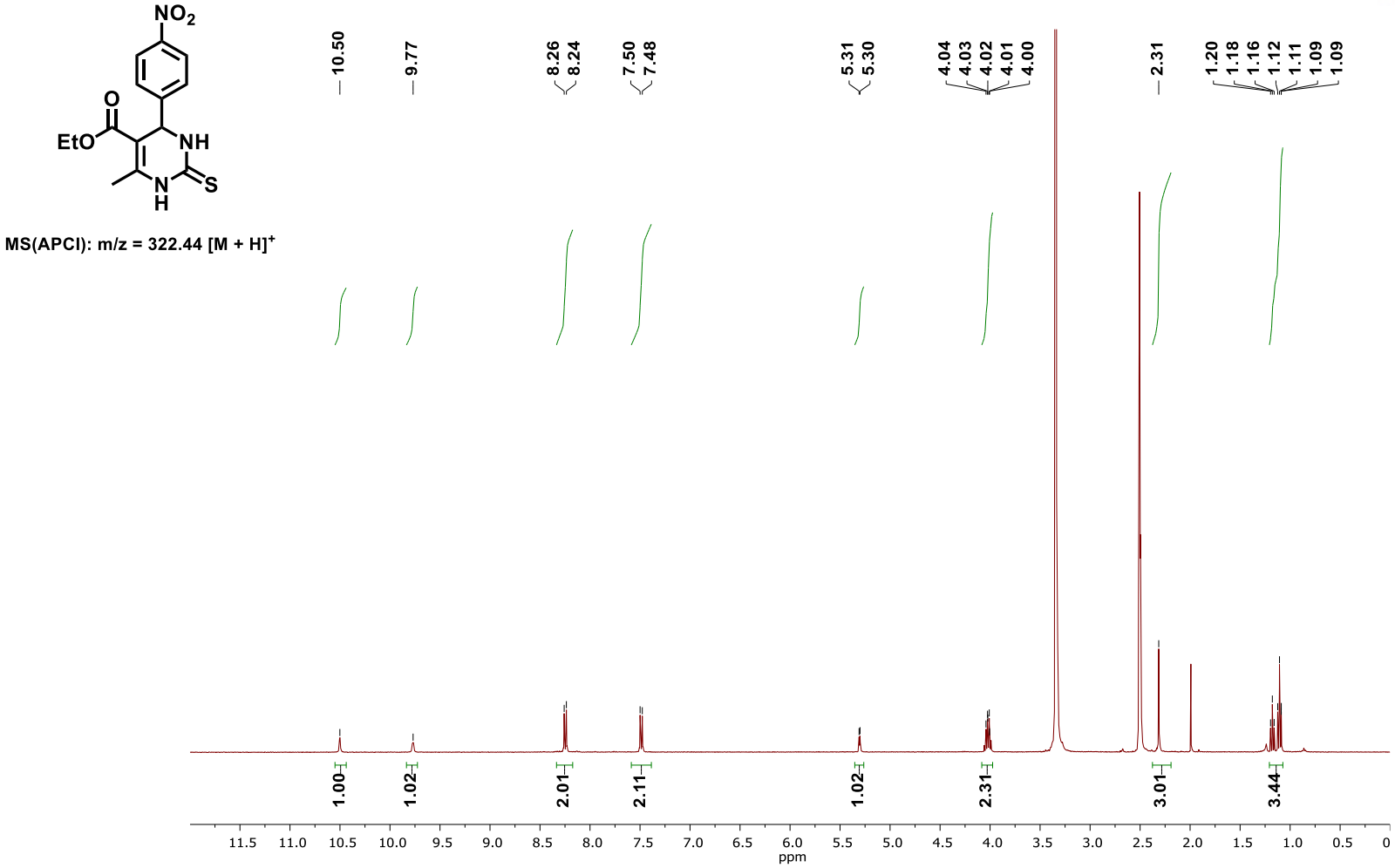

Figure E.3.21 ^{1}H NMR (400 MHz, DMSO-d_6) spectrum recorded for Table A.3.2, Entry 6.

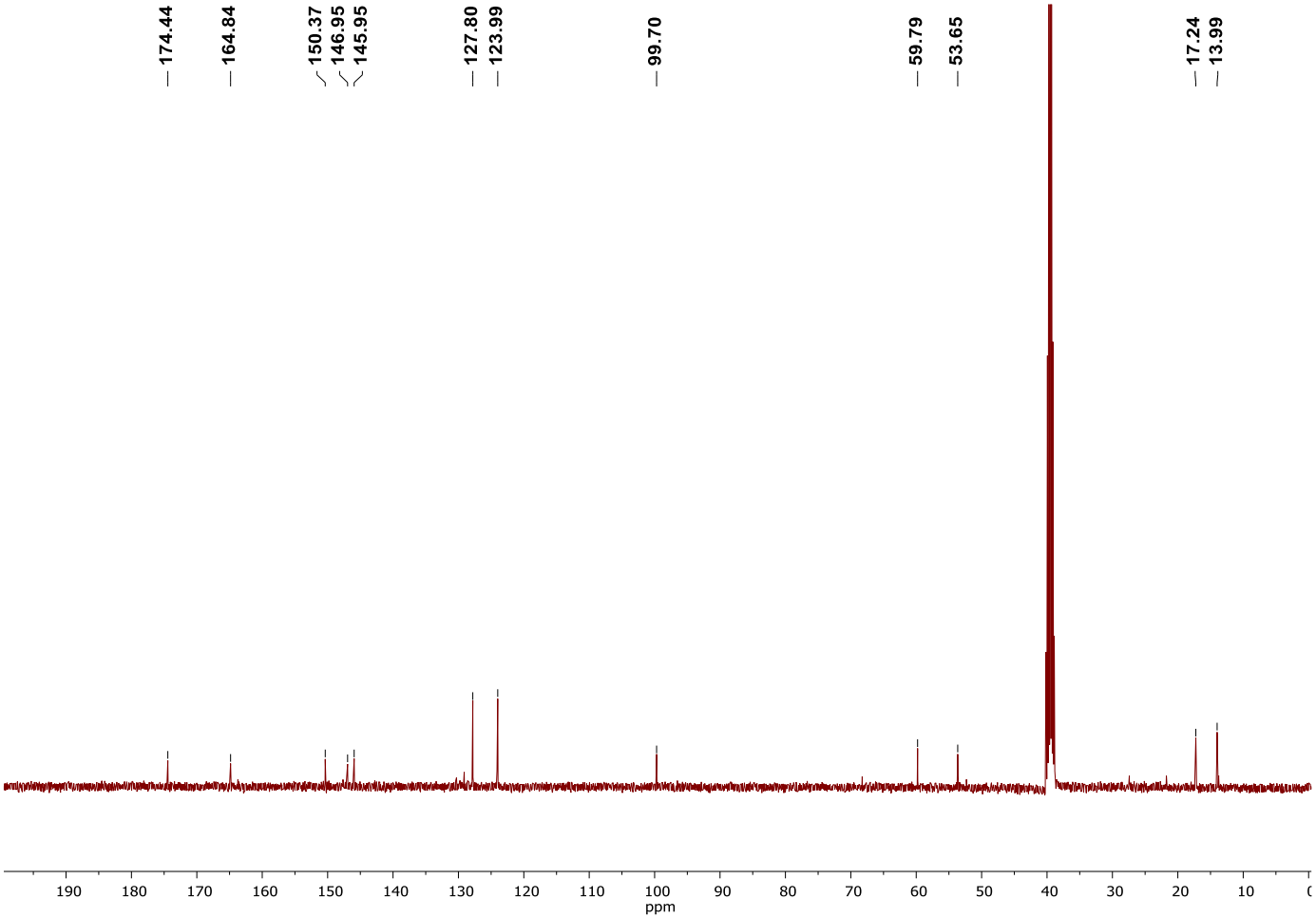

Figure E.3.22 ^{13}C NMR (400 MHz, DMSO-d_6) spectrum recorded for Table A.3.2, Entry 6.

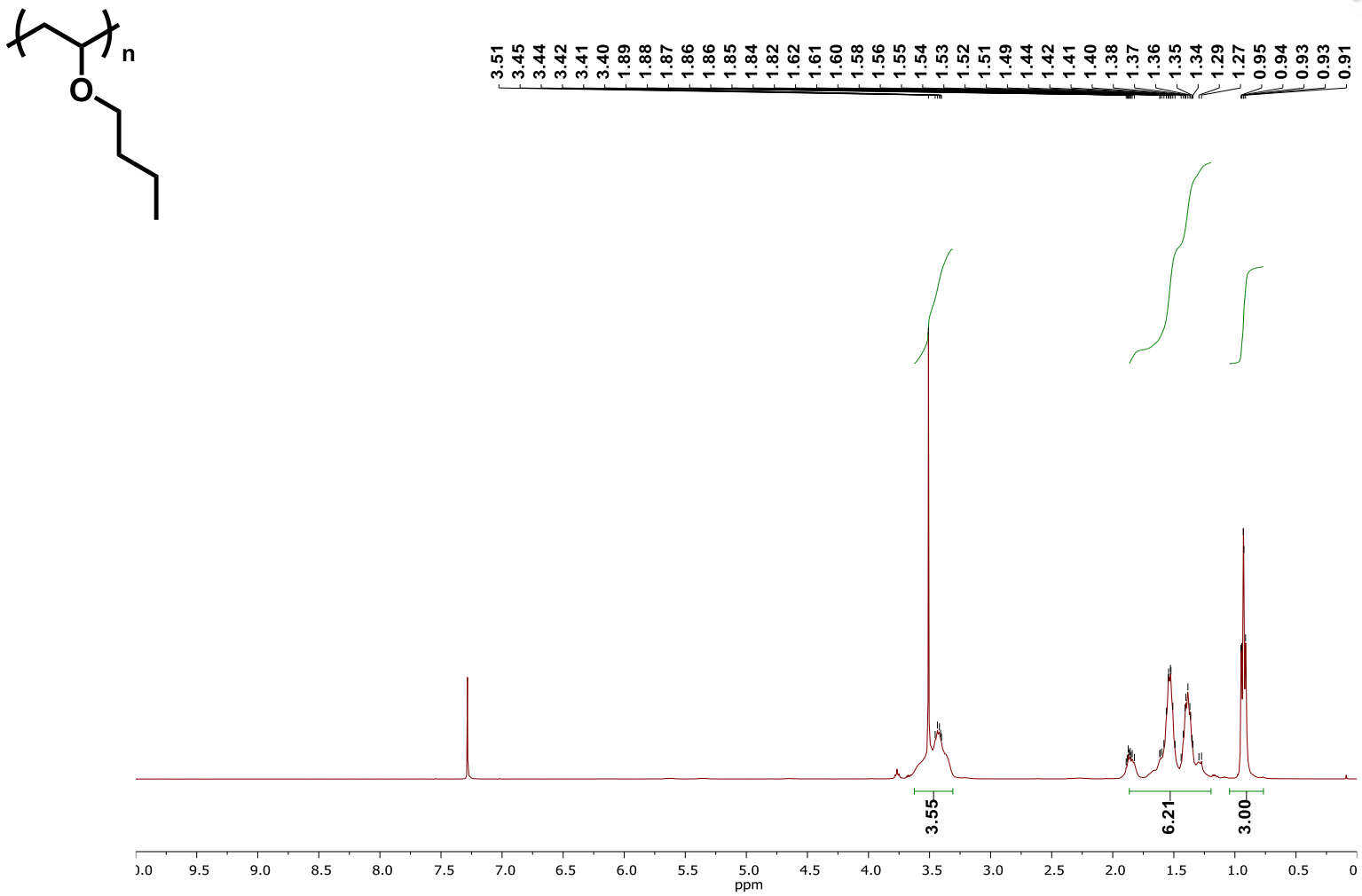

Figure E.3.23 ^{1}H NMR (400 MHz, $CDCl_3$) spectrum recorded for Table 3.5, Entry 1.

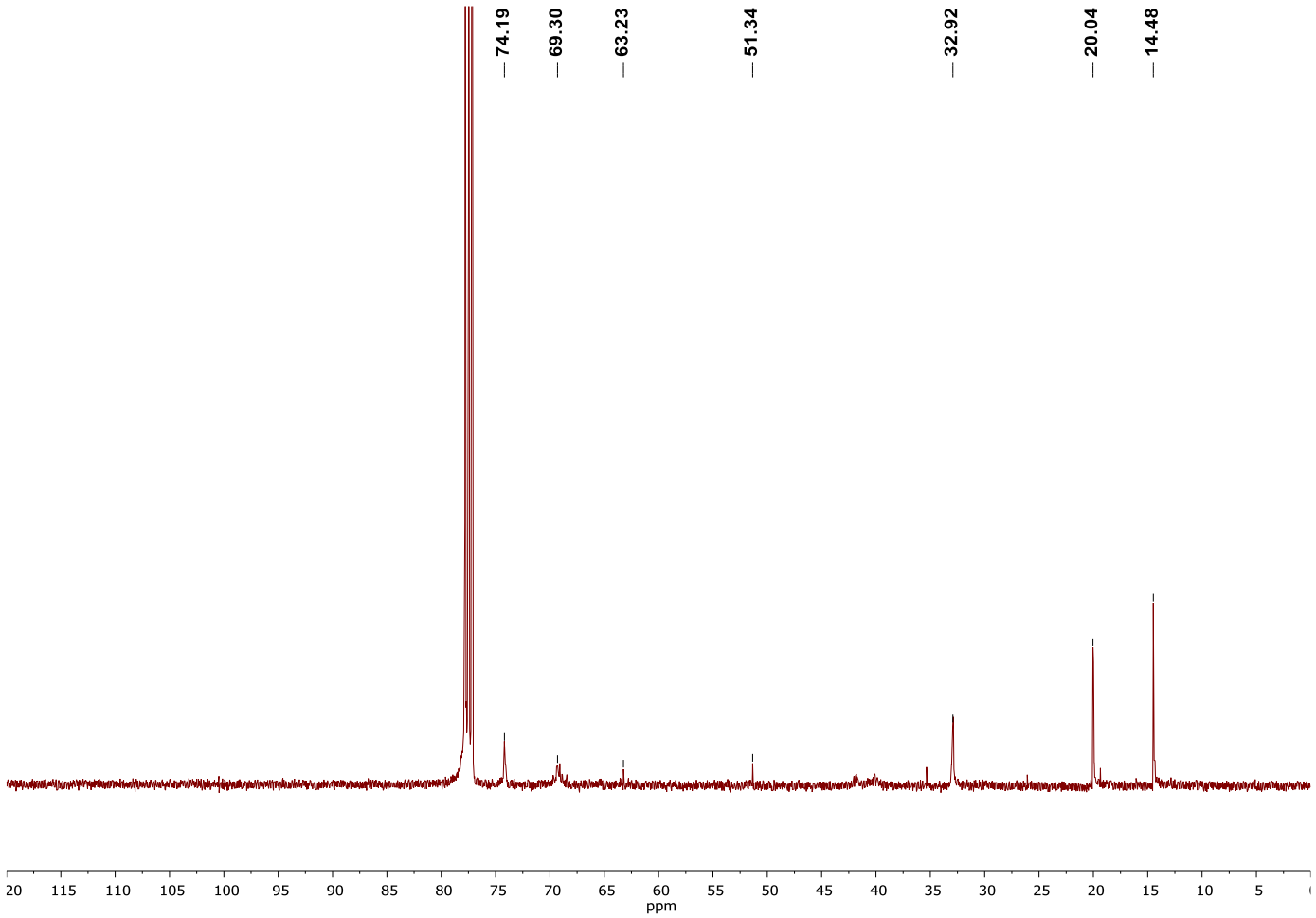

Figure E.3.24 ^{13}C NMR (400 MHz, $CDCl_3$) spectrum recorded for Table 3.5, Entry 1.

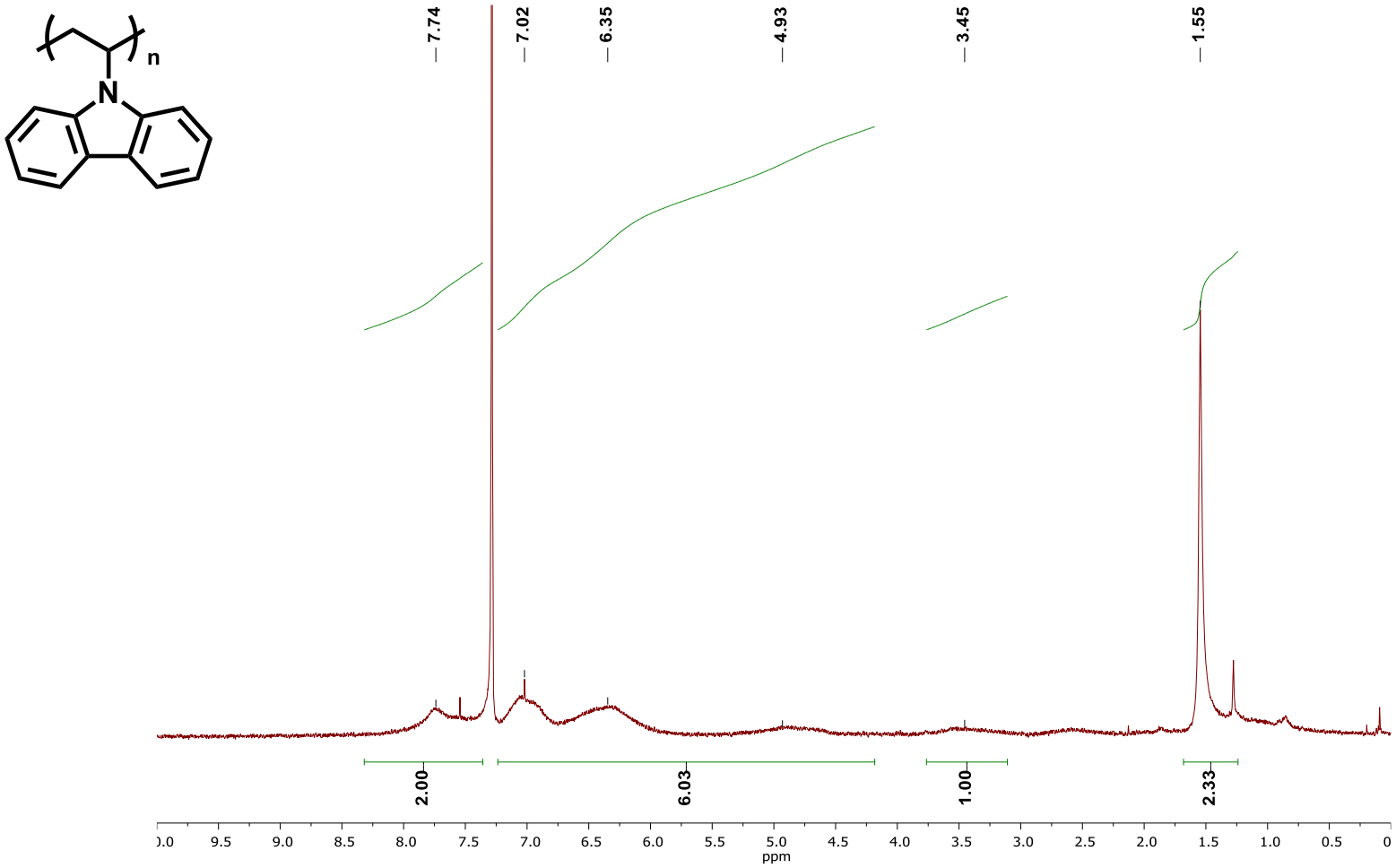

Figure E.3.25 ^{1}H NMR (400 MHz, $CDCl_3$) spectrum recorded for Table 3.5, Entry 2.

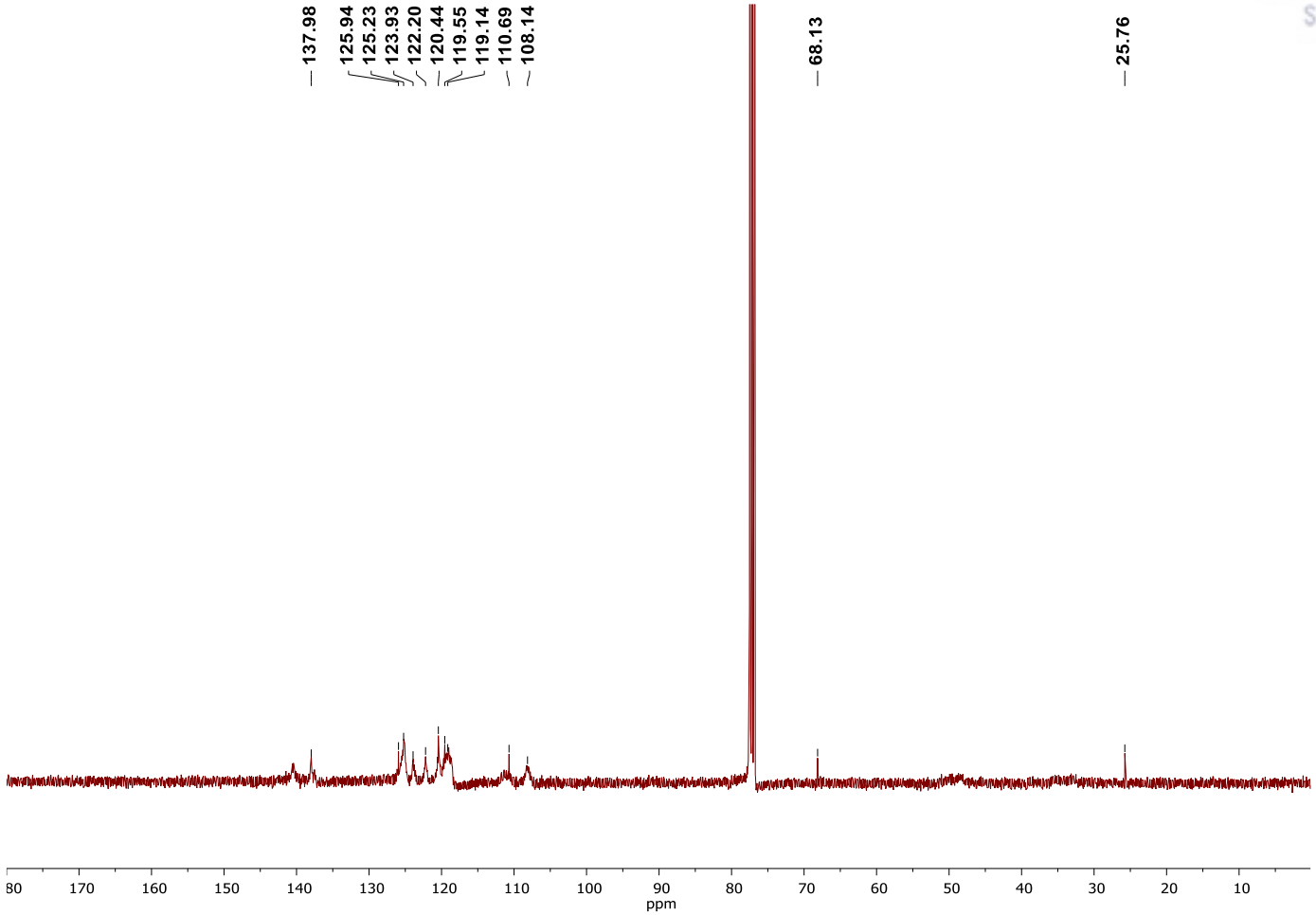

Figure E.3.26 ^{13}C NMR (400 MHz, $CDCl_3$) spectrum recorded for Table 3.5, Entry 2.

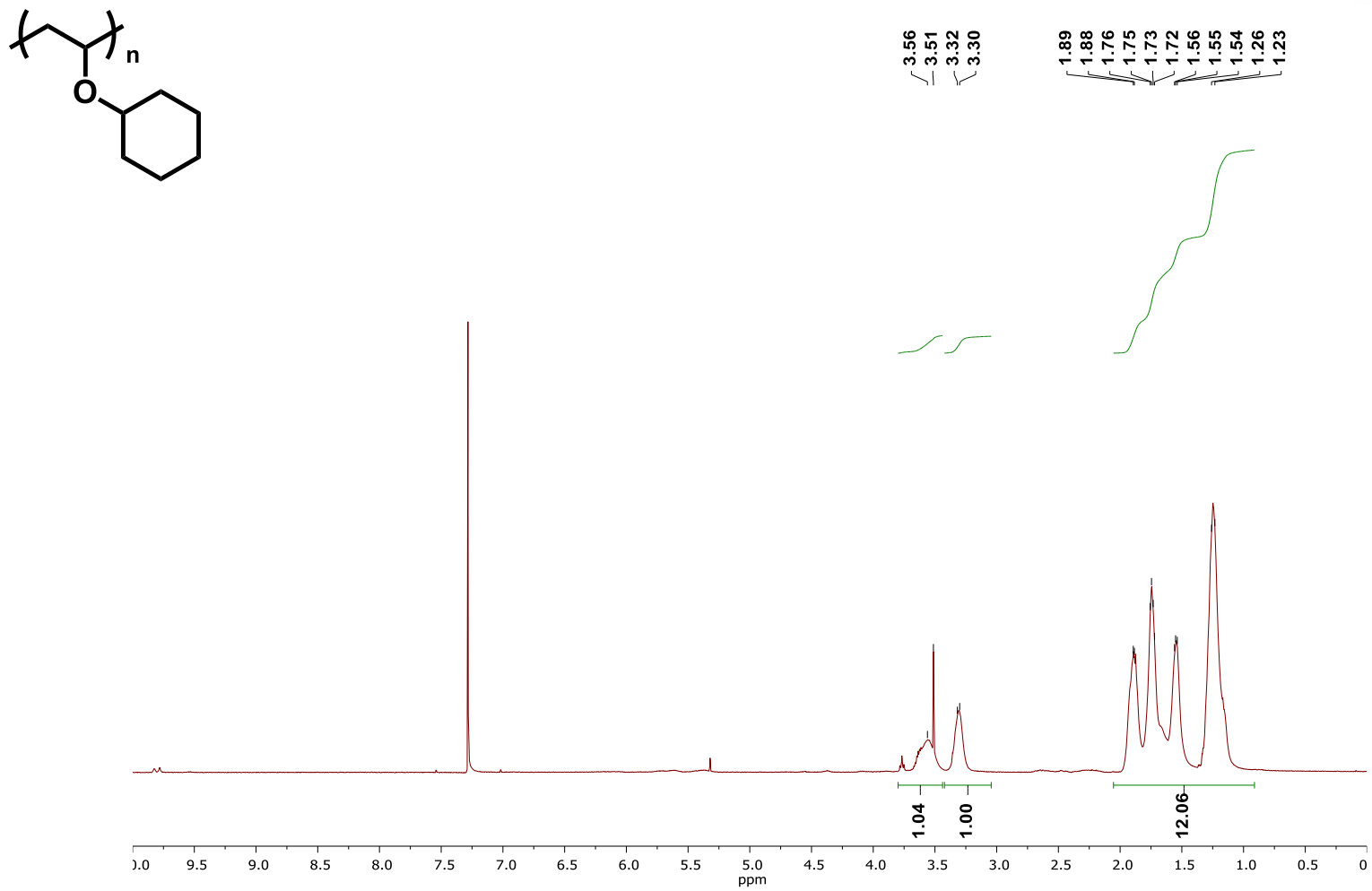

Figure E.3.27 ^{1}H NMR (400 MHz, $CDCl_3$) spectrum recorded for Table 3.5, Entry 3.

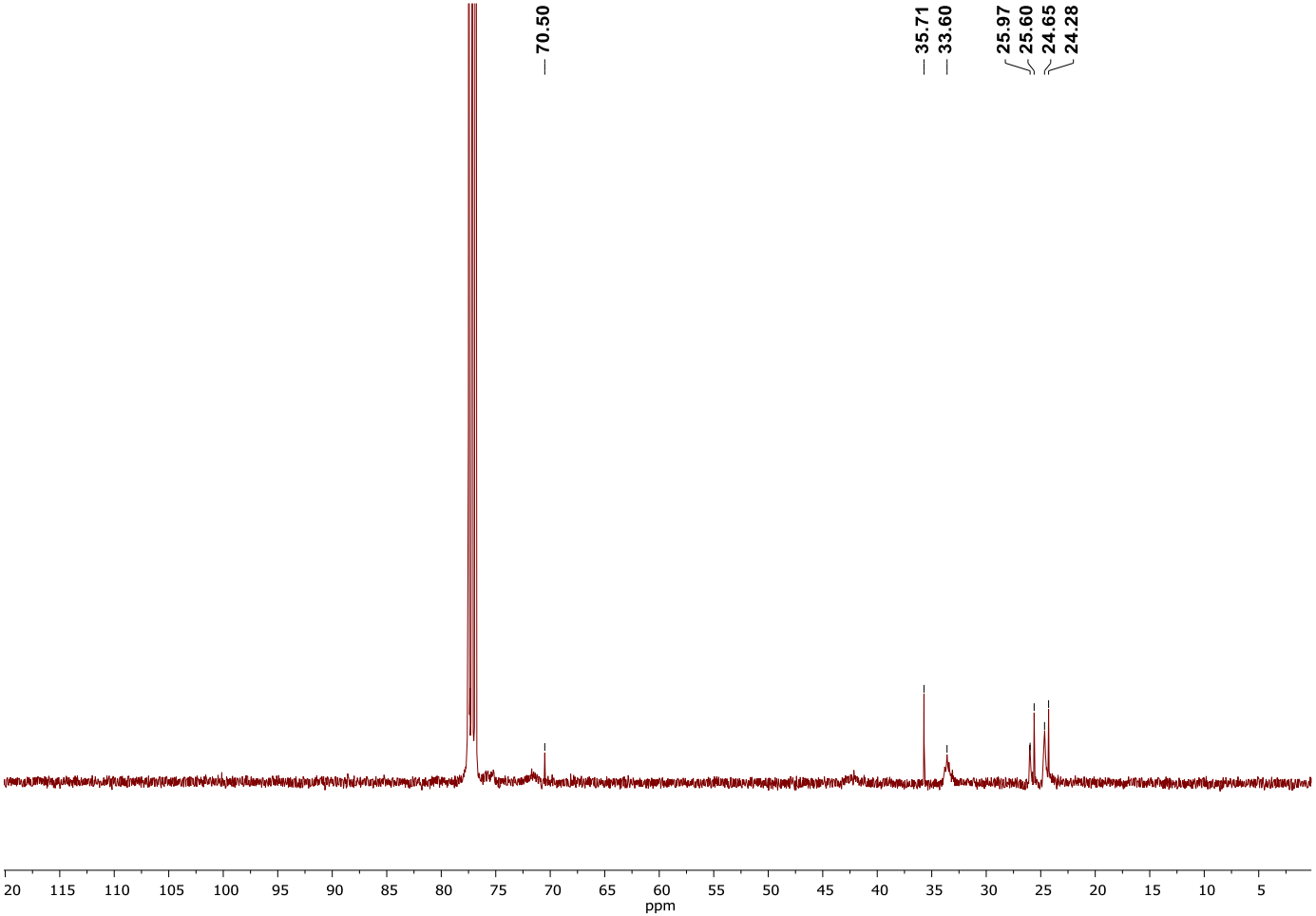

Figure E.3.28 ^{13}C NMR (400 MHz, $CDCl_3$) spectrum recorded for Table 3.5, Entry 3.